

POLITECNICO DI TORINO



FACOLTÀ DI INGEGNERIA

LAUREA MAGISTRALE

In Ingegneria Civile

SEISMIC MONITORING OF STRATEGIC  
STRUCTURES. CASE STUDY: COURT “E. FERMI”  
DURING THE EARTHQUAKE OF CENTRAL ITALY  
(NORCIA 2016)

*Candidato:*

*Alessandro Locchi*

*Relatore:*

*Prof. Rosario Ceravolo*

*Ing. Luca Zanotti Fragonara*

a.a. 2017/2018

In collaboration with:



# INDEX

Table index .....	VI
Figure index.....	VII
ABSTRACT .....	IX
1 GENERAL INTRODUCTION .....	1
2 SEISMIC PREVENTION.....	2
2.1 ReLUIS.....	2
2.2 Seismic Observatory of Structures .....	4
2.3 National Network of Accelerometers (RAN) .....	6
2.4 INGV Ancona .....	7
2.5 Seismic events considered .....	8
2.5.1 24-08-2016 Earthquake (hh.mm 01.36).....	9
2.5.2 26-10-2016 Earthquake (hh.mm 17.10 -19.18).....	10
2.5.3 30-10-2016 Earthquake (hh.mm 06.40).....	12
2.5.4 18-01-2017 Earthquake (hh.mm 10.14).....	12
2.6 Current situation .....	13
3 MONITORING SYSTEM .....	15
3.1 Introduction .....	15
3.2 Architecture of the seismic monitoring system in Fabriano Structure .....	16
3.3 Technologies of SHM.....	17
3.3.1 Experimental technologies.....	17
3.3.2 Analytical technologies .....	18
3.3.3 technologies for the processing of the data .....	19
4 CASE STUDY: COURT OF FBRIANO (EX "E. FERMI" SCHOOL).....	21
4.1 Introduction .....	21
4.2 Territorial classification.....	22
4.3 Description and History of the building .....	23
4.4 Dimensional characteristics .....	24
4.5 Vertical elements .....	24
4.5.1 Tests to define the mechanical parameters.....	26
4.6 Horizontal elements .....	28
4.7 Roof .....	32
4.8 External body joined to the structure .....	33
4.9 Foundations.....	34
4.10 Active monitoring system in the structure .....	34

5	GEOMETRIC MODELING 3D ( <i>RHINO</i> ) AND FEM ANALYSIS ( <i>ANSYS</i> ) .....	37
5.1	Nomenclature and model on <i>RHINO</i> Model .....	37
5.2	Modeling with <i>Ansys</i> .....	39
5.2.1	Definition of Material .....	39
5.2.2	Definition of Section and <i>SHELL</i> element .....	40
5.2.3	Definition of Constraint and Mass .....	42
5.2.4	Definition of type of Analysis .....	45
5.3	Placement of accelerometers .....	45
6	METHODS OF MODEL UPDATING AND CALIBRATION .....	46
6.1	Basic mathematical model and modal analysis .....	47
6.2	Uploading parameters .....	49
6.3	Comparison between measured parameters and model parameters .....	51
6.4	Direct methods of Updating .....	51
6.5	Iterative methods .....	52
6.5.1	Matrix Mixing method .....	52
6.5.2	Lagrange multipliers Method .....	54
6.6	Model Quality .....	56
6.7	Optimization Techniques .....	57
6.7.1	Genetic algorithm .....	57
6.8	Calibration Parameters of Structure .....	58
6.8.1	Stiffness Parameters .....	59
6.8.2	Density Parameters of walls .....	61
6.8.3	Density parameters of slabs .....	62
6.8.4	External parameters .....	62
6.9	Results of Calibration .....	63
6.9.1	Upload parameters found .....	67
6.10	MAC .....	70
7	MODEL BEHAVIOUR UNDER EARTHQUAKE .....	71
7.1	Simulated earthquakes .....	71
7.2	Acceleration comparison .....	78
7.3	Displacements .....	79
7.4	Drift of floor .....	80
7.4.1	Drift variation with the PGA .....	83
7.4.2	Comparison Drift ID and FEM .....	85
7.4.3	Drift for floor height .....	87
8	CONCLUSION .....	89



ATTACHMENT ..... 90

REFERENCES ..... 92

## Table index

Table 3.1 Main experimental technologies used in SHM.....	18
Table 4.1 Type of masonry .....	25
Table 4.2 Test results .....	26
Table 4.3 Results on 8 areas considered .....	26
Table 4.4 Results on 8 areas considered .....	27
Table 4.5 Result of Thermography .....	27
Table 4.6 Soil categories NTC08 .....	34
Table 5.1 Classification adopted .....	38
Table 5.2 Classification adopted .....	38
Table 5.3 Slab and stair characteristic.....	40
Table 5.4 Indicative values of the modulus of elasticity of some soil.....	42
Table 5.5 Composition of Roof.....	44
Table 5.6 Characteristic element mass.....	44
Table 6.1 Stiffness parameters.....	61
Table 6.2 Density parameters .....	61
Table 6.3 Slabs parameters .....	62
Table 6.4 External parameters .....	62
Table 6.5 STARTING, FEM and ID frequency comparison .....	66
Table 6.6 Stiffness MUR_1 MUR_3 .....	67
Table 6.7 Stiffness MUR_2 .....	68
Table 6.8 Density of wall .....	68
Table 6.9 Density of slab .....	69
Table 6.10 External parameters uploaded.....	70
Table 7.1 Earthquake considered.....	71
Table 7.2 Drift under earthquake n.1.....	80
Table 7.3 Drift under earthquake n.2.....	81
Table 7.4 Drift under earthquake n.3.....	81
Table 7.5 Drift under earthquake n.4.....	82
Table 7.6 Table Drift under earthquake n.4 .....	82
Table Attachment n.1 Calibrated Values Parameters.....	91

# Figure index

Figure 2.1 Universities ReLUISS.....	3
Figure 2.2 List of monitored buildings .....	4
Figure 2.3 Monitored buildings locations .....	5
Figure 2.4 National Accelerometer Network .....	6
Figure 2.5 ReSIICO stations .....	7
Figure 2.6 Earthquake list.....	8
Figure 2.7 History earthquakes .....	9
Figure 2.8 Seismic sequence after earthquake 24-08-2016.....	10
Figure 2.9 Model single fault.....	11
Figure 2.10 Model double fault.....	11
Figure 2.11 Seismic sequence after earthquake 30-10-2017.....	12
Figure 2.12 Seismic sequence afeter earhtquake 18-01-2017.....	13
Figure 2.13 Distribution earthquakes from 1997 to 2017 .....	14
Figure 3.1 Accelerometer and cable wiring .....	16
Figure 3.2 Acquisition system .....	16
Figure 4.1 Building on 2017.....	21
Figure 4.2 Fabriano location.....	22
Figure 4.3 Town Hall of Fabriano .....	22
Figure 4.4 Building on 1939.....	23
Figure 4.5 Building on 1940 (up) and on 1943 (down).....	23
Figure 4.6 Bildings's diagram type .....	24
Figure 4.7 Preparing test .....	26
Figure 4.8 Termografhy Southwest side .....	27
Figure 4.9 Features typological basement floor .....	30
Figure 4.10 Features typological ground floor .....	31
Figure 4.11 Features typological first floor .....	31
Figure 4.12 Features typological second floor .....	32
Figure 4.13 typology roof .....	32
Figure 4.14 Steel joint in hight .....	33
Figure 4.15 Steel joint in the corner.....	33
Figure 4.16External body stair .....	33
Figure 4.17 Arrangement of Accelerometers floor basement.....	35
Figure 4.18 Arrangement of Accelerometers ground floor .....	35
Figure 4.19 Arrangement of Accelerometers first floor.....	36
Figure 4.20 Arrangement of Accelerometers second floor.....	36
Figure 5.1 Representation body sud -est RHINO .....	37
Figure 5.2 Representation body nord-vest RHINO.....	37
Figure 5.3 Mechanic characteristic of masonry .....	39
Figure 5.4 Element shell 181 .....	40
Figure 5.5 ANSYS representation .....	41
Figure 5.6 Meshed Structure.....	41
Figure 5.7 Raprsentatio of springs of body Nord .....	42
Figure 5.8 Representation of perimetral soil as springs .....	43
Figure 5.9 Representation of constraint .....	43
Figure 5.10 Coordinates of sensors.....	45
Figure 6.1 genetic algorithm diagram .....	58

Figure 6.2 Ground floor stiffness.....	59
Figure 6.3 First floor stiffness.....	59
Figure 6.4 Second floor stiffness .....	60
Figure 6.5 Roof floor stiffness .....	60
Figure 6.6 I MODE updated Model.....	63
Figure 6.7 I MODE identified.....	63
Figure 6.8 II MODE updated Model, East Side .....	64
Figure 6.9 II MODE updated Model , West Side.....	64
Figure 6.10 II MODE identified .....	64
Figure 6.11 III MODE updated Model , sud Side .....	65
Figure 6.12 III MODE identified .....	65
Figure 6.13 Frequency of model .....	66
Figure 6.14 Stiffness MUR_1 MUR_3.....	67
Figure 6.15 Stiffness MUR_2 .....	68
Figure 6.16 Density of wall.....	69
Figure 6.17 Density of slab .....	69
Figure 6.18 MAC uploaded model.....	70
Figure 6.19 MAC starting model .....	70
Figure 7.1 Earthquake output sensor.....	71
Figure 7.2 Earthquakes distance from Fabriano .....	72
Figure 7.3 Earthquakes distance from Amatrice and Norcia .....	72
Figure 7.4 Shaking map earthquake n.4.....	73
Figure 7.5 Shaking map earthquake n.3.....	74
Figure 7.6 Seismic acceleration Earthquake n.1 .....	75
Figure 7.7 Seismic acceleration Earthquake n.2 .....	75
Figure 7.8 Seismic acceleration Earthquake n.3 .....	76
Figure 7.9 Seismic acceleration Earthquake n.4 .....	76
Figure 7.10 Seismic acceleration Earthquake n.5 .....	77
Figure 7.11 Damage caused by seismic shock 24-08-2016 .....	77
Figure 7.12 Acceleration FEM, ID channel 22 .....	78
Figure 7.13 Acceleration FEM, ID channel 24 .....	78
Figure 7.14 Displacement channel 22 .....	79
Figure 7.15 Displacement channel 24 .....	79
Figure 7.16 Location of DRIFT calculated second floor .....	83
Figure 7.17 Displacement of point 1 with PGA .....	83
Figure 7.18 Displacement of point 2 with PGA .....	84
Figure 7.19 Displacement of point 3 with PGA .....	84
Figure 7.20 Comparison DRIFT point 1.....	<b>Errore. Il segnalibro non è definito.</b>
Figure 7.21 Comparison DRIFT point 2.....	<b>Errore. Il segnalibro non è definito.</b>
Figure 7.22 Comparison DRIFT point 1.....	<b>Errore. Il segnalibro non è definito.</b>
Figure 7.23 DRIFT FEM point 1.....	<b>Errore. Il segnalibro non è definito.</b>
Figure 7.24 DRIFT FEM point n.2.....	<b>Errore. Il segnalibro non è definito.</b>
Figure 7.25 DRIFT FEM point n.3.....	<b>Errore. Il segnalibro non è definito.</b>

# ABSTRACT

This work gives a small contribution about the study of the huge amount of historical buildings which must be protected in the Italian landscape. The model over time can be improved and is an excellent starting point for further exploration.

This thesis is fundamentally divided into three phases of work. The first phase consists in the structural modelling of the building studied, being careful, to the correct individuation of the supporting element and the present characteristics. The modelling through a finite element program must represent in a suitable way the geometry and all the structural particularities of the building. In the second phase, once the geometric model is done, will be carried out a calibration. This operation is used to ensure that the FEM model created has a structural behaviour as close as possible to the real one, which is measured experimentally by the sensors placed in the building. The goal is to have a finite element model that mimics in an adherent way the behaviour of the structure subjected to any earthquake. The last phase concerns the study of the behaviour of the building, under the seismic sequence that struck Norcia and Amatrice in 2016. Will be made an evaluation on the state of damage for the post-earthquake considering the verification of limit state of damage provided by Italian law.

The model created and calibrated at this point will be part of the archive of the project Reluis, which will be available for future studies and dynamic analyses.

# CHAPTER I

## 1 GENERAL INTRODUCTION

Italy is a territory characterized by a high seismic activity. The latest seismic events have reinforced the interest and the study of active and passive mitigation measures for earthquakes. The vulnerability of the Italian territory is dual, at first, the presence of active plaques, and second, the state of conservation of our buildings, which are for the most part historical and in a non-optimal state. Understanding these two factors, is of paramount importance for making progress on earthquake prevention. Most of the Italian heritage consists of masonry buildings, these are often the result of edifications, modifications and alterations, which have succeeded in the years, and are characterized by extremely heterogeneous types of construction and materials. For these reasons, in fact, the evaluation of the current construction status is often delicate and sometimes uncertain.

The tragic consequences of the recent seismic events that took place in Italy, have rooted the idea of a greater protection of the existing buildings respect of earthquakes, and a greater knowledge of historical buildings in order to understand their behaviour under these exceptional events. The study of seismic mitigation starts from the knowledge and monitoring of "strategic" buildings that belong to the public patrimony such as: schools, town halls, courts, bridges etc... The continuous monitoring of a building has a double importance in the study of its dynamic response. First of all, it is possible to understand the evolution over time of the "health condition" of the structure, going to monitor structural parameters, and secondly, in this way is possible to have a seismic data storage network. The structure studied set in Marche region and is the "E. Fermi" School, which after extensive damage by the earthquake of September 1997 has been consolidated with invasive interventions. After 1997 the structure, is subjected to continuous monitoring thanks to the installation of sensors by the Italian Civil Protection. The thesis object, will be the study of this building's behaviour under some chosen earthquakes, and the Thesis work will be divided in three fundamental steps. The first step will involve the creation of the geometrical model, with a 3D graphics program, the next step, will be calibration of the model found, considering the vibration data under the earthquake of that structure provided by the Civil Protection. Finally, once the model is calibrated, simulations will be performed with five different earthquakes, to make some considerations about the level of damage suffered. The simulated earthquakes are real and refer to the seismic swarm that hit central Italy in 2016, in particular the city of Norcia. The calibrated model is an indispensable tool for diagnostic purposes and for the estimation of seismic safety. It also appears to be a valid support in the design of possible consolidation, rehabilitation and seismic protection interventions. From this point of view, with a good calibration of the model it is possible to have simulations more reliable and similar to the real behaviour of the structure with a degree of reliability that is certainly greater than an uncalibrated FEM model. The study of this building is part of a larger project of National interest. The Civil Protection Department collaborates with the Italian Universities and together they work on the monitoring of strategic buildings in Italy. The following chapter aims to give a general but at the same time exhaustive idea about this important collaboration, which is fundamental for the conservation of our constructive heritage.

# CHAPTER II

## 2 SEISMIC PREVENTION

For Seismic Prevention we mean the activity aimed at avoiding, or minimizing, the possibility of damage resulting from seismic events. The prevention activity is based on the knowledge and identification of areas of territory subject to seismic risk and is supported through the introduction of rules, programs and plans, with the implementation of interventions on buildings and infrastructures and actions aimed at training operators and information to the population. The earthquake of Molise in 2002, gave a strong impulse about the numerous strides to be taken in the field of prevention and seismic legislation. This dramatic event, as we recall, made 28 victims, whom 27 were children, shock the consciences of the Italian population a lot, highlighting the enormous need to adopt more rigorous seismic norms. In 2003, with the issuance of the Ordinance of the President of the Council of Ministers (OPCM) 3274, were laid the bases in Italy of a seismic prevention strategy. Because of this hard initiative, was required the help of the Institutions, of the Scientific Community, of the Professional Associations and of the Enterprises, to give Italy a state-of-the-art seismic regulation able to cope with these exceptional events. Specifically, it must be said that the regions of Marche and Umbria, after the earthquake of 1997, immediately provided for the development of seismic vulnerability assessment programs, but nevertheless more space was given to the problem of reconstruction rather than prevention.

The Civil Protection Department thanks to the OPCM 3274 was authorized to promote the establishment of a network of university laboratories of Engineering Seismic (ReLUIs), with the aim of providing scientific, technical and financial organizational support to the universities participating in the project, furthering their participation to activities in the field of seismic engineering. The ReLUIs project began in 2005 involving 137 research units spread across 40 university sites throughout Italy.

### 2.1 *ReLUIs*

The Network of University Laboratories of Seismic Engineering (ReLUIs), constituted by a conventional act signed on April 17 of 2003, is an inter-university consortium whose purpose is to coordinate the activity of University Laboratories of



Seismic Engineering, providing scientific, organizational, technical and financial services to the associated Universities and furthering their participation in scientific and technological activities in the field of Seismic Engineering, in accordance with national and international research programs in this field. The coordination action consist of collaborations between Universities, University Institutes and Interuniversity centers among themselves and with other Research Institutions and Industries, boosting the development of the Seismic Engineering Laboratories, with research activity and dissemination knowledge. The Consortium proposes itself as scientific interlocutor of the various organs of the National Government, of the Regions,

Provinces, Municipalities and of public and private Institutes in order to achieve concrete objectives and valuate and reduce vulnerability and seismic risk. The head office is in Naples, at the Department of Structural Engineering of the Federico II University, and is non-profit-making. Below, we can see the universities that participate in the project, the Polytechnic of Turin is among them.



Figure 2.1 Universities ReLUISS



## 2.2 Seismic Observatory of Structures

The seismic observatory of the structures, OSS, was created to cope the need for a correct seismic prevention and represents the national network of permanent monitoring of the seismic response of construction which belonging to the public patrimony. The Ministry of Infrastructure and Transport, Regions, local authorities and other public bodies collaborate in the identification of the structures of the permanent network of OSS. Through the national network of the Seismic observatory of the structures, the Department of Civil Protection monitors the oscillations caused by the earthquake in 160 buildings of public property: 150 buildings (of which 70 schools equal to 47%, 29 municipalities of 19%, 30 hospitals equal to 20%, 21 other types equal to 14%), as well as 7 bridges and 3 dams. In 2018 two more dams will be added. These buildings are found in municipalities classified mostly in Seismic Zone 1 (34%) and 2 (63%). The OSS allows the evaluation of the damage caused by an earthquake to the monitored structures, which can be extended to those similar ones that fall in the affected area. In this way, it provides useful information to the civil protection activity immediately following the seismic event. When a construction of the OSS is affected by a significant earthquake, the monitoring system records the movement of soil and structure, and immediately sends the recorded data to the central OSS server in Rome. The server automatically processes the recordings flocked from all the affected structures, providing a concise report of some significant parameters that permit to evaluate: the incoming earthquake, the vibrations of the structure and the relative state of damage. There are two monitoring systems:

- **"Detailed" Monitoring system:**

In the "detailed" monitoring system, the sensors are distributed on all floors of the building and on the ground, for an average of 20 acceleration measures, in order to adequately rebuild the vibrations of the structure and estimate the damage

- **"Simplified" Monitoring system:**

In the "Simplified" monitoring system, the sensors are on the ground and on the top floor, independent and connected to the Wi-Fi network only, for about 7 measurements. However, this system is less expensive as supply and as installation, for lack of wiring, but provides less information.

Is possible consult the list of monitored buildings, which are ordered according to a numerical alpha code, on the Civil Protection site ([www.protezionecivile.gov.it](http://www.protezionecivile.gov.it)). Our building ,as seen, from the following image, taken from site above falls into the structures with monitoring "Detailed".

SIGLA	NOME	REGIO	PROVINCI	COMUN	TIPOLOGIA	LATITUDI	NGITU	SEN	CLASSIFICAZI	SISTEMA	A S	ni
01CCO	Chiesa di S. Caterina V.	TOSCANA	MASSA-CARRA	FIVIZZANO	Edificio Monumentale in m	44,239	10,154	26	ALTRO EDIFICIO	DETTAGLIATO	2	
02PME	Ponte ad Arco dello Zin	EMILIA-RC	FORLI'	CESENA	MERCATO S/	43,942	12,184	32	PONTE	DETTAGLIATO	2	
03VTC	Viadotto "Cesi" sulla E/	UMBRIA	TERNI	SAN GEMINI	Ponte in cemento armato	42,614	12,554	32	PONTE	DETTAGLIATO	2	
04ALU	Asilo Nido a Lugo di Ro	EMILIA-RC	RAVENNA	LUGO	Edificio in cemento armato	44,415	11,913	17	SCUOLA	DETTAGLIATO	2	
05SCE	Scuola Elementare "Sal	EMILIA-RC	FORLI'	CESENA	Edificio in cemento armato	44,133	12,264	24	SCUOLA	DETTAGLIATO	2	
BC053	Tribunale di Fabriano	MARCHE	ANCONA	FABRIANO	Edificio in muratura	43,338	12,909	31	ALTRO EDIFICIO	DETTAGLIATO	2	
07IFO	I.T.I. "G.Marconi" - Am	EMILIA-RC	FORLI'	CESENA	FORLI'	44,220	12,053	15	SCUOLA	DETTAGLIATO	2	
08IRI	I.T.I. di Rimini	EMILIA-RC	RIMINI	RIMINI	Edificio in cemento armato	44,047	12,584	17	SCUOLA	DETTAGLIATO	2	
09MIO	I.T. Professionale "G. F	EMILIA-RC	RIMINI	MORCIANO	Edificio in cemento armato	43,816	12,668	16	SCUOLA	DETTAGLIATO	2	

Figure 2.2 List of monitored buildings

The following image shows all buildings monitored by OSS, and their type of use. The map also, refers their geographical location in relation to seismic hazard zones.

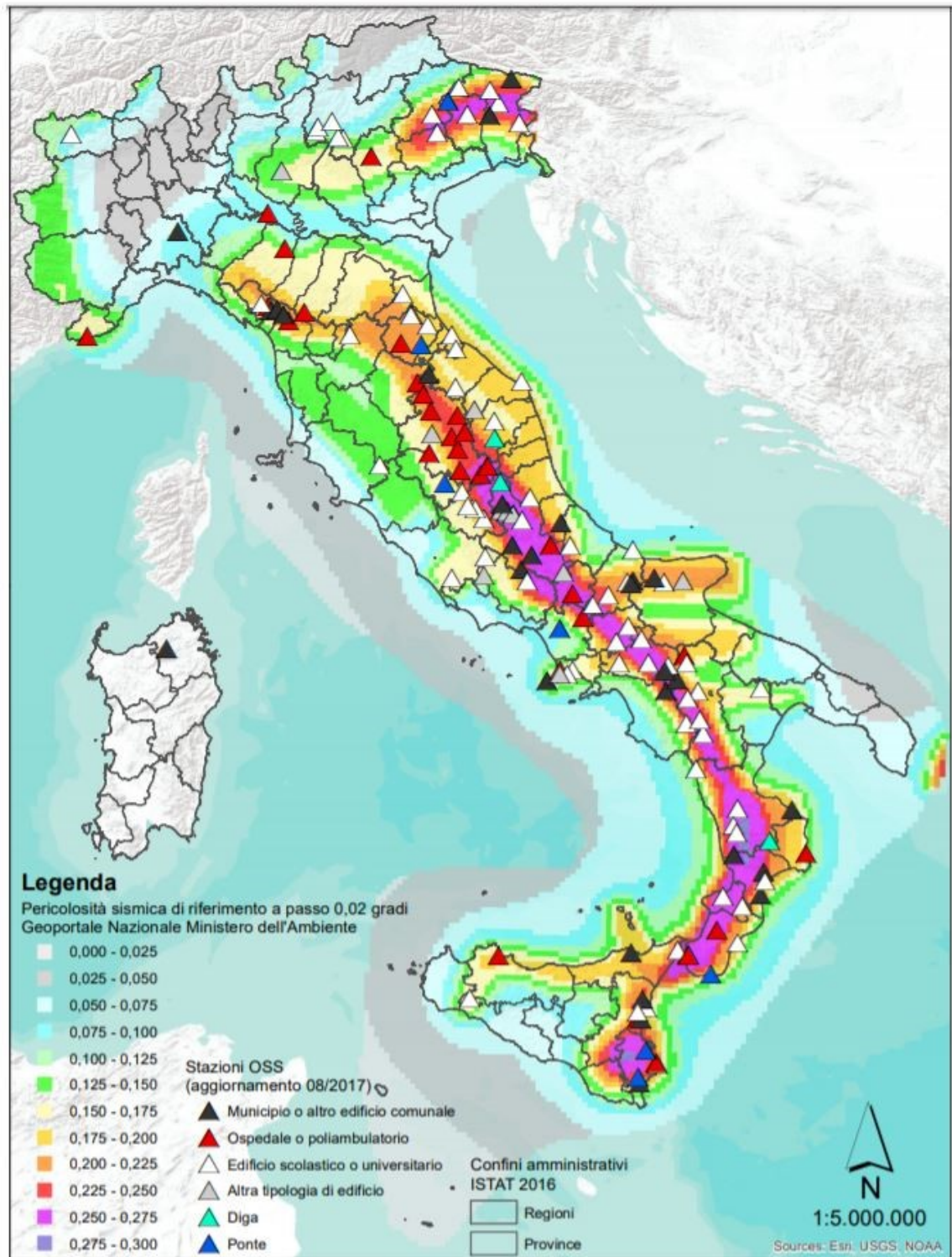


Figure 2.3 Monitored buildings locations

### 2.3 National Network of Accelerometers (RAN)

The RAN is the national accelerometric network of Italian territory that records the response monitoring the earthquake in terms of ground acceleration. The data recorded provide an accurately history of seismic shaking in the Epicentral area. These data also are very useful for studying seismology and seismic engineering and are convenient to defining the seismic action to be applied in the structural calculations. The RAN is distributed throughout the national territory, with a higher density in areas with major earthquake activity. The management of this network is entrusted by the staff of the seismic risk of the Civil Protection Department. The national network consists of permanent and temporary 561 digital workstations, equipped with an accelerometer, a digitizer, a modem/router with an antenna to transmit digitized data via GPRS and GPS receiver to associate the data the universal time UTC and to measure latitude and longitude of the location. Their location is divided into 201 devices in electrical substations of Enel and 360 on publicly owned land. (*data updated to July 2017*). The data flow to the central server of RAN in the headquarters of the Civil Protection Department, where they are automatically collected and processed to obtain an estimate of the main descriptive parameters of earthquake.

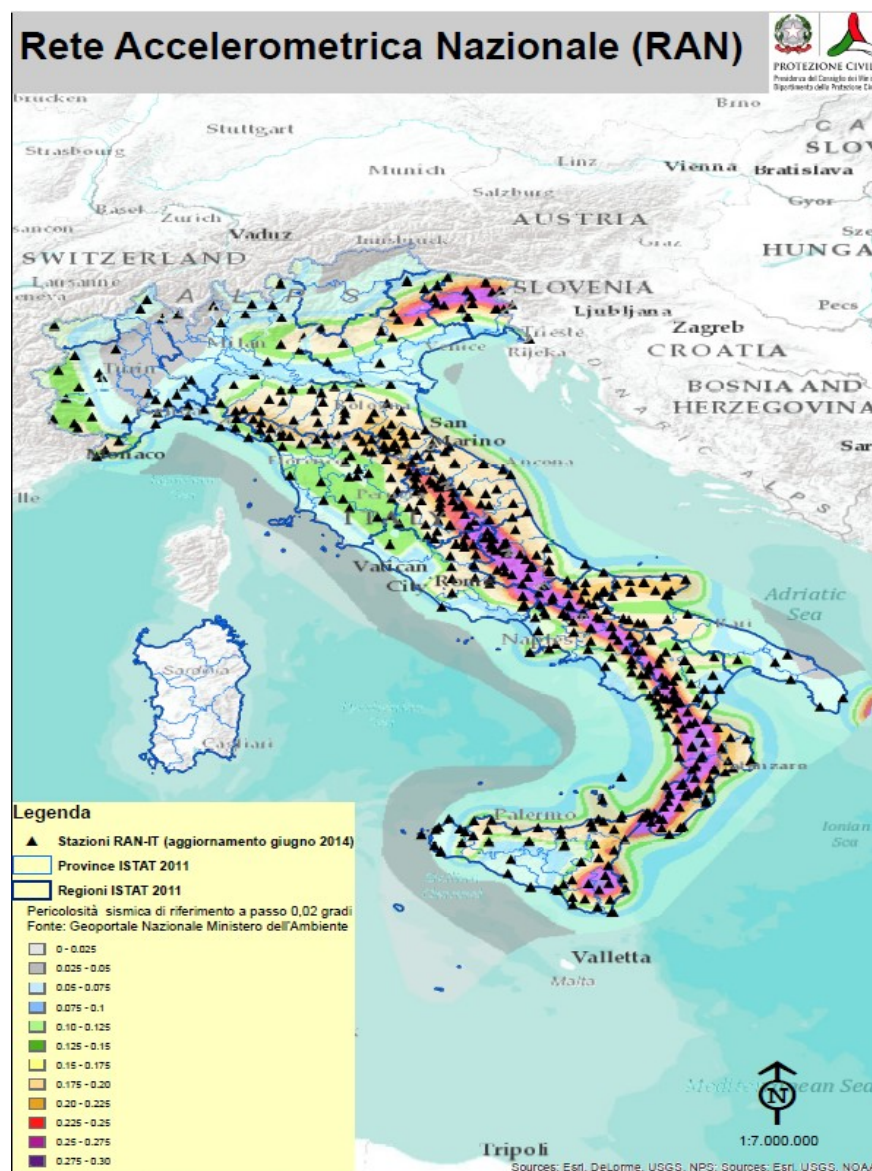


Figure 2.4 National Accelerometer Network



## 2.4 INGV Ancona

The building that will be studied is located in the Marche Region, in the municipality of Fabriano. In this Region, often remembered for the large seismic activity, the monitoring is developed in collaboration with the “*Istituto Nazionale di Geofisica e Vulcanologia (INGV)*”, which is responsible for coordinating national initiatives undertaken by several entities. Since 2002 the Civil Protection Department has started a formal relationship with the INGV seismic contains field and information related to the seismic risk. With this in mind, was created the headquarters of Ancona, significant in this territory, which over the years has seen a modest expansion. Initially it was composed of 10 measurement stations, and subsequently with the absorption of Central Eastern Italy Seismometric network (ReSIICO) has gone to 103 stations. The data obtained from stations are transmitted in real time to Control Centre of Ancona and to the operations room at the INGV of Rome. Multiple initiatives have been developed: activity of monitoring, activity of prevention, vulnerability study of public buildings, measurements to calculate values of ground shaking. All these activities have been designed and developed with a strongly regional characterization through algorithms and improved models of the INGV. The presence of many measurement points also permit to monitor and study in detail the extension of the seismic zone: from the Northern Apennines to the Adriatic coast. The work of INGV is very useful because the collection of the information in a seismic station consent to highlight and study in detail the possible effects of site that should be considered when attempting to study and reproduce the shaking the soil surface. The figure below shows the location of the stations present in the Marche region owned by INGV Ancona

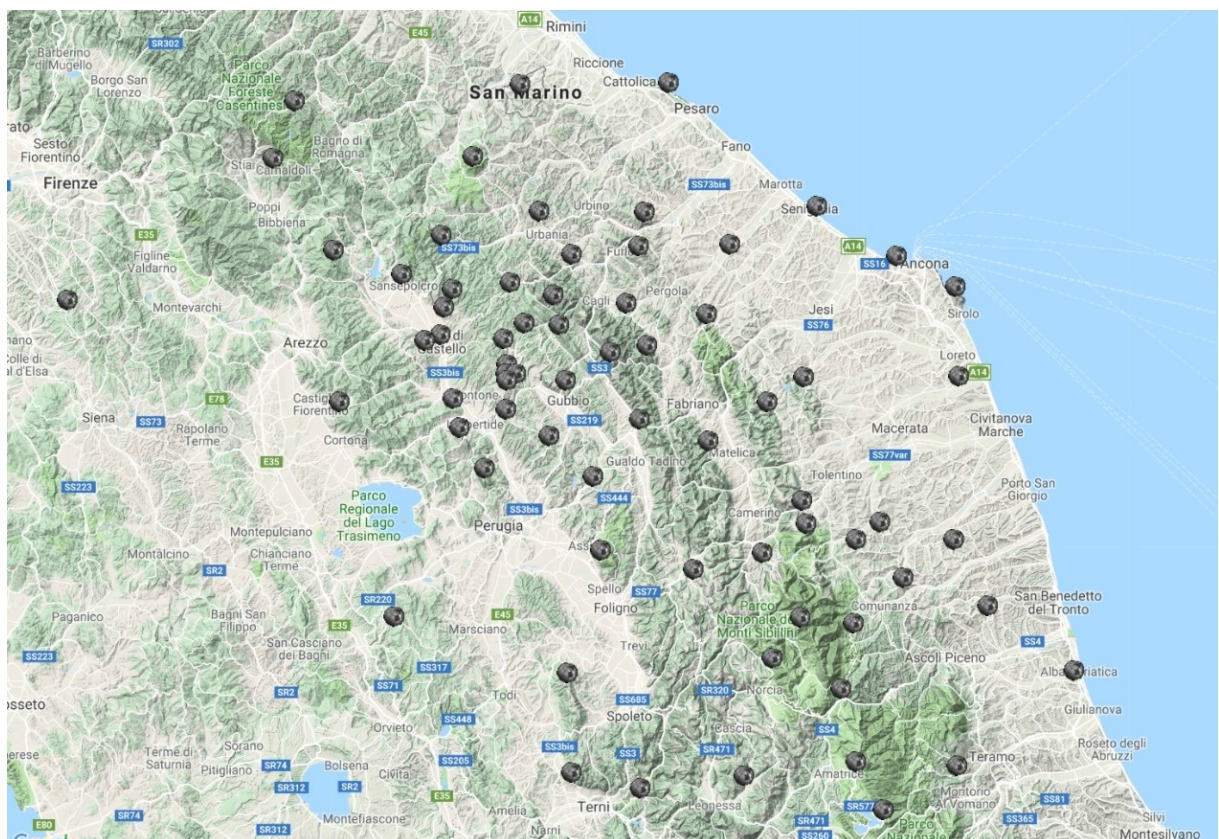


Figure 2.5 ReSIICO stations

## 2.5 Seismic events considered

For the study of the building, five earthquakes were identified belonging to the seismic swarm which struck central Italy in 2016. In the database of recordings into the INGV the site ([www.ingv.gov.it](http://www.ingv.gov.it)), it's possible find these earthquakes with all their information.

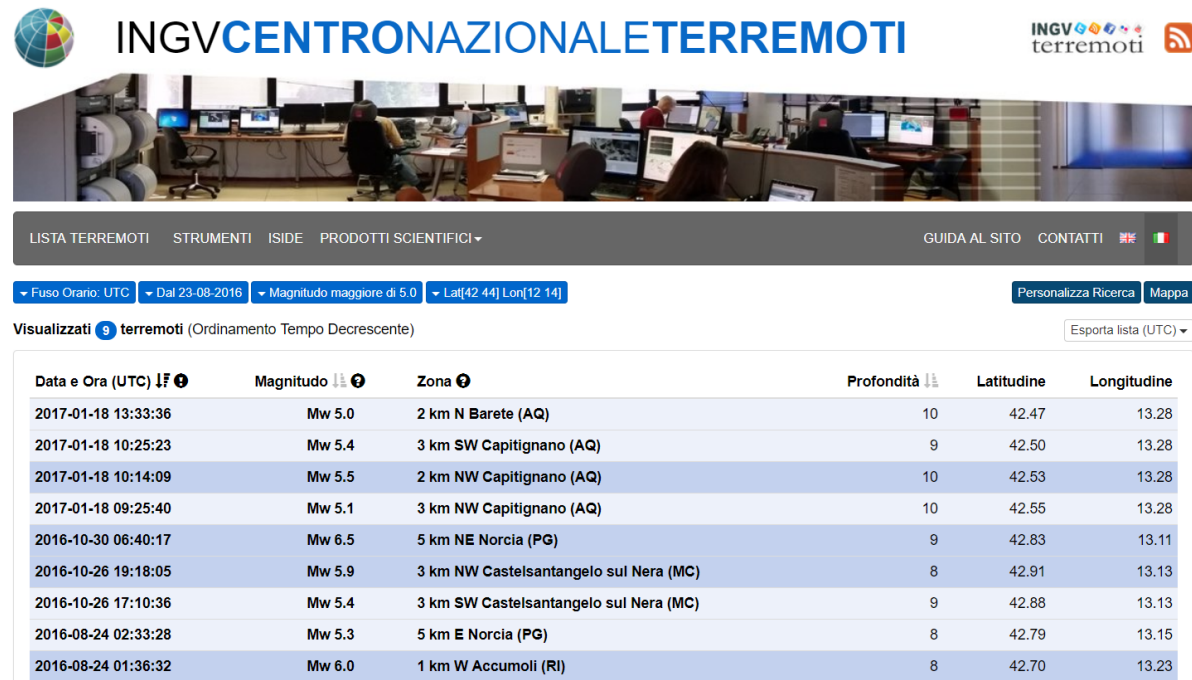


Figure 2.6 Earthquake list

From the previous figure are shown all the information that the INGV makes available. Earthquakes are medium to high intensity and their Epicentral depth not exceeding 10 km. Earthquakes in question were felt even in nearby areas, particularly in Umbria and Abruzzo, and generally in much of Italy. The affected area lies in zone 2 which is characterized by maximum acceleration on the ground, with the 10% probability of exceedance in 50 years (return period of 475 years), refers to soils of category A, equal to 0, 2 g (1, 90m/s<sup>2</sup>). The seismic sequences in detail will be shown in the next paragraph.

### 2.5.1 24-08-2016 Earthquake (hh.mm 01.36)

The seismic shock had an intensity of 6 in the Richter scale. The fault that generated, it extends over 20 km along the axis of the Apennines with a depth of 8 km between the surface. The affected area hosts numerous historic towns and smaller centres of Lazio, Umbria and Marche. The area hit by the earthquake is a dangerous seismic band that runs along the Apennine Ridge. This area has already been stricken by strong earthquakes in the years, as shown in the following figure.

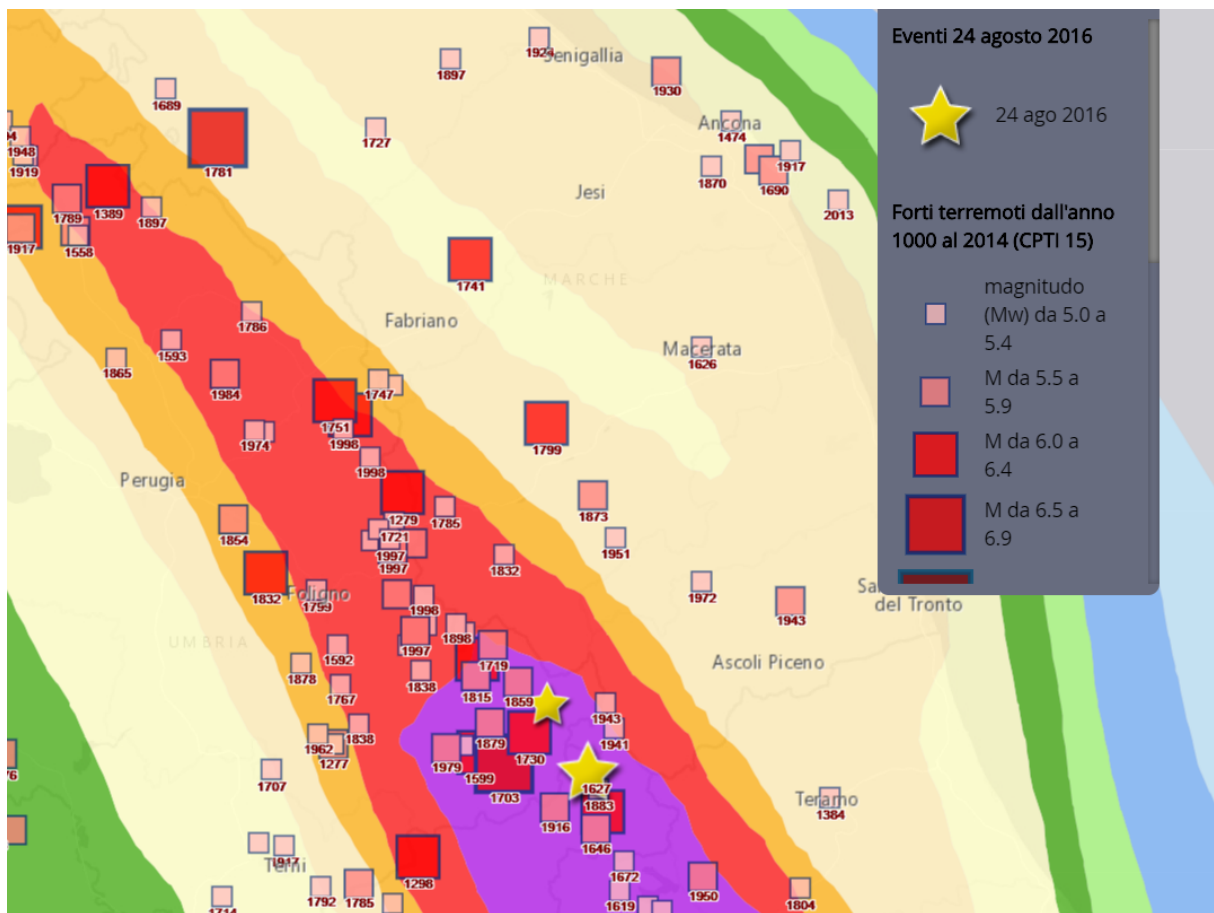


Figure 2.7 History earthquakes

Although the earthquake of 24 August, isn't one of the strongest known seismic events of the historical chronicles but the impact was very serious. Inhabited centers such as Accumoli and Amatrice in fact suffer damage, estimated equal to the X-XI degree MCS (Mercalli-Sieberg). The shock of August 24 arrives without notice, no foreshock in the days and hours before the earthquake. The progress of the sequence after 24 August had a rather complex and



unpredictable trend. After a phase of intense seismic activity with numerous aftershock per day, it seemed that it was going towards a slow return to normality.

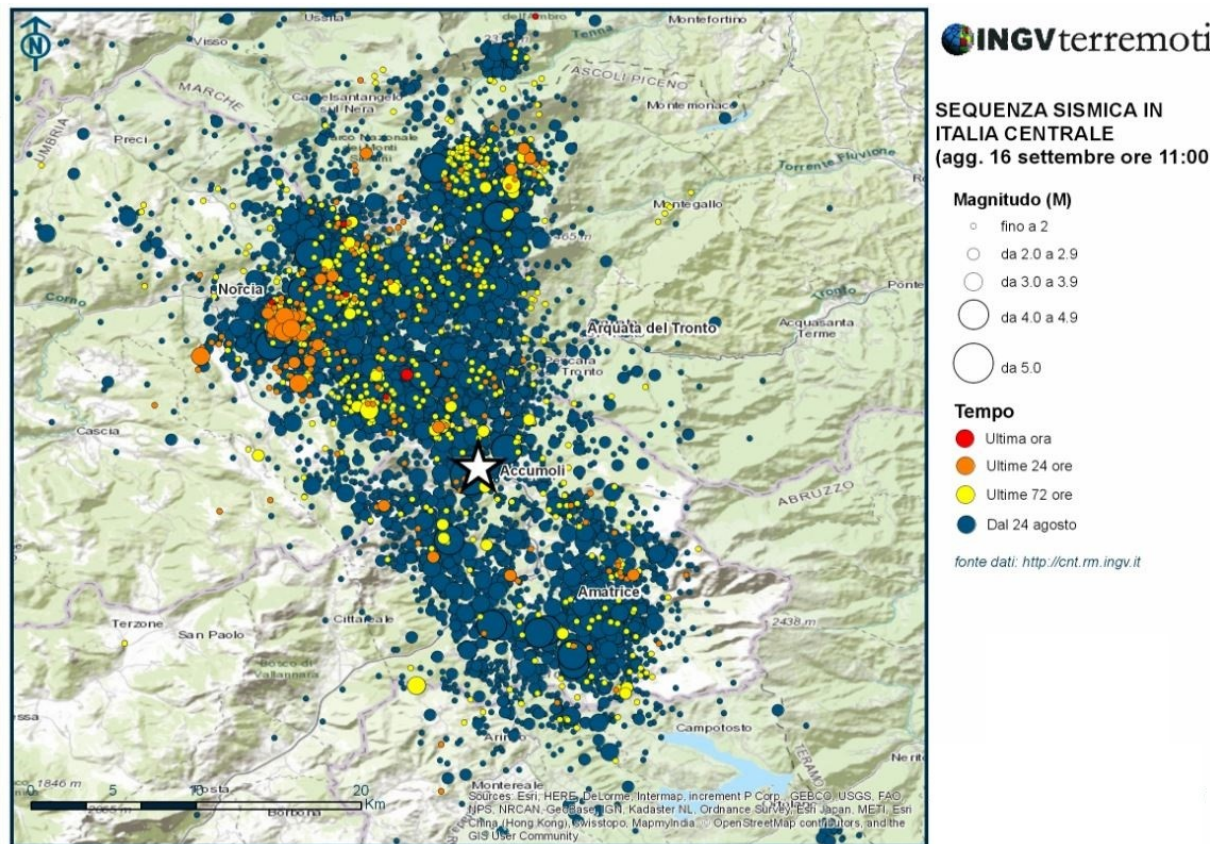


Figure 2.8 Seismic sequence after earthquake 24-08-2016

### 2.5.2 26-10-2016 Earthquake (hh.mm 17.10 -19.18)

On 26 October the sequence of activity recovered with two earthquakes, causing further damage but not victims. The active area moved north between Marche and Umbria. Some think that this earthquake is generated by an independent fault compared to that of August, supporting the idea of an adjacent fault, instead others sustain that it was a "domino effect" with two months later. Here the two images following represent the attempt of experts to want to model the phenomenon according to the many seismic data that were available until then. They thought of two different models one single-fault with one double fault.

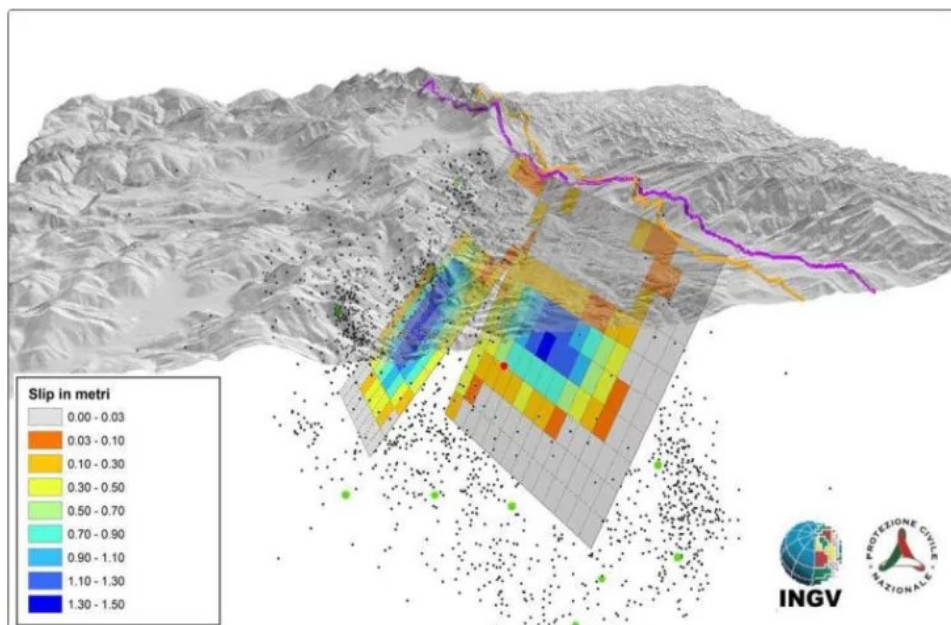


Figure 2.9 Model single fault

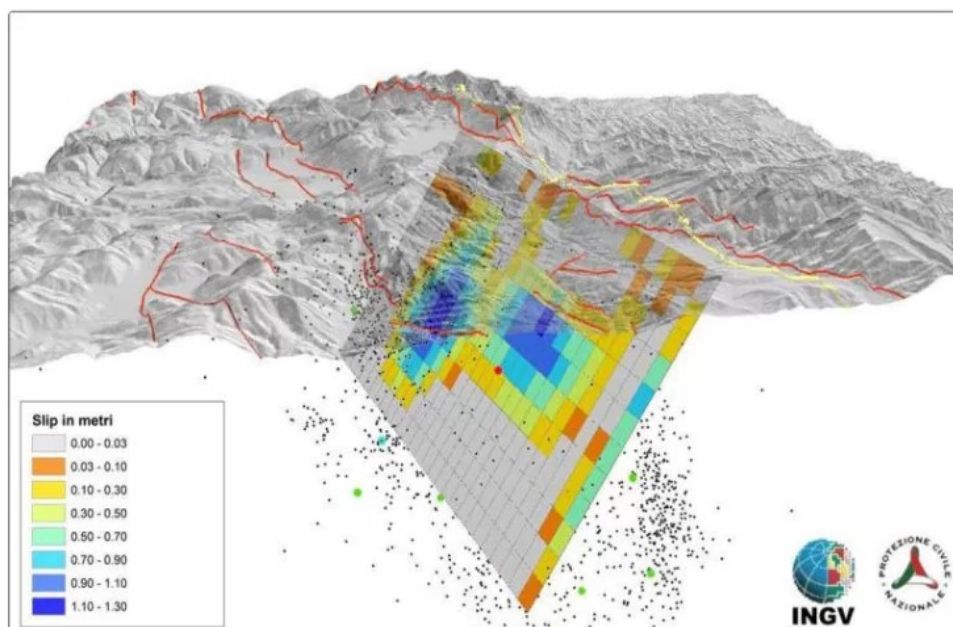


Figure 2.10 Model double fault



### 2.5.3 30-10-2016 Earthquake (hh.mm 06.40)

On the morning of October, millions of people from central Italy ,experienced a new shock, the loudest of the sequence and the strongest in Italy from the earthquake of 1980 in Irpinia. The epicenter was located at 5 km from Norcia, in the middle of the area already affected. The effects of this shock were glaring. Thanks to geological studies, was highlighted a slip of the two fault of 2 m. The following figure shows the sequence of the aftershock and was of fundamental importance to understand the fault system, the deformations of the ground and the forms of the seismic waves.

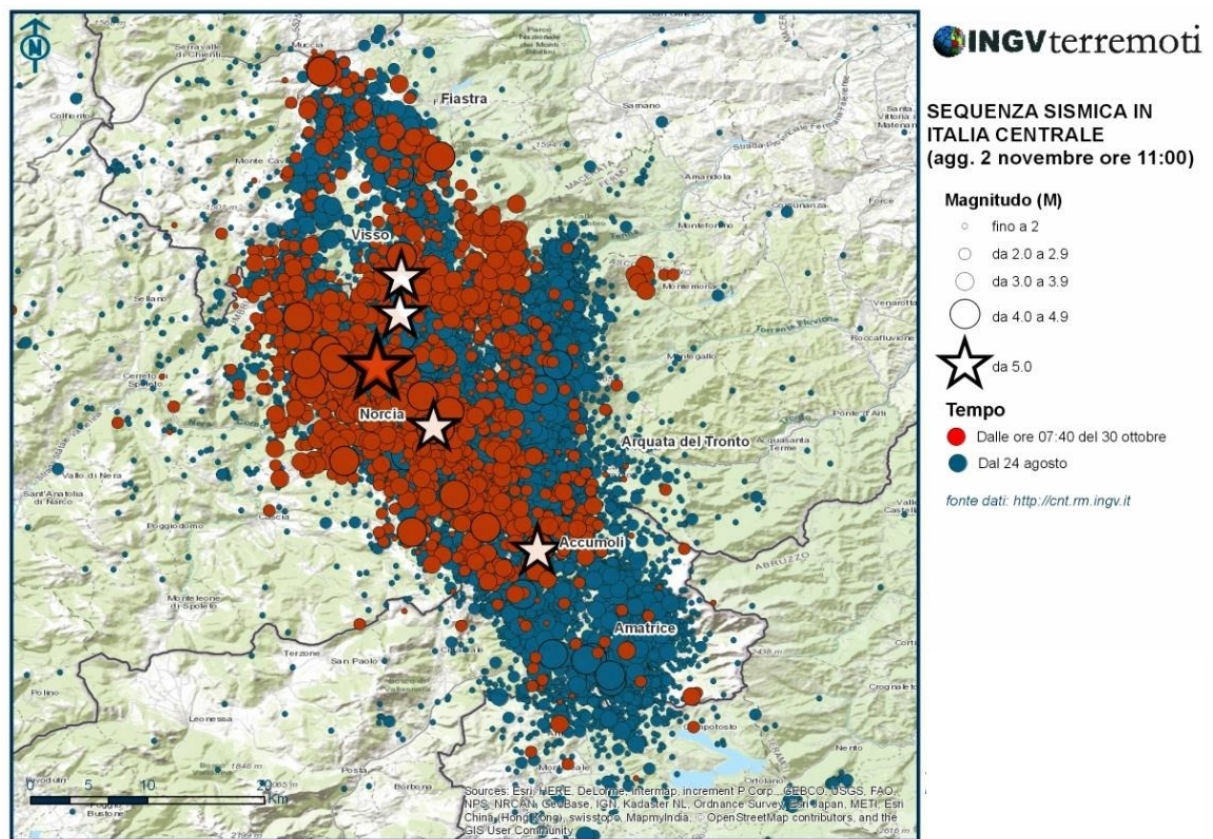


Figure 2.11 Seismic sequence after earthquake 30-10-2017

### 2.5.4 18-01-2017 Earthquake (hh.mm 10.14)

The last sequence taken into account in the study is that of 18 January 2017, almost a year from its inception, with four events between 5 and 5.5 in magnitude in the provinces of L'Aquila. The shock of the 10.14 was the strongest, but it did not cause strong damage.

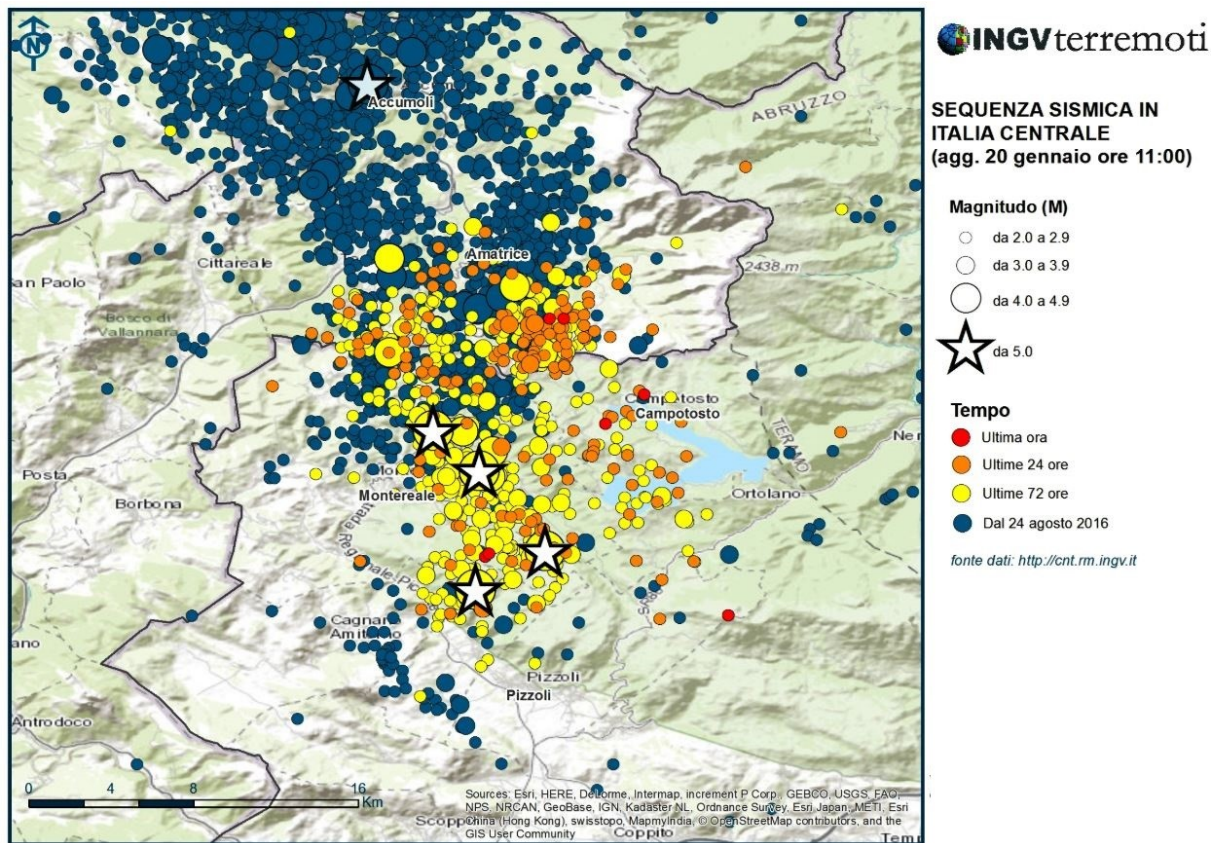


Figure 2.12 Seismic sequence afeter earhtquake 18-01-2017

## 2.6 Current situation

One year after the start of the sequence, more than 75,000 earthquakes were located in an extended area for 80 km from north to south, affecting four regions and several provinces. An interesting aspect to note is how the seismic sequences of 2016/2017 are part of a wider activity started in 1997, and then continue in 2009 and arrive to date. Each event concerned a precise geographic area. From here, the doubt of the geologists and seismologists to have in the near future another area interested by earthquakes. The following figure shows this representation, it's possible see a certain uniformity in the events from 1997 to 2017.



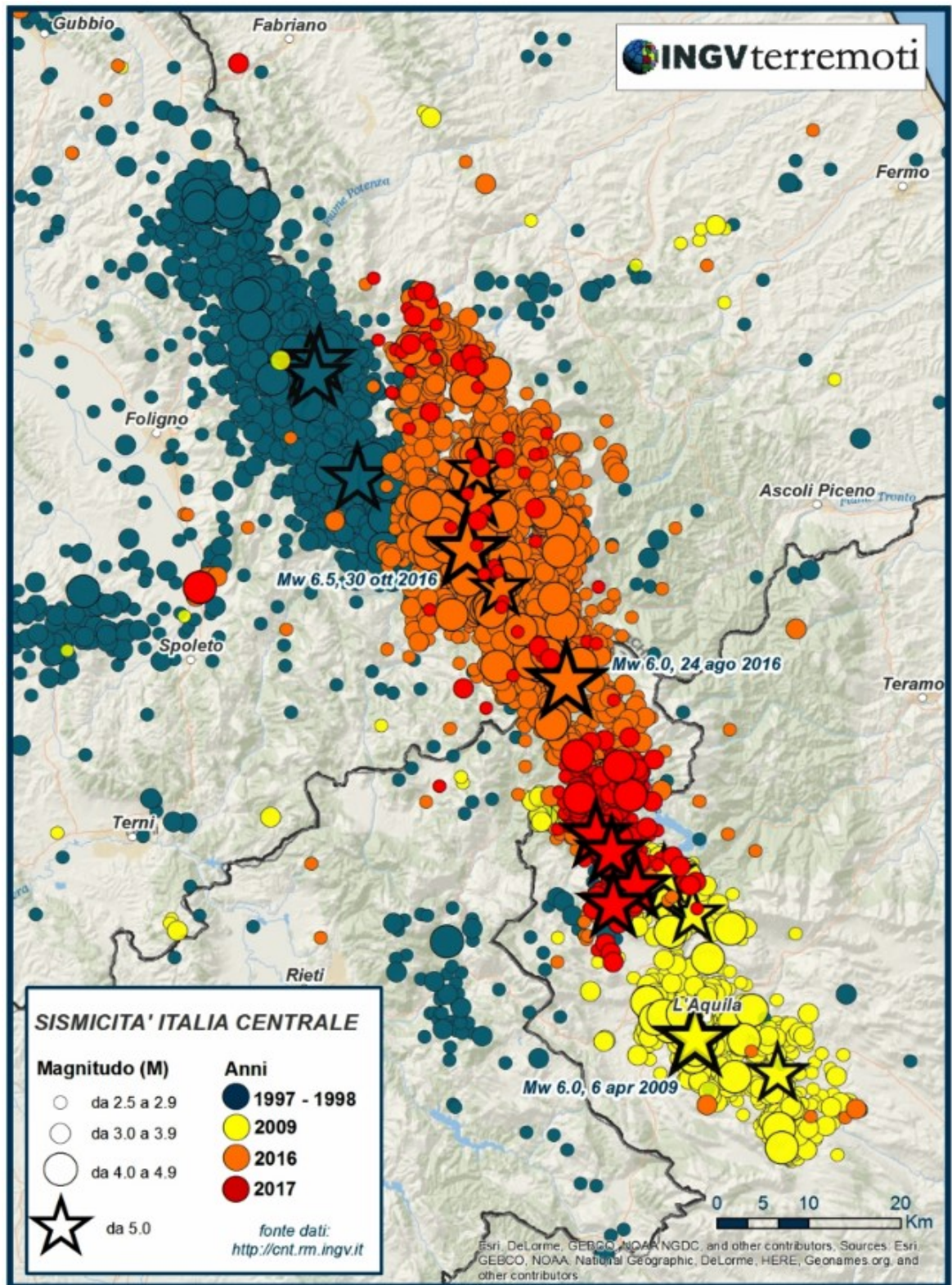


Figure 2.13 Distribution earthquakes from 1997 to 2017

# CAPThER III

## 3 MONITORING SYSTEM

The following chapter will introduce the Structural Health Monitoring (SHM), which belong to monitoring systems, explaining the fundamental components and the reasons that led to their use rather than the traditional methods.

### *3.1 Introduction*

Structural Health Monitoring (SHM) is the process of characterization of existing structures, its proposed is to identify some properties of the building, having information on the real structure and to be able to develop analytical models for the evaluation of the state of the structure or to evaluate changes in structural behaviour. In addition, the installation of a monitoring system permit to have a pre-alarm in order to intervene preventively suspending activities potentially dangerous for the structure (Civil and public sector) so as to identify in detail the vulnerabilities. Another aspect, but not less important, is the economic aspect associated on the reduction of maintenance costs, with targeted and really necessary controls. The great Italian heritage of historic buildings makes our country particularly vulnerable to the seismic events . The costs of securing the buildings are very large due to the unstoppable decay of the materials. In this perspective it is essential to have a permanent evaluation of our structures to guarantee an adequate level of safety. In addition to the visual methods of evaluation, that over the years have always been more consolidated by the experience, it was decided to combine to these, experimental procedures to have a clearer and more precise information about the performance of the structure studied. A monitoring system consists of a periodic detection by means of some basic parameters, from which statistical extraction and analysis it is possible to determine the current state of the system. The need to have an efficient and flexible but simple instrumentation in its installation, to be used in structural applications in civil suit, has encouraged a collaboration between Centre for Research of Civil Protection the University associated.

In fact, remember that the onerous cost of the "visual or traditional monitoring" is due to the use of highly qualified people who periodically inspects the building with a the temporary suspension of the structure's activities on the days of Control ( Double shopping). Talking instead of a permanent monitoring system eliminates completely these expenses, in fact once y faced the initial costs of the instrumentation, the system executes in real time and permanently all the measures required.

A monitoring system is generally divided into several annexed devices that are: a system of measurement, data acquisition, an alarm system, a modelling and identification system and a decision-making system

SHM systems pursue the same objectives that had traditional visual inspection. In this perspective there is a real integration. In fact, it's possible talking about an evolution of new technologies discovered to have a single intelligent system, overcoming the limits that often traditional practices had.

### *3.2 Architecture of the seismic monitoring system in Fabriano Structure*

The monitoring system consists on a network of accelerometer sensors distributed within the structure, which communicate in real time with one or more units of acquisition and interpretation of the data. The transmission can be done with a wireless connection or through a wiring of the sensors with the central acquisition device. The main components that make up the system are:

- **The Data Acquisition unit**

This device also known as the "Master " node consists of a real time controller and an input-output module for connecting the measuring points.

- **Accelerometer Sensors**

The accelerometers are attached to the cable acquisition units and measure the accelerations in real time, at the most in 3 directions.

- **Power supplies**

Next to each control unit there is a power supply box necessary for the electrical supply of the sensors. Each accelerometer has a single cable which provides for both the data and the electric charge.

- **Continuity Group**

In order to cope with sudden electrical interruptions, due also to the earthquake itself, a Continuity Group is foreseen that can guarantee the electrical supply to the system for a certain time.



*Figure 3.2 Acquisition system*



*Figure 3.1 Accelerometer and cable wiring*

### 3.3 Technologies of SHM

This is a multidisciplinary subject that concerns new structural monitoring techniques, modern measurement systems, modelling and non-destructive investigation techniques. The application of the SHM allows the implementation of interventions only when it is necessary in order to optimise the costs of structural maintenance. The analysis is fundamentally based on the development of global methodologies that are based on the analysis of the variations of the dynamic characteristics of the structure. This technique of investigation requires a dense network of measures distributed in the structure under examination, which are transferred to a central system to be then processed, as to understand the health conditions of the building. The techniques available are clearly distinguishable from (NDE not destructive evaluation), which are a method of field investigation and allow only local inspection due to their limited areas, not observing the global behaviour of the structure.

Regarding the methodologies used, is possible distinguish three methodologies that are referenced in three different technologies:

- experimental technologies,
- analytical technologies,
- technologies for the processing of the data

#### 3.3.1 Experimental technologies

Experimental technologies use techniques developed in the course of the last decades. These techniques allow the survey of structural response. They are based entirely on the use of experimental data of dynamic response of the system and the variability of the measurements compensated automatically from a statistical method. The techniques used can be static or dynamic depending on the acquisition of measures, on the basis of a destructive nature or not, and depending on the duration of monitoring. The table below shows the most important experimental technologies, classified according to the type of tests: static dynamic, hybrid.

Class	Name	Description
Static tests	<i>Not destructive</i>	These tests are carried out for a limited portion of the structure, by applying controlled load you can characterize materials
	<i>destructive</i>	In this category fall the laboratory tests designed to characterize samples collected in situ. These tests are often expensive and little generalizable, performing in the field of scientific research

<b>Dynamic tests</b>	<i>Not destructive</i>	These tests involves vibration analysis in order to extract the modal properties of the structure and its dynamic behaviour. The excitation of the input comes from the impact of a hammer or can be done impulsively by falling weight. It is possible even use the natural vibrations caused by wind or traffic.
	<i>permanent monitoring</i>	The measuring system is set on the structure. And acquire periodically different amount related to structure behaviour. In this way it is possible to study the data evolution in order to provide reliable warnings
<b>Hybrid tests</b>	<i>geometric monitoring</i>	These tests make use of tools such as: laser scanning, Photogrammetry and remote sensing, with the purpose of having a Visual framework of geometrical changes during the time.
	<i>not destructive</i>	These tests are used to detect hidden construction details, defects or damages, for physical-chemical characterization of materials. investigate a limited portion of the structure. There are a wide range of these tests.

Table 3.1 Main experimental technologies used in SHM

### 3.3.2 Analytical technologies

In view of a good prevention and an accurate diagnosis, analytical technologies play a key role. When it is necessary to do a diagnostic study of the building, the measured signals will be analysed and correlated. Instead when is required do dell forecast, will be taken into account the temporal evolution of the data. These technologies provide structural simulation tool, both in operating condition and in presence of damages. Nothing can be done without structural modelling, which can be geometric or numeric. However because of uncertainties concerning the characteristics of historic buildings, has been accompanied stochastic study of these

parameters, as boundary conditions, non-linear effects and mechanical properties of materials. However it is preferable to have a fitting model to reality, in which uncertainties are handled with a deterministic approach, considering a maximum range of variation of these parameters. To have a template as much as possible adhering to reality, knowledge of experimental data is of great help, because they give valuable information that will be useful for proper calibration of the model. The first step in analytic modelling turns out to be the computer-aided design CAD. Thanks to a 3D rendering you can define the macro elements that are part of the structure as a whole. The photogrammetric techniques in this stage play an important role, thanks to these it is possible to define precisely size and details the most significant. The photographic images obtained from the photogrammetric techniques can also be used to make important assessments, for example: using triangulation of strategic points is possible to calculate the displacements at the base during time.

The numerical modelling, depending on the purpose of study, may be more and less into detail, if is required high precision, the computational burden will be higher, so as to take more time.

There are three methods that can be implemented:

- finite element method (FEM)
- boundary element method (BEM)
- finite difference method (FDM)

FEM solution turns out to be the most suitable, also due to the presence of numerous software on the market, many of which are easy to use. Three-dimensional models are indispensable for studying on a building in the complex. The idealization of geometry, constraints, and the interaction between the structural elements are important choices that must be made before start the modelling, these wrong choices lead to significant errors at the time of calibration. A correct template provides a starting point for the control system, it is also a good indicator for comparison to the results obtained from the structural identification. This is also useful for evaluating the critical elements of the structure and evolution of possible damage.

The methods of analysis are divided into linear and non-linear. Masonry models are designed with linear regression analyses, which are slimmer. Linear analysis takes into account the constitutive materials non considering second order effects. Non-linear analysis especially in heterogeneous materials, such as masonry, makes it difficult to interpret the results and an error in the mechanical parameters can lead to very high errors.

### *3.3.3 technologies for the processing of the data*

In the design of a monitoring system, not only the correct position of the sensors and data acquisition, are the steps where need to be accurate and precise. In order to avoid systematic failures, it must be adopt an appropriate methodologies such as: a tidy archiving, an analysis and interpretation of data acquired. In the preliminary stages of the design of the monitoring system, are to define procedures for: the collection, classification and archiving of data. A key parameter affecting the technical implementation is the choice of the number of sensors an



the use of the number of channels. Some of the most common operations that are performed after data collection are:

- **formatting data**  
It makes a similar formatting to all acquired signals to facilitate their treatment
- **data classification**  
out-put data must be organized into a structure with a appropriate nomenclature to facilitate data collection and storage
- **prior checking,**  
is an initial check to verify the correctness of the signals, the formatting and their classification
- **data communication**  
devices communicate with the remote unit via wired lines or wireless systems. Hopefully in the near future to have a communication in real time to the control system
- **data storage,**  
It is important to have database management programs and data storage systems for signal processing become sequentially
- **data pre-processing,**  
are operations that prepare data before extraction of certain characteristics. may be the cleansing of the signal from the noise, the outlier removal, the waste of some of these
- **extraction of characteristics**  
in this phase, we proceed with the extraction of useful information to the purposes sought.
- **data interpretation**  
in this operation we proceed to diagnose the health of structure based on experimental data
- **presentation of results**  
Depending on the nature of the results and achievements, we proceed to the representation of the results using charts, summarizing the information obtained.
- **decision-making**  
is the final step where you decide based on the results whether to intervene or not, and what actions to take

# CHAPTER IV

## 4 CASE STUDY: COURT OF FBRIANO (EX "E. FERMI" SCHOOL)

### *4.1 Introduction*

The building belongs to the public patrimony for over 50 years, it falls into the category of buildings bound by law 1089 of 1939. The property in question has undergone a change of use in the last year, which will be explained later. That appertain to the artistic buildings in seismic areas and for this reason there are stringent constraints on method seismic improvement. The structure is located in the immediate vicinity of the historic centre of Fabriano (AN), at the intersection of streets of Porta Pisana.



*Figure 4.1 Building on 2017*



## 4.2 Territorial classification

The town of Fabriano is located 325 m s.l. m between hills in the Umbria-Marche Apennines. The municipality of Fabriano with its 57 fractions counts 31,075 inhabitants but the town itself has no more than 6,000 inhabitants. With its 27.2018 km<sup>2</sup>, it is the largest town of the Marche region. The city plays a primary role in the economy of the area, very important are its leading industries in the production of paper and appliances.

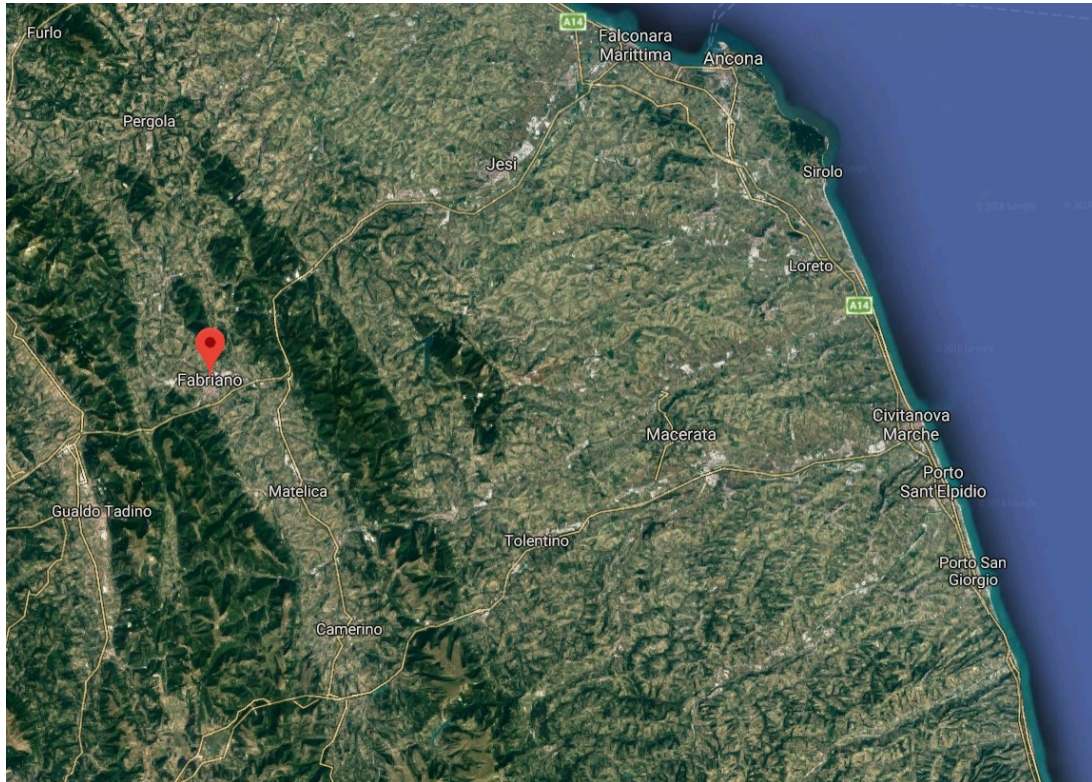


Figure 4.2 Fabriano location

The origins of this ancient Italian village date back to the iron age, and over time has undergone several influences of foreign populations. The cultural heritage of this community is huge, the houses in the historical centre, the Town Hall, churches, teathers, dating to the middle ages.



Figure 4.3 Town Hall of Fabriano

### 4.3 Description and History of the building

From the historical archives of the municipality, the ceremony of "cornerstone" was attended by Prince Umberto II on 28-06-1922. The area for the building of the Royal industrial school was expropriated to count Carlo Corbelli, and the construction of the building was entrusted to company "Crocetti Pacifico ". On this occasion, the City Council reorganized also the urban layout and the entire surrounding area.

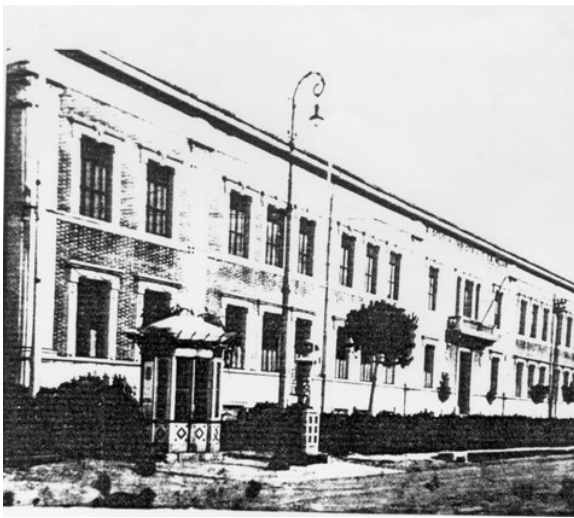


Figure 4.4 Building on 1939

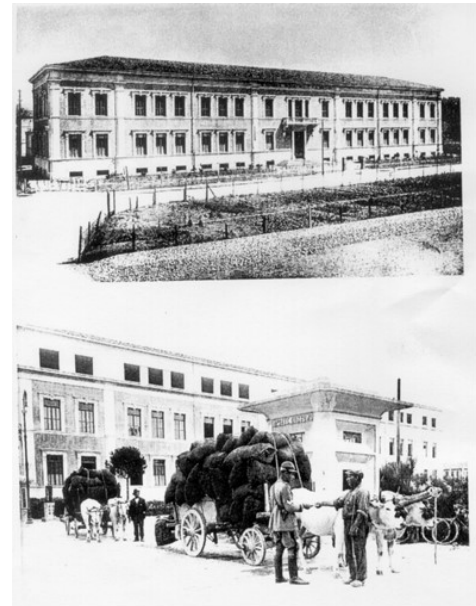


Figure 4.5 Building on 1940 (up) and on 1943 (down)

In 1941 the building was raised by one floor, arousing criticisms and controversies of the population about the architectural look. Important works were made at the beginning of the years 50, there were set up the body of toilets adjacent to the two outer wings. The raising of one floor was done with little care of prospectuses and finishes. The building also holds a very clear symbol: the willingness of the city of expansion along the direction of the road to Ancona, this area is still a key interchange node. The earthquake that struck central Italy in September 1997, severely damaged the school, making it unfit for use. In 1999 after the allocation of funds to the affected areas of the earthquake, the building has undergone a change of use from school building in legal-administrative. Today, however, there have been changes. Only the second floor is home to the administrative offices, while the ground floor is home to a kindergarten and the first floor is waiting for a target by the municipal administration.

#### 4.4 Dimensional characteristics

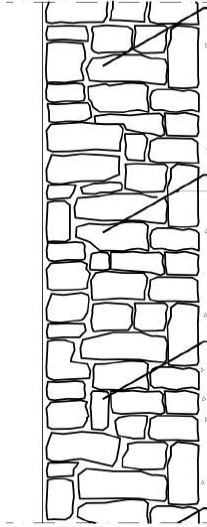
The property is developed over four levels, three above ground and one basement, the maximum eaves height is 16.8 , the diagram repeats itself identical on every floor, and his form refers to "T". It is possible to distinguish two bodies, one geared more elongated in a North-South direction and another more small linked to this on East.



Figure 4.6 Buildings' diagram type

#### 4.5 Vertical elements

The building is masonry. The walls are constituted in split stone, whose thickness grows to full height with good regularity. The thicknesses of wall vary from floor to floor: the first floor between 110 and 80 cm, and between 50 and 60 cm remaining ones. The different types of walls can be divided into three categories. The following table summarizes these types:

Type	Representation	Description
<b>MUR1</b>		<p><b>Original structure</b>  <i>This is the most common type of walls in the building. Is filled with rocks split with good texture, and also from solid brick, as seen by some polls. The thickness of these walls varies between 110 and 50 cm.</i></p> <p><b>After consolidation of 1999</b>  <i>Were executed consolidation: plaster reinforced with welded mesh <math>\phi</math> 6 and mesh 10 x 10, armed with mortar injections and reinforced bolting bar <math>\phi</math> 16</i></p>

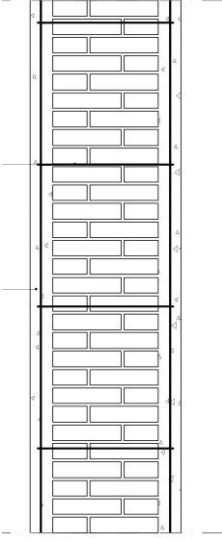
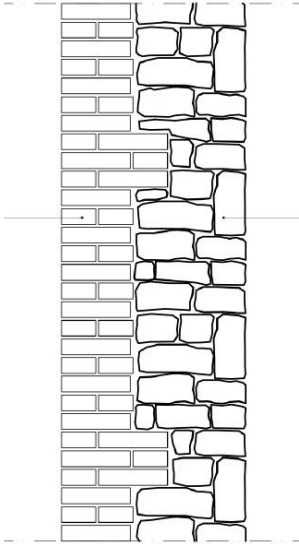
MUR2		<p><b>Original structure</b>  <i>This type of wall is made of bricks. that category has spread on the top floor and in some interior walls of the lower floors. The thickness varies between 35 and 45 cm.</i></p> <p><b>After consolidation of 1999</b>  <i>were executed consolidation: plaster reinforced with welded mesh <math>\phi</math> 8 and mesh 10 x 10, armed with mortar injections and reinforced bolting bar <math>\phi</math>16</i></p>
MUR3		<p><b>Original structure</b>  <i>This type of walls are the walls of the ground floor and the first floor. As for type MUR_1 split stones are characterized by the presence of a brickwork variable. the total thickness of the walls varies between 75 and 45 cm.</i></p> <p><b>After consolidation of 1999</b>  <i>were executed consolidation: plaster reinforced with welded mesh <math>\phi</math> 6 and mesh 10 x 10, armed with mortar injections and reinforced bolting bar <math>\phi</math> 16</i></p>

Table 4.1 Type of masonry



#### 4.5.1 Tests to define the mechanical parameters

Tests conducted for the characterization of mechanical properties of materials is provided below:

- **DOUBLER PLATES JACKS**

The test was carried out in a section of the basement. Were recorded the following stress:

- $\sigma = 0,43 \text{ N/mm}^2$  operating stress of the wall before cutting
- $\sigma = 0,33 \text{ N/mm}^2$  loss of linearity on stress-strain diagram
- $\sigma = 0,82 \text{ N/mm}^2$  stress limit value corresponding to the cracking of mortar



Figure 4.7 Preparing test

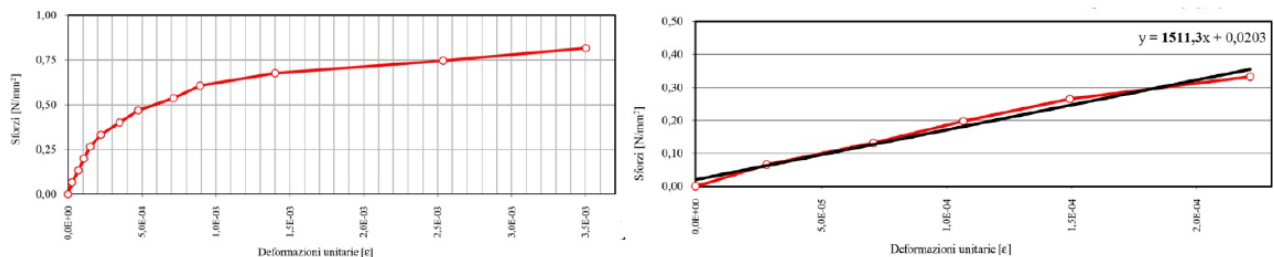


Table 4.2 Test results

- **PENETROMETRO FOR MALTA**

This test is performed on 8 zone, going to relate the energy that comes from the realization of a blind hole with the compressive strength of the material.

Call sign	compressive strength [N/mm <sup>2</sup> ] $f_m$
PE1	0,51
PE2	0,35
PE3	0,48
PE4	0,42
PE5	0,41
PE6	0,38
PE7	0,57
PE8	0,61

Table 4.3 Results on 8 areas considered

- SAMPLING OF MANSORY**

Eight samples were taken for compression tests and punching of mortar in the laboratory

Call sign	compressive strength of specimen of mortar $f_m$	compressive strength of the element $f_{bk}$
PM1	-	104,8
PM2	-	91,0
PM3	-	100,4
PM4	-	40,2
PM5	-	106,8
PM6	-	90,6
PM7	2,24	9,5
PM8	2,26	87,3

Table 4.4 Results on 8 areas considered

PM7 element refers to brick material and everyone else are blocks of natural stone. Most samples do not eligible to try punching of the mortar, so is not possible calculated the compression resistance, and also not within the rage of the legislation. For these reasons it wasn't can estimate the compressive resistance of mortar.

- THERMOGRAPHY ON MASONRY**

This test is run in 8 areas, and aims to ensure consistency and homogeneity of the masonry. the test was conducted with indirect methods.

Call sign	Average Speed [m/s]
TS1	1031
TR2	956
TS3	948
TS4	1020
TS5	1003
TS6	1050
TS7	972
TS8	1082

Table 4.5 Result of Thermografy

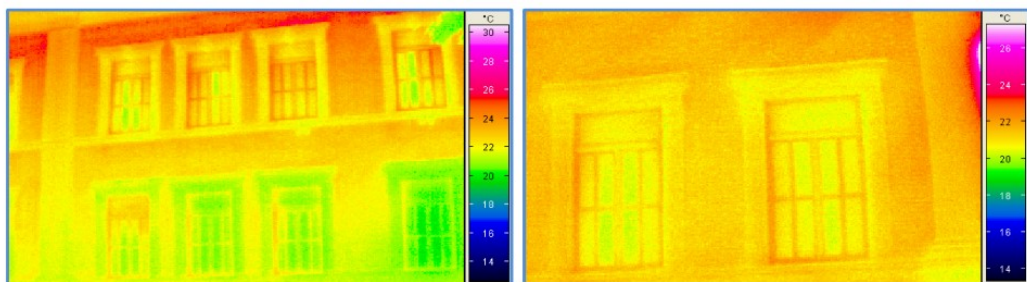
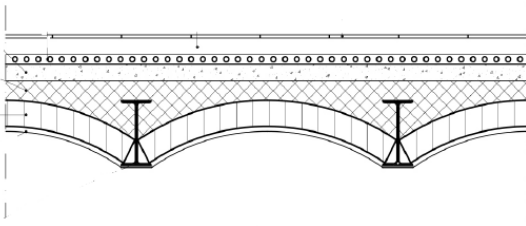
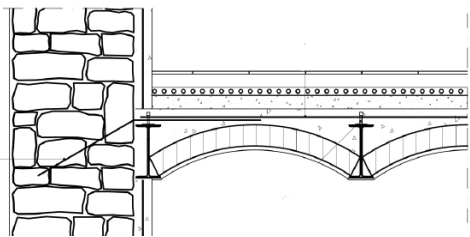


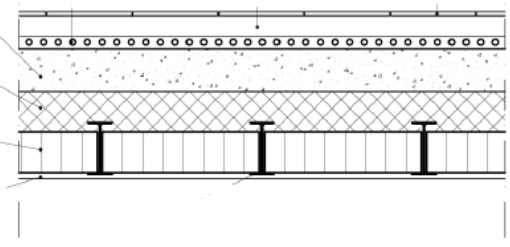
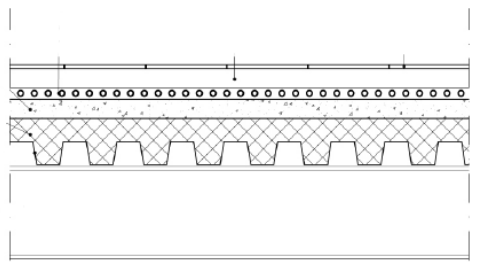
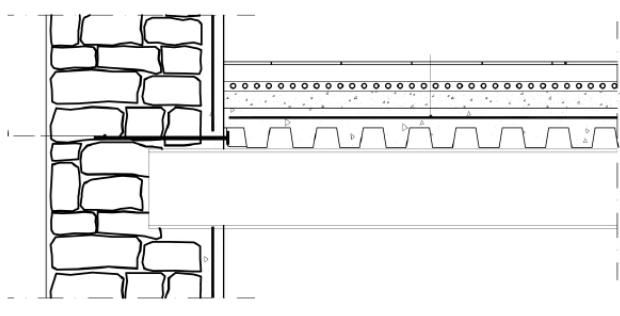
Figure 4.8 Termografy Southwest side


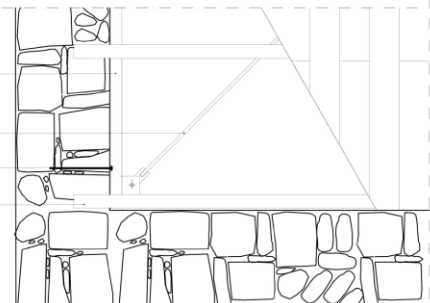


## 4.6 Horizontal elements

The building has different types of horizontal closures because of the different construction epochs. The types that will be identified refer to the investigations carried out by the SGM company during the improvement of the 1999. It is specified that the company found inconsistencies from the analysis of the documents that were available to them. It was decided to divide into five categories as the table follows:

Type	Representation	Description
<b>SOL0</b>	—	<p><b>Original structure</b>  <i>The investigation by radar shows the presence of an armed slab with probable implants inside. More precise considerations are complicated to do.</i></p> <p><b>After consolidation of 1999</b>  <i>From the material available there is no intervention</i></p>
<b>SOL1</b>		<p><b>Original structure</b>  <i>The floor is made of steel beams, with wheelbase of 80 cm. Above is an armed slab of 6 cm and a screed where the floor is placed, the thickness of which is uncertain. Due to the presence of the floor heating the surveys have not identified the thickness of the slab.</i></p>
		<p><b>After consolidation of 1999</b>  <i>With the consolidation intervention were arranged the connectors welded on the steel profiles, was distributed a welded net and was filled with a concrete Rck25 for a thickness of 6 cm. To ensure a good connection to the masonry, <math>\phi 16</math> irons have been inserted throughout the perimeter.</i></p>

<b>SOL2</b>		<p><b>Original structure</b>  <i>It is a steel-brick slab with a profile wheelbase of 35/40 cm. The thickness of the brick cone is 10 cm while the section of the steel joist is IPE 120. There is also a probable presence of floor heating.</i></p> <p><b>After consolidation of 1999</b>  <i>There is no information available in the cut-out regarding this typology. It is possible to hypothesize that the same techniques of SOL_1 have been used.</i></p>
<b>SOL3</b>		<p><b>Original structure</b>  <i>we do not have information about the type of the slab originally before the consolidation</i></p>
		<p><b>After consolidation of 1999</b>  <i>The floor consists of steel profiles of type IPE with wheelbase 84 cm with corrugated sheet. Above it is a jet of concret with a 6 cm thick electro-welded mesh. Two different dimensions of the IPE were used, depending on the distances to be covered more precisely: IPE 160 and IPE 240. The connection to the masonry was improved with a chemical anchorage</i></p>

<b>SOL4</b>		<b>Original structure</b> It is consisted of profiles Y with wheelbase of 145 cm and wood panel of 3.5 cm. The size of the steel profiles varies from 9 to 16 cm depending on the lights to be covered.
		<b>After consolidation of 1999</b> The interventions concerned the replacement of the flooring, the construction of braces of steel top and a connection with chemical anchorage to the masonry

The layout of the types of walls and slab for each floor is as follows:

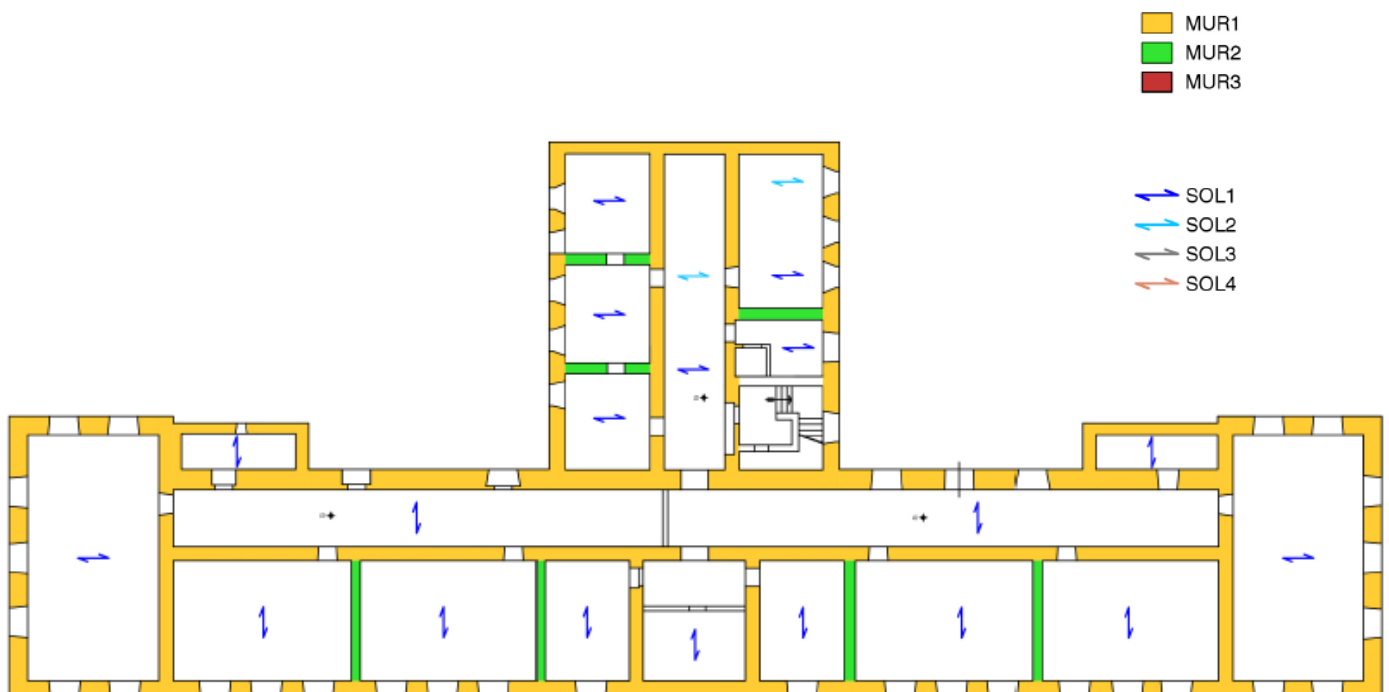


Figure 4.9 Features typological basement floor

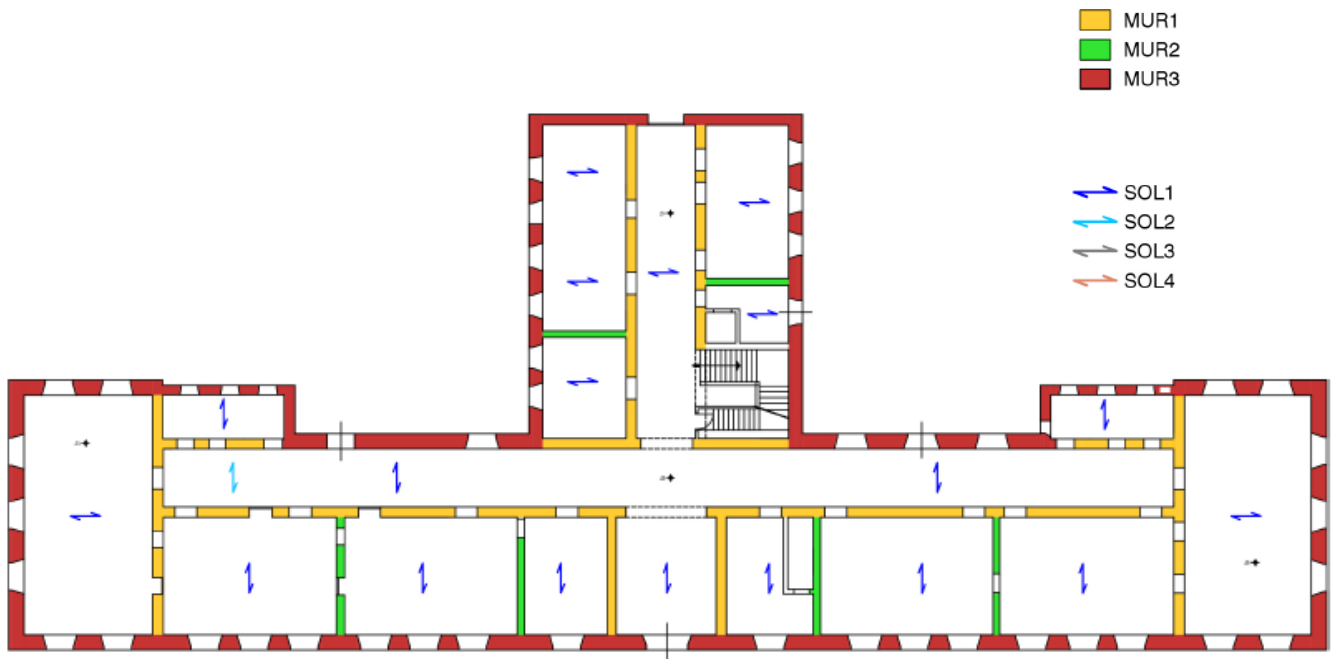


Figure 4.10 Features typological ground floor



Figure 4.11 Features typological first floor

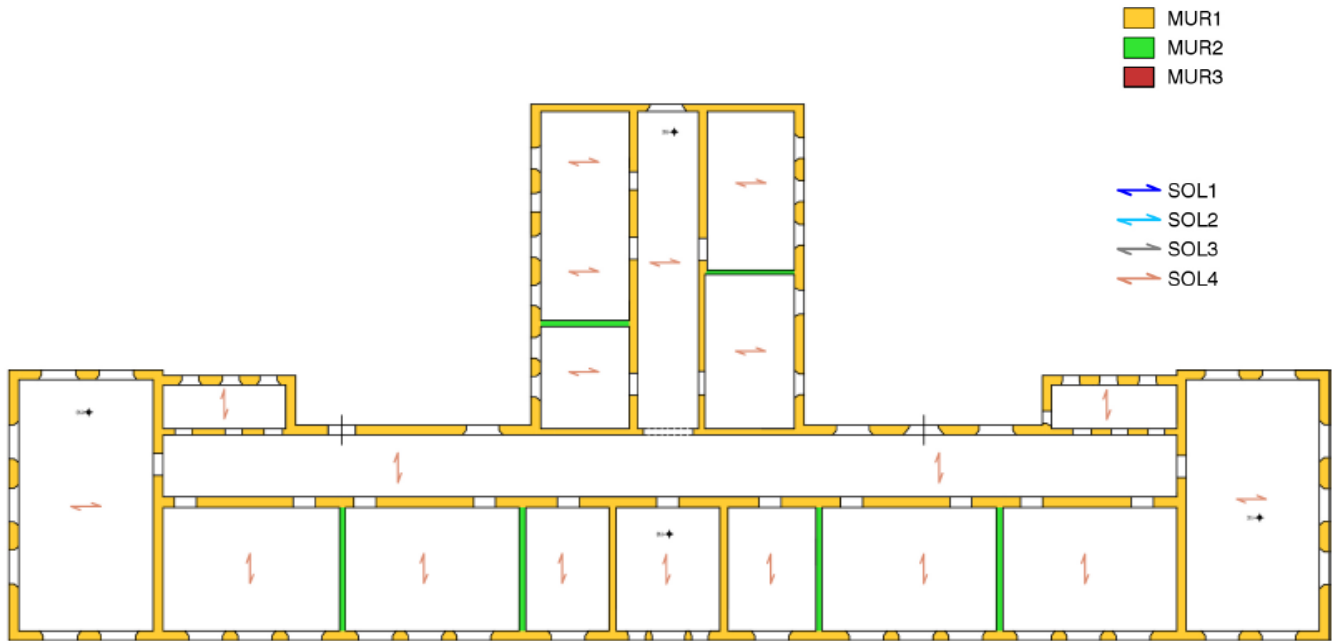


Figure 4.12 Features typological second floor

## 4.7 Roof

The roof is made up of wooden trusses, so as to have a light and non-pushing cover. The trusses support a warping of joists on which the wooden plank and the tiles are resting. In the north-south oriented body the two pitch have the top at different altitude as a result the trusses are divided. On the transverse body the trusses are raised chain. However a real stratigraphy of the roof isn't available, the maps share reports only the position of the trusses.



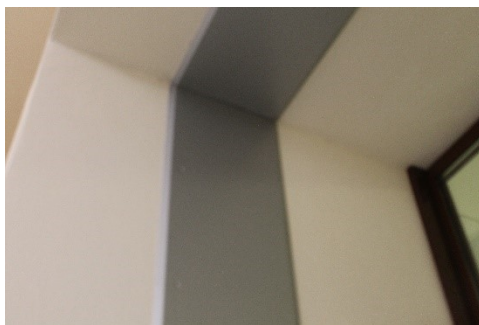
Figure 4.13 typology roof

#### 4.8 *External body joined to the structure*

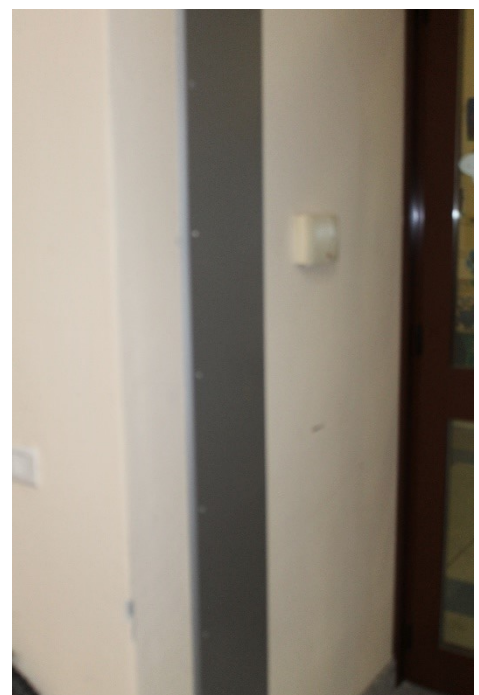
As is shown from the plants, in the West right side, recently was built a scale body, this structure of concrete and steel is spliced to the structure for all its height. This body was built for the autonomous access of the second floor of the structure, which is predispose for the offices of the Court. The staircase being joined does not constitute an increase in weight but in the points where it is connected to the structure turns out to be a strong constrain. In the next chapter will be developed to take this stiffness into account.



*Figure 4.16 External body stair*



*Figure 4.15 Steel joint in the corner*



*Figure 4.14 Steel joint in high*

## 4.9 Foundations

The investigations that have been made, including that video endoscopic have shown that the foundations are formed by the continuation of the masonry blocks, at least equal to 1.90 m from the trampling quote of the basement. From the information available there are no consolidation interventions to the foundations. Also through surveys done in 1999, it was possible to characterize the soil. Thanks to the MASW method, calculating the speed of the cutting waves  $V_s = 472 \text{ m/s}$ , the soil the land has been classified belonging to category B.

Ground type	Description of stratigraphic profile	Parameters		
		$v_{s,30}$ (m/s)	$N_{SPT}$ (blows/30cm)	$S_u$ (kPa)
A	Rock or other rock-like geological formation, including at most 5 m of weaker material at the surface.	> 800	—	—
B	Deposits of very dense sand, gravel, or very stiff clay, at least several tens of metres in thickness, characterised by a gradual increase of mechanical properties with depth.	360 – 800	> 50	> 250
C	Deep deposits of dense or medium-dense sand, gravel or stiff clay with thickness from several tens to many hundreds of metres.	180 – 360	15 – 50	70 – 250
D	Deposits of loose-to-medium cohesionless soil (with or without some soft cohesive layers), or of predominantly soft-to-firm cohesive soil.	< 180	< 15	< 70
E	A soil profile consisting of a surface alluvium layer with $v_s$ values of type C or D and thickness varying between about 5 m and 20 m, underlain by stiffer material with $v_s > 800 \text{ m/s}$ .			
$S_1$	Deposits consisting, or containing a layer at least 10 m thick, of soft clays/silts with a high plasticity index ( $PI > 40$ ) and high water content	< 100 (indicative)	—	10 – 20
$S_2$	Deposits of liquefiable soils, of sensitive clays, or any other soil profile not included in types A – E or $S_1$			

Table 4.6 Soil categories NTC08

## 4.10 Active monitoring system in the structure

The monitoring system consists of accelerometers. The number of devices installed is 16 elements. Twelve of these have a double channel (X, Y), another 3 are single channels (X). Finally there is one tri-channel ground attack. A data acquisition unit is installed in the basement. The accelerometers are powered by cables for power supply and for data transfer, these cables pass from floor to floor through special passages. On each floor of the building are installed five sensors, except for the basement that also has the earth sensor. The arrangement of the sensors is shown in the following figures.



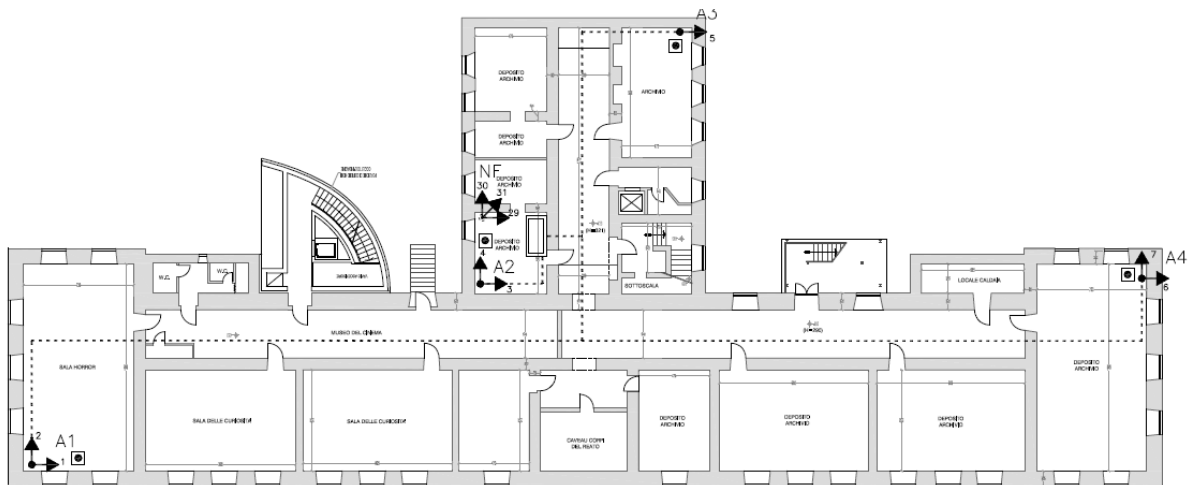


Figure 4.17 Arrangement of Accelerometers floor basement

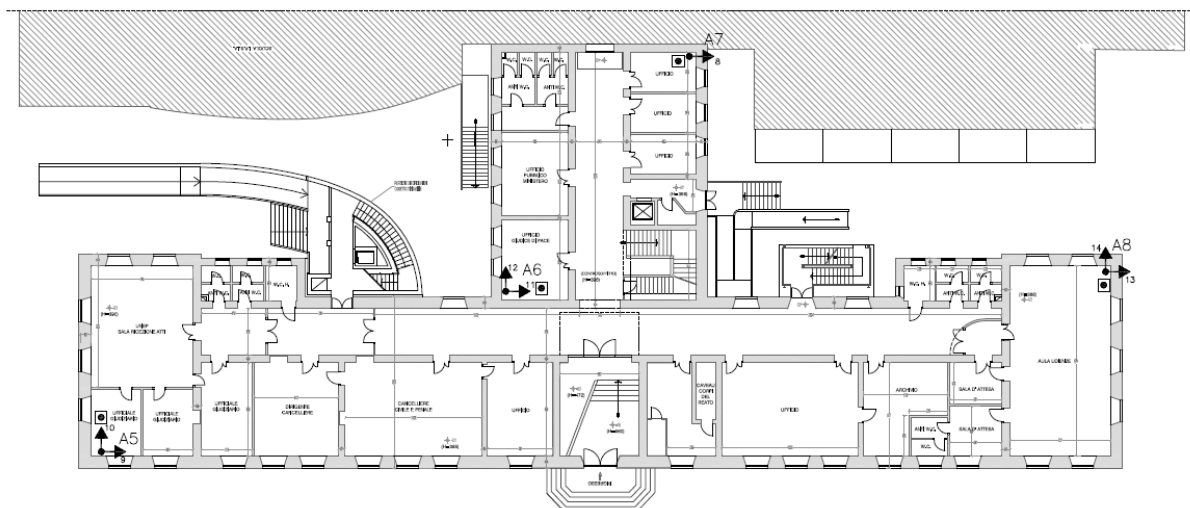


Figure 4.18 Arrangement of Accelerometers ground floor

[illegible]

36

# CHAPTER V

## 5 GEOMETRIC MODELING 3D (*RHINO*) AND FEM ANALYSIS (*ANSYS*)

Once the phase of the study of the characteristics of the structure is completed, the next step will be to build a FEM model to reproduce its geometry in a adherent way. The design of the model was entrusted to the 3D graphics and visualization program: *RHINOCEROS*. In this first preliminary phase, by means of the maps at disposal, was made a division of the elements constituting the structure according to: material and floor of walls, and their thickness.

### 5.1 *Nomenclature and model on RHINO Model*

For the design of the structure with the Rhino program, in the first place has been done a list of all the components of walls that constitute the structure. The division adopted, element by element is based on its location of floor, depending on the material and the thickness. The following tables carry all the elements created. The column "**n. Rhino**" lists the element created with the 3D program, the element with the same colour have the same material characteristic (as seen from name too M1 or M2 or M3). The column immediately next called "**n. Ansys**" is the number of the respective element given by Ansys. This number is important because Ansys only makes faith in its numerical listing. The nomenclature for the walls of the basement was simplified because in this plan the walls are all of the same material, so it was granted only a letter of recognition "S" (Seminterrato) associated with an identification number. The following table, more than the main elements created, refers even the horizontal elements such as "SOLAIO" divided according to existing type, and sloping elements like internal stair. Elements like "TRAMEZZI" refer to the walls that make up the internal body stair, and "TETTO" that are those that hold up the roof. Is important to remember that all the elements created in Rhino are plane, it has worked with surfaces.

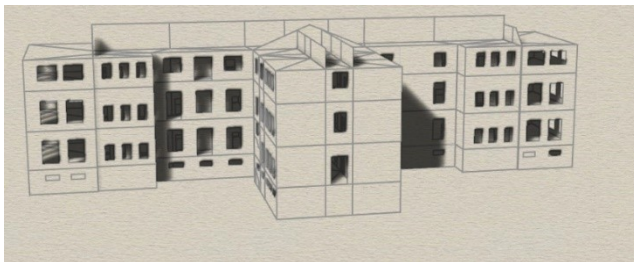


Figure 5.1 Representation body sud -est RHINO

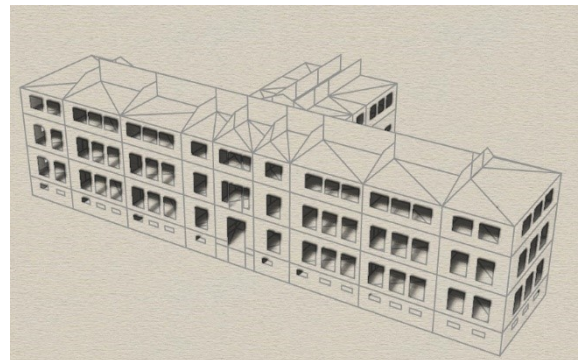


Figure 5.2 Representation body nord-vest RHINO

UNDERGROUND FLOOR				GROUND FLOOR	
n. ANSYS	n.RHINO	n. ANSYS	n.RHINO	n. ANSYS	n.RHINO
1	S1	16	S16	32	M1_pr_52.5cm
2	S2	17	S17	33	M1_pr_60cm
3	S3	18	S18	34	M1_pr_62cm
4	S4	19	S19	35	M1_pr_64cm
5	S5	20	S20	36	M2_pr_36.5cm
6	S6	21	S21	37	M2_pr_38cm
7	S7	22	S22	38	M2_pr_40.5cm
8	S8	23	S23	39	M2_pr_42cm
9	S9	24	S24	40	M2_pr_44cm
10	S10	25	S25	41	M2_pr_47cm
11	S11	26	S26	42	M3_pr_57.5cm
12	S12	27	S27	43	M3_pr_59cm
13	S13	28	S28	44	M3_pr_62.5cm
14	S14	29	S29	45	M3_pr_62cm
15	S15	30	S30	46	M3_pr_80cm
		31	SOLAIO_1	47	M3_pr_90cm

Table 5.1 Classification adopted

FIRST FLOOR		SECOND FLOOR		SPECIAL PIECES	
n. ANSYS	n.RHINO	n. ANSYS	n.RHINO	n. ANSYS	n.RHINO
48	M1_p1_38cm	70	M1_p2_38cm	95	M3_p1_65cm_V
49	M1_p1_40cm	71	M1_p2_57cm	96	M3_p1_65cm_O
50	M1_p1_44cm	72	M1_p2_40cm	97	M3_p1_65cm_V1
51	M1_p1_51cm	73	M1_p2_59cm	98	M3_p1_65cm_V2
52	M1_p1_55cm	74	M1_p2_48cm	99	M1_p1_60cm_V
53	M1_p1_60cm	75	M1_p2_58cm	100	M1_p1_60cm_V1
54	M2_p1_30.5cm	76	M1_p2_60cm	101	M1_p1_55cm_V
55	M2_p1_35cm	77	M1_p2_57,5cm	102	M3_pr_90cm_V
56	M2_p1_36.5cm	78	M1_p2_42cm	103	M3_pr_90cm_V1
57	M2_p1_38.5cm	79	M1_p2_50cm	104	M3_pr_90cm_O
58	M2_p1_41cm	80	M1_p2_56cm	105	M3_pr_90cm_O1
59	M2_p1_44cm	81	M1_p2_53cm	106	M1_pr_60cm_O1
60	M3_p1_50cm	82	M2_p2_38cm	107	M1_pr_60cm_O
61	M3_p1_52cm	83	M2_p2_35cm	108	M3_pr_80cm_V
62	M3_p1_53cm	84	M2_p2_24,5cm	109	M1_pr_60cm_V
63	M3_p1_57.5cm	85	M2_p2_36,5cm	110	M1_pr_60cm_V1
64	M3_p1_64cm	86	M2_p2_40cm	111	M1_p2_57cm_V2
65	M3_p1_65cm	87	SOLAIO_4_90	112	M1_pr_64cm_V
66	M3_p1_66cm	88	SOLAIO_4_160	113	TRAMEZZI_56,5cm
67	M3_p1_78,4cm	89	M1_p2_57cm_V	114	TRAMEZZI_38cm
68	SOLAIO_3_160	90	M1_p2_57cm_O	115	SCALE
69	SOLAIO_4_240	91	M1_p2_38cm_V	116	TETTO_38
		92	M1_p2_57cm_V1	117	TETTO_60
		93	M1_p2_50cm_V	118	TETTO_50
		94	M1_p2_56cm_V	119	TETTO_35

Table 5.2 Classification adopted

## 5.2 Modeling with Ansys

At this point did the geometrical model, the various elements were saved in .iges format and hence have been recalled in the finite element software Ansys. It is important to know, as already mentioned before for all assignments the features of the different elements, it must refer to the numerical order given from Ansys (Table 5.1,5.2 n. Ansys). So far, is been defined the model in its "graphical view", the modelling phase continue with:

- definition of **Material**
- definition of **Section**
- definition of **Constraint and Mass**
- definition of type of **Analysis**

### 5.2.1 Definition of Material

The materials used in the model are three: the concrete for the floors and stairs, wood for the ceiling of the top floor, and the brickwork. For the latter category is a further subdivision into three types as has been reported in Vertical .

- **Masonry**

The values shown in the table were taken from the report of civil protection. the investigations have led to the characterization of MUR1 and MUR2, however for type MUR3, as stated by the report, it has not been possible to classify. For MUR3 it was thought to hypothesize the mechanical characteristics, choosing intermediate parameters. it wasn't given any information about the Poisson's ratio, and was considered equal to  $\nu = 0,2$  for all type.

Type	$f_m$ [N/cm <sup>2</sup> ]	E [N/mm <sup>2</sup> ]	$\tau_0$ [N/cm <sup>2</sup> ]	G [N/mm <sup>2</sup> ]	w [KN/m <sup>3</sup> ]	Density[kg/m3]
MUR1	320	1500	6,5	580	21	2142,9
MUR2	320	1500	7,6	500	18	1836,7
MUR3	320	1800	6	500	19	1938,8

Figure 5.3 Mechanic characteristic of masonry



- **Concreet**

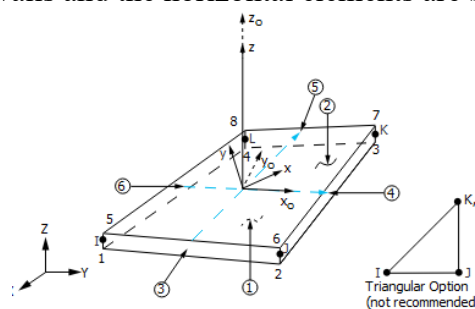
For the reinforced concrete elements, was calculated the density of each slab, going to view the Autocad drawing for their thickness. The SOL4 is wooden slab. Note that for both the type SOL3 and SOL4, for the same category, we used two different profiles depending on the light cover. The values of the elastic module were hypothesized, about it there was not information.

	TYPOLOGY	Thickness [m]	Density [KN/m2]	Density [Kg/m3]	E [N/mm <sup>2</sup> ]
<b>SLAB</b>	1	0,315	2,31	747,7	3,00E+10
	2	0,300	2,10	600,5	3,00E+10
	3_IPE_160	0,295	1,82	630,6	3,00E+10
	3_IPE_240	0,375	2,00	544,2	3,00E+10
	4_90	0,125	0,36	291,4	3,00E+08
	4_160	0,195	0,42	219,8	3,00E+08
<b>STAIR</b>	-	0,255	0,81	323,3	3,00E+10

Table 5.3 Slab and stair characteristic

### 5.2.2 Definition of Section and SHELL element

The building counts 119 sections, coming from the subdivision made before, and all elements belong to the same shell element selected. To these sections must be set the thickness and the material of belonging, This operation was done in Ansy, considering the numerical correspondence of each element. The choice of the shell element is critical to the behaviour of the structure. The structural components, are elements where one size, thickness, is much lower than others that define its geometry. These items ,can't be assimilate to beam (1-Dim), where the length is predominant on the size of the section and neither to solid elements, due to the heaviness of FEM model. The masonry elements have been assimilated to plates endowed of a certain orientation, this assimilation can be done by virtue of two hypotheses: infinitesimal deformations of the element with respect to its transverse dimensions and presence of membrane actions. The walls and the horizontal elements are SHELL181 elements of ANSYS.

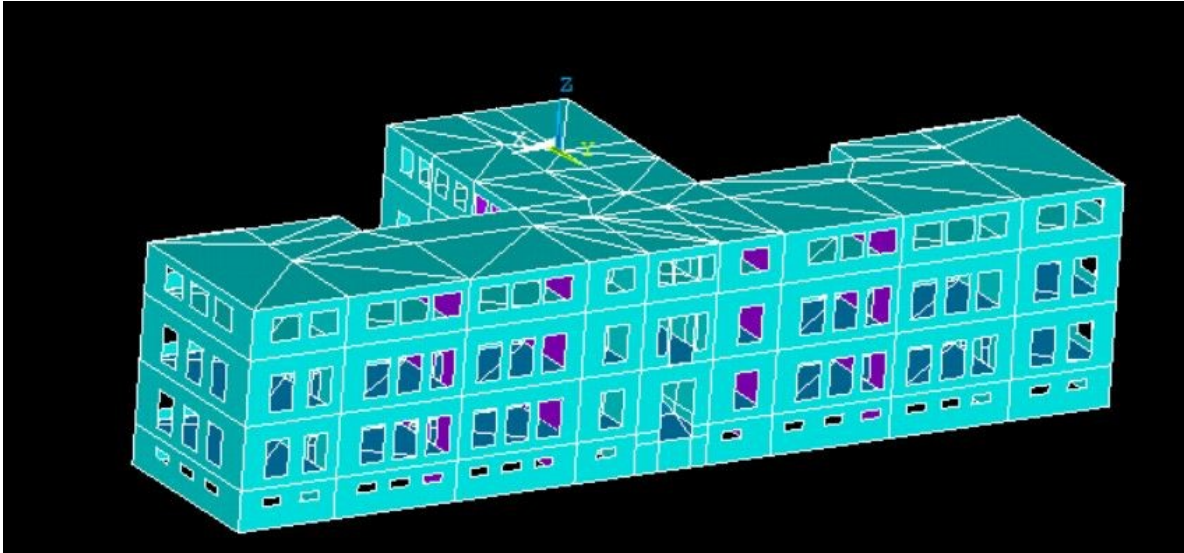


$x_0$  = Element x-axis if ESYS is not provided.

$x$  = Element x-axis if ESYS is provided.

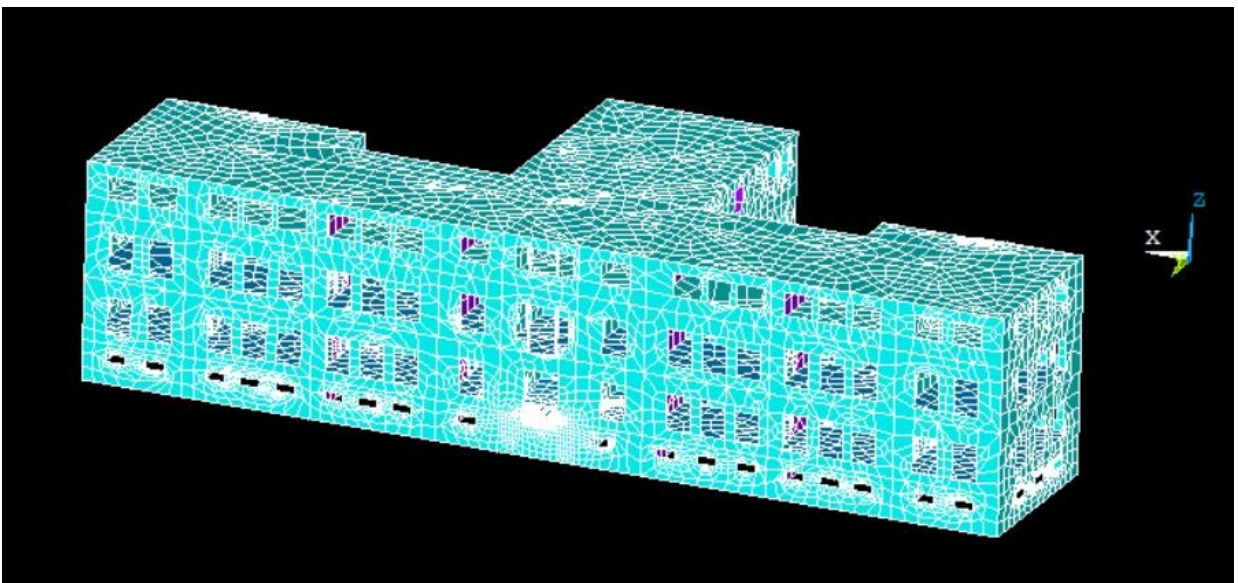
Figure 5.4 Element shell 181

Ansys recalls the saved items in the. *iges* format, one by one until the entire structure is composed as a whole.



*Figure 5.5 ANSYS representation*

Once you have imported the model into Ansys and assigned all the section and material characteristics, it will be meshed, the size of the mesh is a parameter to set. More dense is the mesh and the more calculations will be onerous, but not always will accurate. It been chosen a mesh of 0.6 in the Ansys settings , later will see how to a thickening of mesh would change the results of analysis



*Figure 5.6 Meshed Structure*

### 5.2.3 Definition of Constraint and Mass

The constraints play a key role in the structural behaviour under seismic excitation. Their determination is not often intuitive and requires experience and characterization tests. The constraints characterize in the model are: ground at the base, the perimeter ground and the external stair of the body.

#### - Constraints at the base

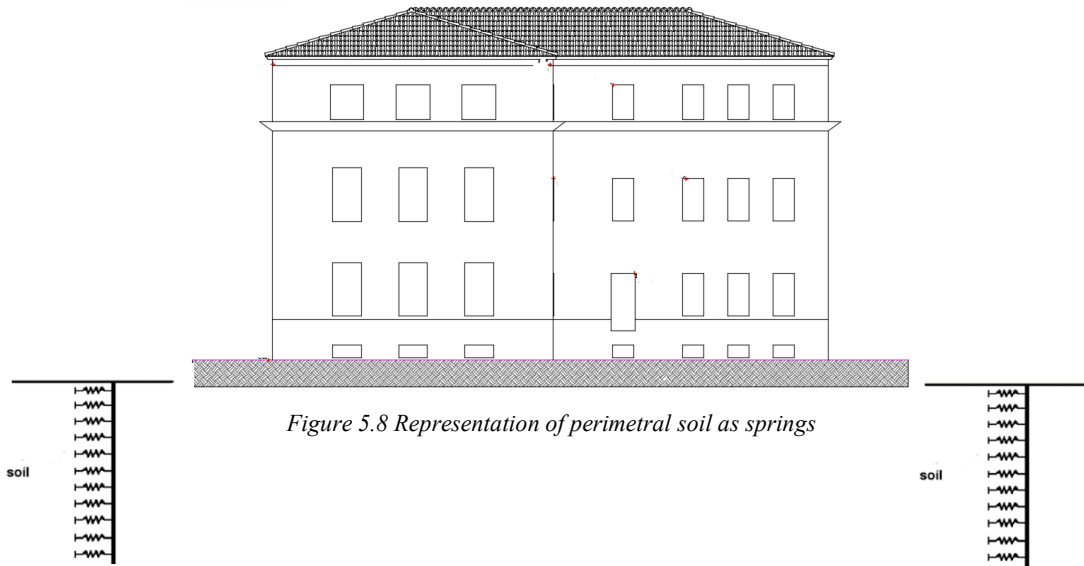
The type of foundation that owns the building is made up of the extension of the walls that go in depth. For this reason it was thought to assume a rigid constraint at the base quote by going to block the three translations and rotations.

#### - Perimeter Terrain

The soil thanks to the surveys carried out in 1999 was catalogued as B. Belong to category B semi-rigid terrain. However, the perimeter ground is not a rigid constraint, and so it is characterized by reagent springs in longitudinal direction. The stiffness of the springs has been hypothesized with an imposed value, but then it will be a parameter to calibrate.

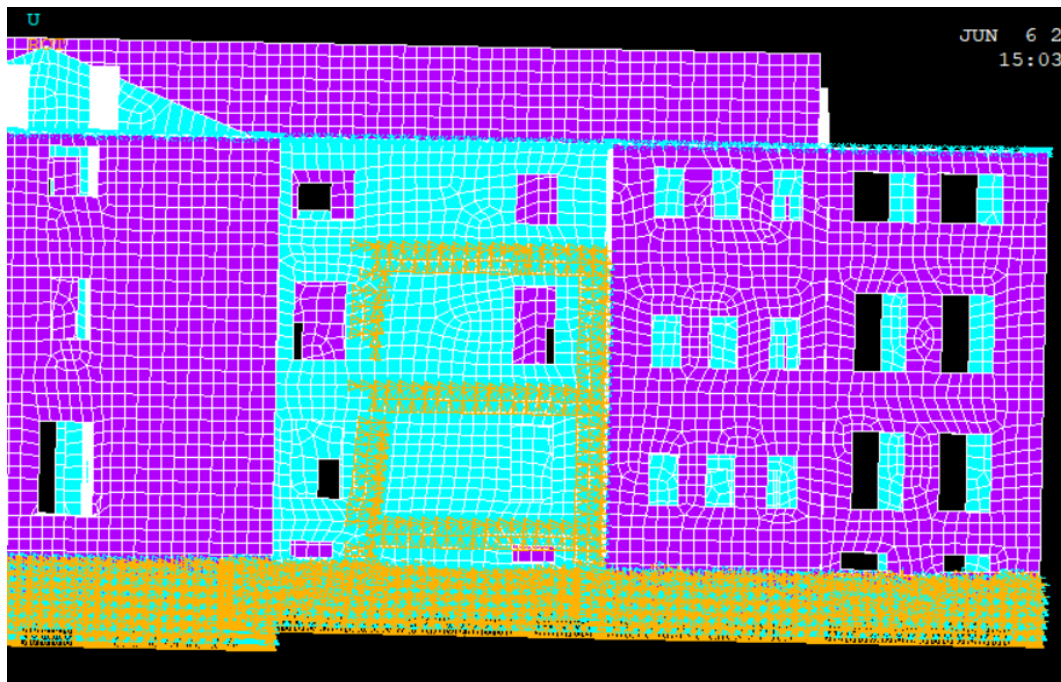
Terreno	E (Kg/cm <sup>2</sup> )	
	valore massimo	valore minimo
Argilla molto molle	153	20.4
Argilla molle	255	51
Argilla media	510	153
Argilla dura	1020	510
Argilla sabbiosa	2550	255
Loess	612	153
Sabbia limosa	204	51
Sabbia sciolta	255	102
Sabbia compatta	816	510
Argilloscisto	51000	1530
Limo	204	20.4
Sabbia e ghiaia sciolta	1530	510
Sabbia e ghiaia compatte	2040	1020

Table 5.4 Indicative values of the modulus of elasticity of some soil



### -Outdoor Staircase

The external staircase must be shaped. In this case, it has taken the nodes along the attack with the structure along all its height, creating spring which react longitudinally. Because of the great geometry of the scale it was thought that this is a considerable stiff constraint, and is used a very high stiffness value of the springs at first. However, this will also be a parameter to be calibrated



## -Mass

For the masses of the walls and floors, Ansys takes into account automatically, going to set the density of the materials used. For loads in serviceability, were taken into account by going to increase the density of the slabs in the calibration phase. The roof which represents a not indifferent load on the structure was not modelled but was operated in another way. There was no stratigraphy of the cover, and therefore is made a general load analysis.

The first step in the analysis of the roof loads is going to calculate the roof area. Thanks to the maps available, and going to consider the inclinations of the roofs is possible calculate it:

$$\text{Area\_Roof} = 1466.5 \text{ m}^2$$

progressing to calculate the weights:

	PESO [Kg]
TEGOLE	58658,8
TAVOLATO	44891,9
IMPERMEAB.	14964,0
ORDITURA	74819,9
CAPRIATA	
TOTALE	193335

Table 5.5 Composition of Roof

Now that the weight of the roof first hypothesis is found, after, this is distributed between all the perimeter nodes of the septa of the top floor, and to these nodes is assigned the MASS21 element of ANSYS.

M_tot [kg]	193335
TOTAL NODES	244
Meq/NODE [kg]	792,4

Table 5.6 Characteristic element mass21

How can it be seen from the table below, the total perimeter nodes are 244 and they have been assigned a uniform mass each. This parameter will also be calibrated given its uncertainty.



### 5.2.4 Definition of type of Analysis

The analysis chosen is the modal one in order to evaluate the own frequencies and the magnitude of the deformed. For a structure of this size, the analysis is set on the first seven ways of vibrating. At this stage, have to be careful to exclude local ways that could impair the results.

### 5.3 Placement of accelerometers

The 17 accelerometers are arranged in the structure's floor and need to be identify them on the basis of a main reference system. This coordinate system is very important because the recorded data refers to these points for identifies displacements and accelerations of structure. The reference system is the one that was created in modelling with Rhino and which is then taken back to Ansys.

	n_Accelerometers	COORDIATES		
		X [m]	Y [m]	Z [m]
UNDERGROUND	A1	65,842	63,765	0
	A2	35,533	51,815	-0,7
	A3	19,603	32,575	-0,7
	A4	-10,948	48,025	0
GROUND	A5	65,842	63,765	3,32
	A6	35,533	51,815	3,32
	A7	19,603	32,575	3,32
	A8	-10,948	48,025	3,32
FIRST FLOOR	A9	65,842	63,765	8,5
	A10	35,533	51,815	8,5
	A11	19,603	32,575	8,5
	A12	-10,948	48,025	8,5
SECOND FLOOR	A13	65,842	63,765	13,85
	A14	35,533	51,815	13,85
	A15	19,603	32,575	13,85
	A16	-10,948	48,025	13,85
	NF	35,533	45,555	-0,7

Figure 5.10 Coordinates of sensors

# CHAPTER VI

## 6 METHODS OF MODEL UPDATING AND CALIBRATION

The model updating is the tool through which is possible improve the performance of mechanical systems and structures of civil engineering. With the passing of time, instruments available for the resolution of more and more specific problems, were not suitable, just think of the solution with some mathematical models that foresee the resolution of differential equations of high order, whose solution is complicated and difficult to interpret. Then was tempted another approach, detecting a tool that could be a support to the mechanical model realized, able to identify it and improve its behaviour and if need to correct it. From these necessity were formulated the updating models, able to correlate the results obtained from the processing with those proceeds from experimental tests. The first stride of the calibration process is the choice of model parameters. This phase is of fundamental importance, because these parameters must be chosen in order to characterize the model with a strong physical meaning and not only in order to have an optimal calibration. In the civil field a fundamental parameter is the rigidity, thanks to its calibration it is possible to detect any problems and defects in the real structure. A wrong choice of the model or its incompleteness leads to inevitable and coarse errors, but also an inaccurate acquisition of the data, due to background noises, lead to very common errors. Another aspect concerns the measurements that are often made by sensors in a not high number of points, so that do not have a complete database.

Is possible divide the Updating techniques into two categories:

- **Indirect methods**  
Correct the starting model in one step
- **Direct methods**  
The model is corrected step by step, updating the parameters each time

Both categories incur errors typical of these processes. In fact, the data can often be inaccurate, in some cases it is not possible to have a unique solution and the presence of non-linear functional relationships does not allow an adhering simulation of the physical phenomenon studied. A non-minor point is the identification of boundary conditions that are not fast-identifying.

In both cases the steps to be done in a Model Updating algorithm are as follows:

- Creation of a numerical model of the system to be studied, with a program of finite elements FEM
- Assignment of the updating object parameters
- Choosing a model that can correlate the measured parameters and those of the model by means of suitable algorithms
- Calibration of parameters by direct or indirect methods (choice of updating criterion)

### 6.1 Basic mathematical model and modal analysis

The problem is solved through a discretization to infinite degrees of freedom with the techniques of Finite Element analysis. The first step is the construction of local matrices of the system and then with the processes of assembly and expansion are obtained the global matrices. These permit the solution of the dynamic problem, deriving a system of differential equations of the second order:

$$[M]\{\ddot{x}\} + [C]\{\dot{x}\} + [K]\{x\} = \{f(t)\} \quad (6.1)$$

Where:

- $[M]$  global matrix of mass
- $[K]$  global matrix of stiffness
- $[C]$  global matrix of Viscous damping

Assuming an harmonic force and neglecting the damping  $[C]$ , the solution to the problem is:

$$x(t) = x(\omega) \cdot e^{i\omega t} \quad (6.2)$$

The system of autovectors and eigenvalues corresponding respectively to the modal forms and to their own frequencies are obtained:

$$[K]\{\Phi\}_j = \lambda_j [M]\{\Phi\}_j \quad (6.3)$$

Where:

- $\lambda_j$  is j-th autovalue, also is the square of the modal frequencies
- $\{\Phi\}_j$  is j-th modal formis j-th modal form

For the Orthogonality property of the modes result:

$$\begin{aligned} \{\Phi\}_j^T [M] \{\Phi\}_k &= m_j & \text{for } k = j \\ \{\Phi\}_j^T [M] \{\Phi\}_k &= 0 & \text{for } k \neq j \end{aligned} \quad (6.4)$$

$$\begin{aligned} \{\Phi\}_j^T [K] \{\Phi\}_k &= k_j & \text{for } k = j \\ \{\Phi\}_j^T [K] \{\Phi\}_k &= 0 & \text{for } k \neq j \end{aligned} \quad (6.5)$$

When is set up modal analysis of a building modelled with finite element program, the mode of vibration that can be found are elevated, by virtue of the many degrees of freedom. When is analysed a structure, the Italian regulations, like the European ones, takes into account the participant mass of each mode. To find the modal mass, it is indispensable to make a decoupling of the equation of motion considering:

Firstly a normalization respect of mass matrix:

$$\{U\} = \frac{\{\Phi\}}{\sqrt{\{\Phi\}^T [M] \{\Phi\}}} \quad (6.6)$$

In this way it have:

$$\{U\}_i^T [M] \{U\}_j = \begin{cases} 0 & i \neq j \\ 1 & i = j \end{cases} \quad (6.7)$$

$$\{U\}_i^T [K] \{U\}_j = \begin{cases} 0 & i \neq j \\ \omega^2 & i = j \end{cases}$$

and furthermore:

$$\begin{aligned} [U]^T [M] [U] &= [I] \\ [U]^T [K] [U] &= [\Omega] \end{aligned} \quad (6.8)$$

Where:

- $[\Omega]$  is the matrix of the modal pulses of all modes
- $[I]$  is the identity matrix
- $[U]$  is the normalized modal matrix

Then by virtue of this, is possible rewrite (6.1) introducing the modal coordinate:

$$\{x\} = [U] \{p\} \quad (6.9)$$

$$[I] \{\ddot{p}\} + [\Omega] \{p\} = [U]^T \{f(t)\} \quad (6.10)$$

and corresponds to the generic decoupled equation associated with the i-th mode

The matrix system contains the following equations:

$$\ddot{p}_k + \omega_k^2 p_k = -\{U\}_k^T [M] \{t\} \cdot \ddot{u}_g(t) \quad (6.11)$$

Notice how the to force was replaced  $f(t) = m \cdot \ddot{u}(t)$

These equations can be developed separately for finding the effect of each mode on the structure.

it distinguish:

$$\Gamma_k = -\{U\}_k^T [M] \{t\} = \sum_i \gamma_{ik} \quad (6.12)$$

Where:

- $\Gamma_k$  is the coefficient of modal participation
- $\gamma_{ik}$  Is the participation factor of plan

The modal mass participant of each mode can be derived from the equivalent static forces and is:

$$m_{mod,k} = (\{U_k\}^T [M] \{t\})^2 \quad (6.13)$$

Where:

$\{t\}$  dragging vector of the problem

In the analysis the modal mass that will be calculated will be a useful parameter to verify if the ways we have taken in the consideration are the most important.

## 6.2 Uploading parameters

The selection of the parameters subject to calibration is one of the most delicate passages. The number of parameters is the function of the measured data that are available. Having a limited number of data, in fact, it will not be able to calibrate too many parameters, otherwise it will be enlarged to problems of bad-conditioning. A good criterion of choice could be that which selects the parameters able to correct the uncertainties localized in the model.



As studied by Wittrich (1962) and Fox-Kaapoor (1968) , variation of the system in function of the parameter  $\theta$  is:

$$\left[ [K] - \lambda_j [M] \right] \frac{\partial \{\Phi_j\}}{\partial \theta} = - \left[ \frac{\partial [K]}{\partial \theta} - \lambda_j \frac{\partial [M]}{\partial \theta} - \frac{\partial \lambda_j}{\partial \theta} [M] \right] \{\Phi_j\} \quad (6.14)$$

It is possible to extract the sensitivity of the autovector, thanks to the symmetry of the stiffness matrix and the masses:

$$\frac{\partial \lambda_j}{\partial \theta} = \{\Phi_j^T\} \left[ \frac{\partial [K]}{\partial \theta} - \lambda_j \frac{\partial [M]}{\partial \theta} \right] \{\Phi_j\} \quad (6.15)$$

From the formula just obtained, can be seen, how the sensitivity of the i-th autovector is a function itself.

Generally, to the parameters object of calibration are associated a range of variability due to their mechanical limits. For example, if in a masonry structure as an updating parameter, chosen is the Poisson coefficient  $\nu$ , this parameter in the Updating process will undergo constant variation. However these variations are limited, as from literature,  $\nu$  has a range that varies, and especially for the walls will hardly exceed 0.4. Another choice that can be made is to calibrate not only individual elements but groups, making sure that these groups have similar characteristics. The mass and stiffness matrices defined earlier refer to the structure overall, but in the analysis it is not going to vary these in their entirety, but in their components. In fact, as will explained below, it will calibrate groups of walls, from that, the global matrices depend directly.

What just said is confirmed in the following formulas:

$$[M] = [M_0] + \sum_{i=0}^n \theta_i [M]_i \quad (6.16)$$

$$[M] = [M_0] + \sum_{i=0}^n \theta_i [M]_i \quad (6.17)$$

Where:

- $[K]_i$  stiffness matrix of the single or group of calibrated elements
- $[M]_i$  mass matrix of the single or group of calibrated elements
- $\theta_i$  parameter to be calibrated

### 6.3 Comparison between measured parameters and model parameters

The criterion underlying the comparison between the experimental data and those related to the FEM model, is the one that sees the identification of a parameter called MAC, whose formulation is:

$$MAC_{jk} = \frac{(\{\Phi_m\}_j^T \{\Phi_a\}_k)^2}{(\{\Phi_a\}_j^T \{\Phi_a\}_k)(\{\Phi_m\}_j^T \{\Phi_m\}_k)} \quad (6.18)$$

Where:

- $\{\Phi_m\}_j$  J-Ith Autovector referred to structural reliefs
- $\{\Phi_a\}_k$  J-Ith Autovector referred to model analysed

It is important to have a streamlined computational model that uses little onerous analytical methods, because every time is calculated the MAC, time to time is done a modal analysis. The MAC has a range of variability between 0 and 1. Values close to 1 denote an optimal correlation, on the contrary, values close to 0 indicate an uncorrelation.

In general, on numerator the values are non-zero, due to the orthogonality property of the modes. MAC is calculated for all possible pairs of modal shapes. In this way it is possible to construct a square matrix, which in the case of perfect coincidence between the data, has unit values in the diagonals, while in the others equal to 0

### 6.4 Direct methods of Updating

As the name indicates, these methods perform in a small number of stages and do not require iterations. In this way the convergence of the solution is assured and the calculation times are not long. These methods are able to reproduce exactly the measures available, but this could also be a weakness, because of the wrong measurements, also those affected by noises become an integral part of the analytical model. When is used these methods, is recommended careful caution on the experimental data acquisition procedure. The modal frequencies are identified with good precision, on contrary for the modal deformed, the measurement is more delicate. There is a pre-requisite that never occurred: the number of degrees of freedom measured must be equal to the number of degrees of freedom of the analytical model. Another problem concerns the sensors, in fact the measurements can be carried out only in a range of frequencies, thus leading to the not knowledge of certain modes of vibrating out of this range. However, in civil applications, the sensors are calibrated in a range in which most of the frequencies of the structure fall. Is not demanded to know all the ways, but only the most important ones, in general the top ten are fine

## 6.5 Iterative methods

The iterative methods are a very useful tool, because they allow an accurate choice of the parameters to be optimized. However, these methods require a good understanding of the physical nature of the problem. Iterative methods, are based on the measurement of modal data such as frequencies and deformed ones, trying to minimize the differences between the experimental data and the updated model. By subsequent iterations is tempted to minimize this difference, only the selected parameters are calibrated in this procedure. This optimization is based on the search for the cost function, which is built on frequencies and modal forms, it is the sum of the squares of the differences between estimated and measured data. The parameters that can be used can be of a high number but it is recommended not to have an excessive number because of the calculation times. A good parameterization of the system allows a better efficiency of the iterative methods, and not all the chosen parameters have the same role in the system. A model can be more or less sensitive to certain parameters, in fact some of these varying little, can create a great variation of the response. The MAC index is a great way to have an estimate of this comparison

### 6.5.1 Matrix Mixing method

The measurement of all modal forms of structure in all its degrees of freedom, in a practical way is unfeasible, but if it were possible the construction of the matrices of mass and stiffness would be immediate:

$$[M]^{-1} = [\Phi_m][\Phi_m]^T = \sum_{i=1}^n [\Phi_m]_i [\Phi_m]_i^T \quad (6.19)$$

$$[K]^{-1} = [\Phi_m][\Lambda]^{-1}[\Phi_m]^T = \sum_{i=1}^n \frac{[\Phi_m]_i [\Phi_m]_i^T}{\omega_{mi}^2} \quad (6.20)$$

Where:

- $\omega_{mi}^2$  Observed natural frequencies
- $[\Phi_m]_i$  Natural eigenvalues observed

However, the provisions data are limited and often incomplete and refer to a number of degrees of freedom significantly lower than ones of the model. The mixing approach aims to solve the problems that affect this difference between the few degrees of freedom considered and the many belonging to the model. The problem around the incompleteness of the data is solved with the passage of the expansion of the Autovectors.

So the matrices are derived with the following expression:

$$[M]^{-1} = \sum_{i=1}^m [\Phi_m]_i [\Phi_m]_i^T + \sum_{i=m+1}^n [\Phi_a]_i [\Phi_a]_i^T \quad (6.21)$$

$$[K]^{-1} = \sum_{i=1}^m \frac{[\Phi_m]_i [\Phi_m]_i^T}{\omega_{mi}^2} + \sum_{i=m+1}^n \frac{[\Phi_a]_i [\Phi_a]_i^T}{\omega_{ai}^2} \quad (6.22)$$

Where:

- The subscript "a" indicates the analytically calculated quantities
- The subscript "m" indicates the quantities obtained experimentally
- The subscript "n" indicates number of degrees of freedom of the model

This formulation requires the calculation of the high frequency modes, and does not always lead to a suitable solution to obtain the matrices. Assuming that the number of modes is much less than the order of the model,  $m \ll n$ , Indirectly is possible get to the following formula of modal deformation:

$$\sum_{i=m+1}^n [\Phi_a]_i [\Phi_a]_i^T = [M_a]^{-1} - \sum_{i=1}^m [\Phi_a]_i [\Phi_a]_i^T \quad (6.23)$$

$$\sum_{i=m+1}^n \frac{[\Phi_a]_i [\Phi_a]_i^T}{\omega_{ai}^2} = [K_a]^{-1} - \sum_{i=1}^m \frac{[\Phi_a]_i [\Phi_a]_i^T}{\omega_{ai}^2} \quad (6.24)$$

### 6.5.2 Lagrange multipliers Method

The method of Lagrange multipliers is a technique for studying the maximums and the minimums of a multi-variable function, in reference to one or more constraints. The application of this method in this study takes into account three quantities: the measured modal data, the mass matrix, and the stiffness matrix. Although in the past it was preferred to compute the mass matrix with static methods because it came to better results than dynamic analysis. A fundamental point of the analysis is the limited number of sensors to disposition, which acquire data on the points where they are installed, which are not in all degrees of freedom of the model (Operation impossible in reality). To cope with this deficiency, it is performed, an expansion of modal shapes or a reduction of the analytical model matrices. However these techniques could compromise the orthogonality of the modes. The  $[\Phi]$  matrix is determined by going to minimize the Euclidean norm:

$$J = ||N([\Phi] - [\Phi]_m)|| = \sum_{i=1}^n \sum_{k=1}^m \left[ \sum_{j=1}^n [N]_{ij} ([\Phi]_{jk} - [\Phi]_{m,jk}) \right]^2 \quad (6.25)$$

In which the condition of normality results:

$$[\Phi]^T [M_a] [\Phi] = [I] \quad (6.26)$$

Where :

- $N = \sqrt{[M_a]}$
- $[M_a]$  Analytic mass matrix
- $[\Phi]_m$  Matrix Autovectors measured
- $m$ , Number of autovectors measured
- $n$ , Number of degrees of freedom analytical model

The array of autovectors is weighed with the parameter  $N$ , which represents the square matrix of the mass matrix, so that the true function is minimized.

$$J = \sum_{i,j,h=1}^n \sum_{k=1}^m \left\{ [N]_{ij} ([\Phi]_{jk} - [\Phi]_{m,jk}) \cdot [N]_{ih} ([\Phi]_{hk} - [\Phi]_{m,hk}) \right\} + \sum_{i,h=1}^m \gamma_{ih} \left\{ \sum_{j,k=1}^n ([\Phi]_{ij} [M_a] [\Phi]_{kh} - \delta_{ij}) \right\} \quad (6.27)$$



Where :

- $\delta_{ij}$  Kronecker operator
- $\gamma_{ih}$  Lagrange operators

Lagrange operators can be collected in the matrix  $[\Gamma]$ . Because of the redundancy of the number of equations, which could cause the non-uniqueness of the solution, the following constraint arises:

$$[\Gamma] = [\Gamma]^T \quad (6.28)$$

The minimization of the function (6.27), is obtained by placing the derivatives equal to zero relative to each element of the autovectors, thus obtaining the following expression

$$[\Phi][I] + [\Gamma] = [\Phi_m] \quad (6.29)$$

And by means of a replacement it becomes:

$$[\Phi] = [\Phi_m][[\Phi_m]^T[M_a][\Phi_m]]^{1/2} \quad (6.30)$$

Considering the exact mass matrix, so as to respect the equation of motion, the modal matrix found, is used to determine the stiffness matrix, by means of the direct formulation:

$$[K][\Phi] = [M_a][\Phi][\Lambda] \quad (6.31)$$

Where:

- $[\Lambda]$  Diagonal matrix of measured frequencies

The function to be minimized refers to the differences between the correct and analytical stiffness matrix, and has the following formulation:

$$J = \frac{1}{2} ||[N]^{-1}([K] - [K_a])[N]^{-1}|| \quad (6.32)$$

and to make the solution unique it poses the condition:

$$[\Gamma]_k = -[\Gamma]^T \quad (6.33)$$

It is possible to differentiate the formula to be minimized in relation to the elements of the stiffness matrix, reaching the expression of the analytical stiffness matrix as a function of the matrix with Lagrange multipliers:

$$[K] = [K_a] - [M_a][\Gamma_\Lambda][\Phi]^T[M_a] - [M_a][\Phi][\Gamma_\Lambda]^T[M_a] \quad (6.34)$$

And of the one where all the terms that compose it are known:

$$\begin{aligned} [K] = [K_a] - [K_a][\Phi][\Phi]^T[M_a] - [M_a][\Phi][\Phi]^T[K_a] \\ + [M_a][\Phi][\Phi]^T[K][\Phi][\Phi]^T[M_a] \\ + [M_a][\Phi][\Lambda][\Phi]^T[M_a] \end{aligned} \quad (6.35)$$

In case that the mass matrix is not correct, the following expression must be minimized to determine the  $[M]$  values:

$$J = \frac{1}{2} \left\| [M_a]^{-1/2} ([M] - [M_a])[M]^{1/2} \right\| \quad (6.36)$$

Another approach is the correction of the matrices of mass and stiffness at the same time, using as input data the array of autovectors and having as constraint the orthogonality. In this case the function to minimize becomes:

$$\begin{aligned} J = \frac{1}{2} \left\| [M_a]^{-1/2} ([K] - [K_a])[M]^{1/2} \right\| \\ + \frac{1}{2} \left\| [M_a]^{-1/2} ([M] - [M_a])[M]^{1/2} \right\| \end{aligned} \quad (6.37)$$

## 6.6 Model Quality

The methods of Updating are al lots and are consolidated over time, however, it is necessary to validate the quality of the obtained parameters and the same procedures that are used. A procedure that can be proposed is the one which provides for the division into two categories of the acquired data. The first category will be developed to correct and calibrate the uncertain parameters, while the second will be used to verify the quality of the parameters and the model obtained. The quality of a model refers to three parameters:

- Adherence between normal measure and the analytical model
- Selection of parameters and correction algorithm
- Weights and variance assigned to estimation of measured data and initial parameters

## 6.7 Optimization Techniques

The techniques of optimization are all those techniques that are meant to minimize a certain function. Working with an indirect-type Updating model, the iterative calculations that are performed aim to the minimum point of the cost function. The mathematical optimization counts of many techniques, specialized in different fields, from the economic one to the structural one, but all have a common basis. The main problem that is faced, is the presence of numerous parameters to be calibrated and the presence of their relative minimums that inevitably leads to very long calculation times.

### 6.7.1 Genetic algorithm

This algorithm was created by John Holland at the beginning of the years 70', and is considered as an excellent optimization technique. This is part of the category of heuristic algorithms, and the genetic term defines their way of implementation: they are inspired by mechanisms similar to biochemical ones and also to the process of Darwinian evolution. The idea is to select better solutions and to recombine them in some way, evolving each time toward the best selected points. The main elements that characterize it are:

- Fitness function, is the function to maximize
- Individual or population, are the variables belonging to the fitness function in a certain interval
- Chromosome, is the sequence of 0 or 1 that make up an individual

The structure of a genetic algorithm is articulated in these phases:

- **Defining the initial generation**  
It is defined, even at random, a first set of possible solutions to the problem under consideration
- **Definition of each solution and selection of the best**  
Each solution is evaluated, associating a quality indicator with each one so that they can be ordered
- **Defining a new generation**  
for generation it is intended the population of a given moment of time, at this stage, is defined a new group of solutions with high quality, in order to promote the development at the expense of the worst ones
- **Conclusion of the processing**  
If the number of iterations established has been reached or the quality of the best available solution is acceptable, processing can terminate, otherwise a new solution group is generated

It is important to know, that the selection of an individual depends on its value of fitness, a high value of this corresponds to a greater possibility of being chosen as a parent to create a new generation

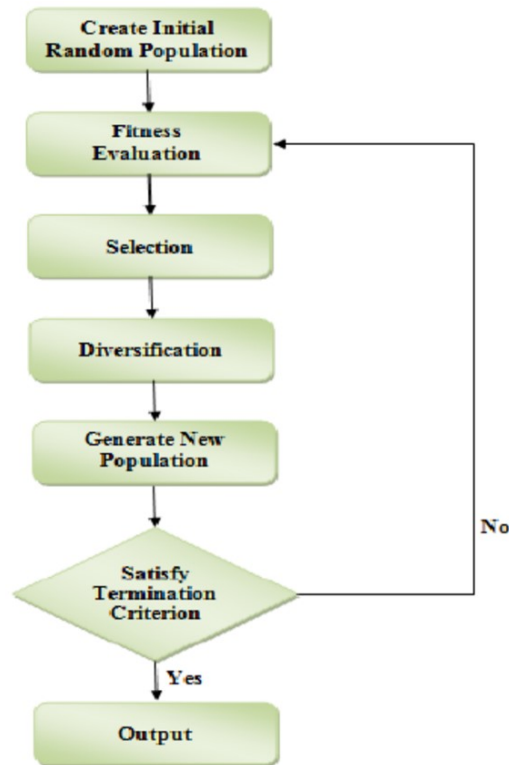


Figure 6.1 genetic algorithm diagram

## 6.8 Calibration Parameters of Structure

The calibration of the structure was made by going to subdivide all its components into blocks that had the same characteristics. As parameters of updating were considered: the stiffness and the density of the walls, the stiffness of the ground and the external staircase, and the mass of the roof. In a first phase, few parameters were chosen, but seeing that the model reached poor MAC values, it was thought of a schematization of the parameters, floor by floor, that could better capture the structural behaviour. A single parameter has been taken for the rigidity of the slabs, considering that it must be a rigid plane and knowing that this value does not deviate much from the different typologies that make up the structure. However, for each of these, the density was taken into account as the updating parameter. With regard to the ground around, and the external staircase, these were schematized by elastic Springs, whose stiffness represent two independent updating parameters. From the technical reports of the structure, it was not possible to analyse in detail the components of the roof, and to have a precise mass of the cover, for this reason, the weight of the roof was taken as a parameter to calibrate. It started however from starting values shown in table 5.5 and 5.6.

### 6.8.1 Stiffness Parameters

The schematization of stiffness is subsequently reported for each block of wall considered:

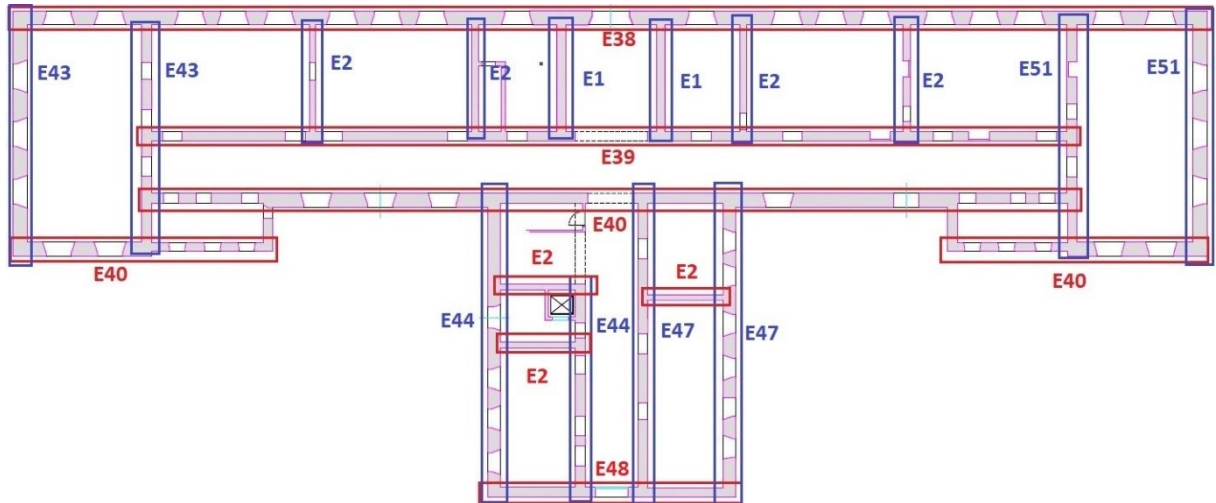


Figure 6.2 Ground floor stiffness

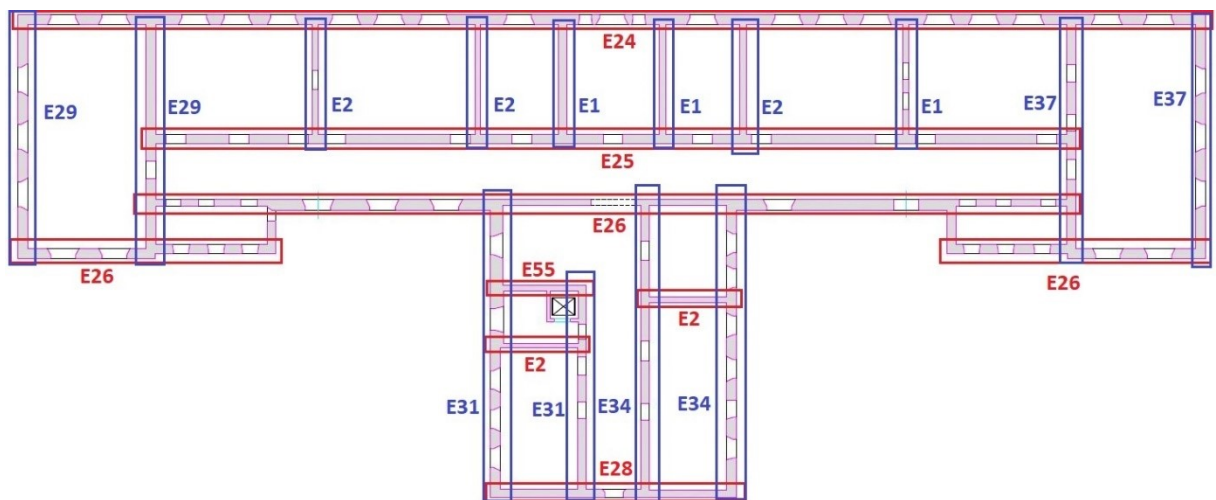


Figure 6.3 First floor stiffness



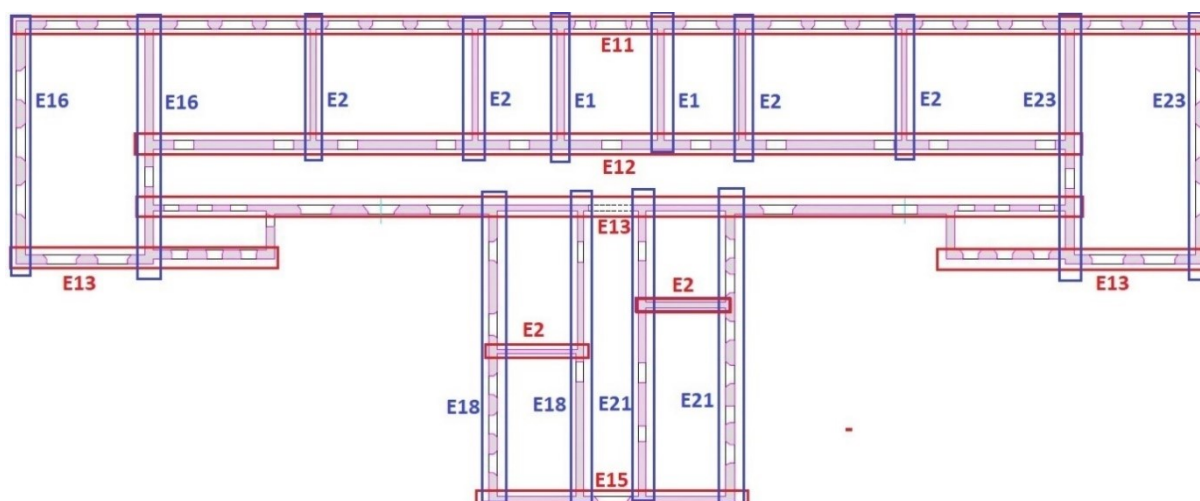


Figure 6.4 Second floor stiffness

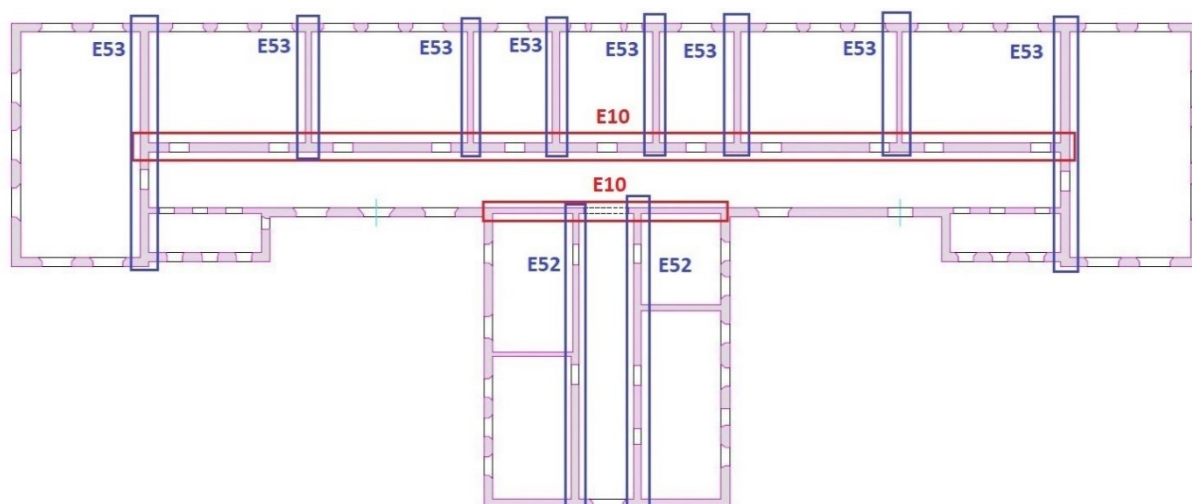


Figure 6.5 Roof floor stiffness

The figure 6.5 reports the walls that belong to the roof, are those that support in part the cover, are nothing else the continuation of the walls of second floor. The selected stiffness parameters are shown in the following table.

FLOOR	PARAMETERS
UNDERGROUND	E1
GROUND	E48
	E39
	E40
	E44
	E47
	E51
	E38
	E43
FIRST	E28
	E25
	E26
	E31
	E34
	E37
	E24
	E29
SECOND	E15
	E12
	E13
	E23
	E18
	E21
	E11
	E16
WALLS OF ROOF	E53
	E10
	E52
PARTITIONS	E55
	E2

Table 6.1 Stiffness parameters

### 6.8.2 Density Parameters of walls

Instead, for the density, were chosen two parameters for each plane, considering the types of materials present, which were exhibited in Chapter III. Only for the second floor, because it has only one type of masonry the two density parameters were divided for the walls in the X-direction and for the walls in the Y-direction.

FLOOR	MASONRY TYPE	PARAMETER
UNDERGROUND	MUR_1	D1
GROUND	MUR_2	D38
	MUR_3	D49
FIRST	MUR_3	D24
	MUR_2	D30
SECOND	MUR_2 on Y	D16
	MUR_2 on X	D11
ROOF	MUR_2	D54'
	MUR_2	D10'
	MUR_2	D52
	MUR_2	D53

Table 6.2 Density parameters

The parameters D10, D52, D53, D54, refer to the wall of thorns that support the roof.

### 6.8.3 Density parameters of slabs

The same thing was done for the slabs, remembering that each floor has two different types, and for this reason two parameters have been chosen by floor:

FLOOR	SLAB TYPE	PARAMETER
GROUND-FIRST	SOL_1	D49
SECOND	SOL_3 Ω160	D24
	SOL_3 Ω240	D30
PLANE OF ROOF	SOL_4 Ω90	D16
	SOL_4 Ω160	D11

Table 6.3 Slabs parameters

### 6.8.4 External parameters

In addition to the parameters of the structure, three other parameters have been chosen which modify in part the structural behaviour and which must be taken into account. The first concerns the rigidity of the ground, which surrounds the structure for a depth of about 1.70 m, the second parameter refers to the stiffness from the ladder spliced along the north-east side, which constitutes an alley, and finally the third parameter that represents the weight of the roof, distributed perimeter on top of the walls of the second floor.

TYPE	PARAMETER
STIFFNESS OF TERRAIN	K_SOIL
STIFFNESS OF STAIR	K_SPRING
WEIGHT OF ROOF	MASS_ROOF

Table 6.4 External parameters

It was decided to calibrate also the value of the Poisson's module whose range is limited.

TYPE	PARAMETERS
MODULE OF POISSON	vpoiss

In total the calibrated parameters are 51.

## 6.9 Results of Calibration

For the calibration of the model, were considered, the first three modes of vibration, which constitute a good approximation of the structural behaviour, as they excite more than 80% of the mass of the building.

### I MODE

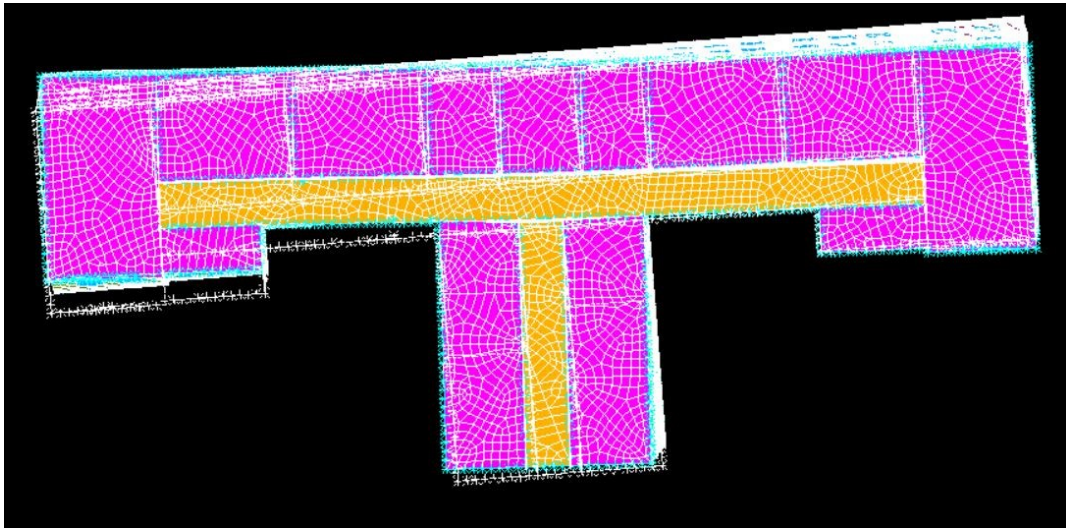


Figure 6.6 I MODE updated Model

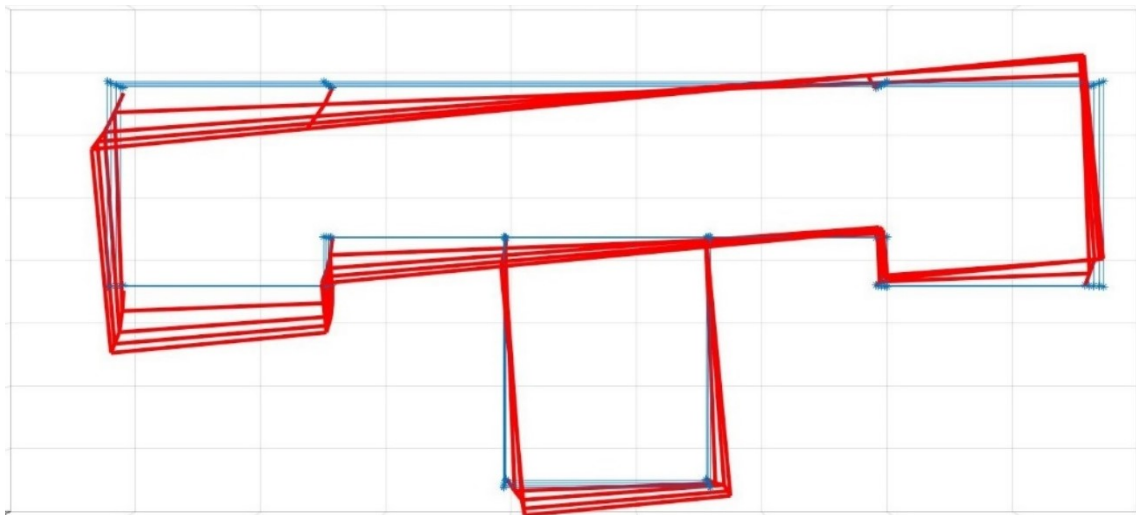


Figure 6.7 I MODE identified

The first mode of vibrating is a torsional mode, from the comparison with Figure 6.7, which represents the mode identified by the sensors, it is possible to grasp a good approximation with the torsional mode obtained from the calibrated FEM analysis



## II MODE

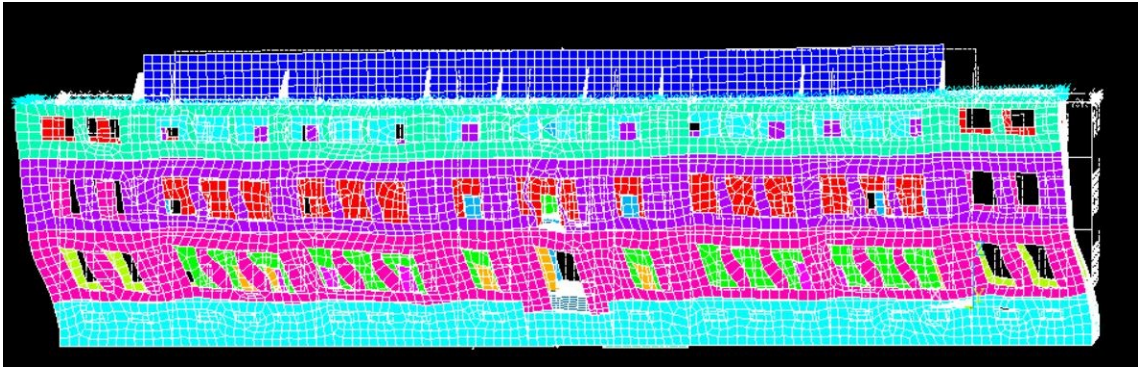


Figure 6.8 II MODE updated Model, East Side

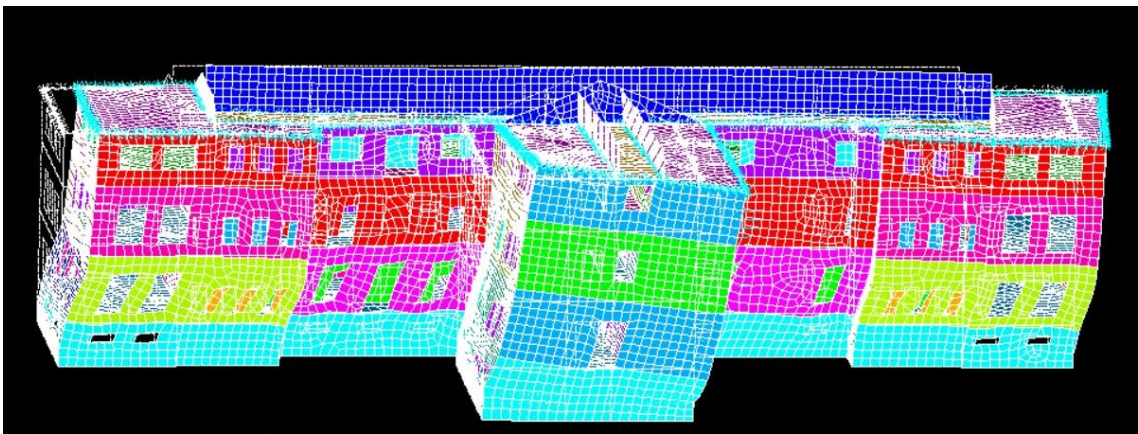


Figure 6.9 II MODE updated Model, West Side

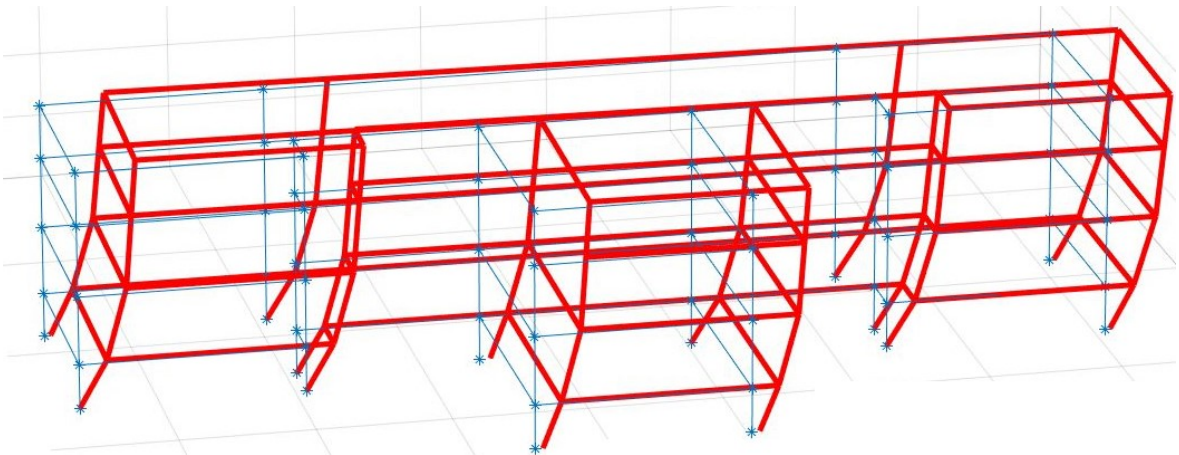
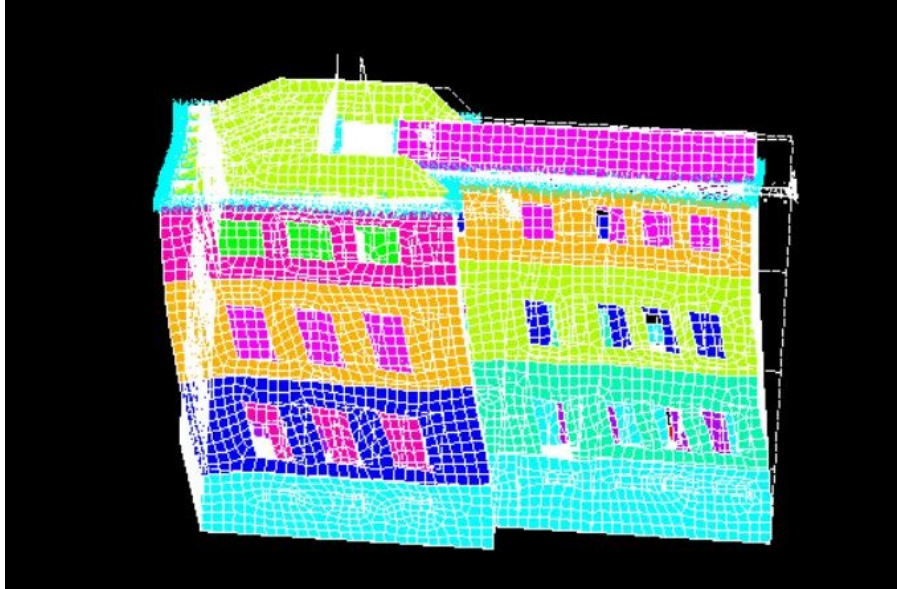


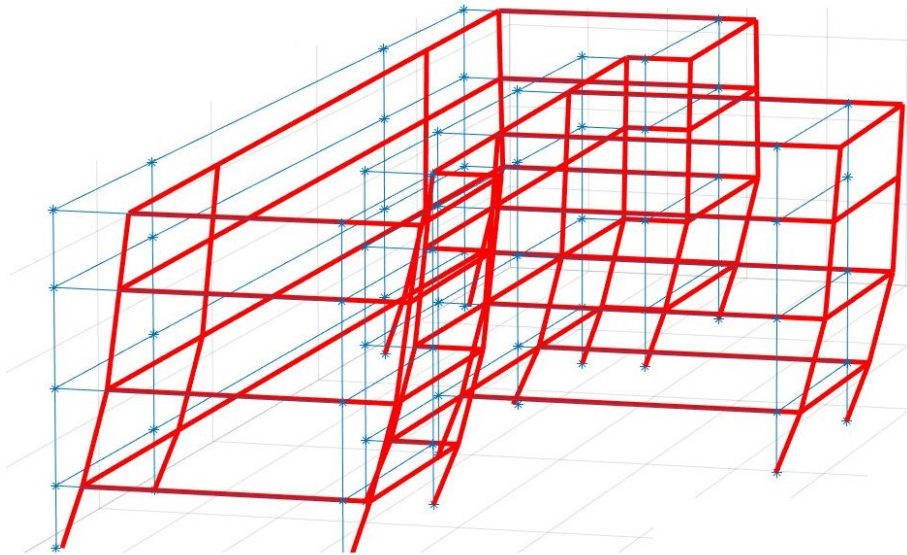
Figure 6.10 II MODE identified

The second way of vibrating represents the heel in the Y direction, here too, it is possible to compare the two results, the mode of the calibrated structure Fig 6.10 and the experimental modes obtained by sensors fig 6.11

### III MODE



*Figure 6.11 III MODE updated Model , sud Side*



*Figure 6.12 III MODE identified*

The third mode instead corresponds to a skid along the X-axis



Comparing the result obtained in terms of frequencies between the two model : FEM and IDENTIFICATED is possible observe that the error is less than 1%. The following table show the values of frequency of the starter model too:

	FREQUENCY [Hz]			Error [%]
	STARTING	FEM	ID	
I° MODE	4,511	4,157	4,162	0,12
II° MODE	4,982	4,826	4,827	0,02
III° MODE	6,120	4,928	4,917	0,22

Table 6.5 STARTING, FEM and ID frequency comparison

The values of the MAC parameter is very good for the first mode, as far as the second one is at a lower value, but always satisfactory, the same for the third mode.

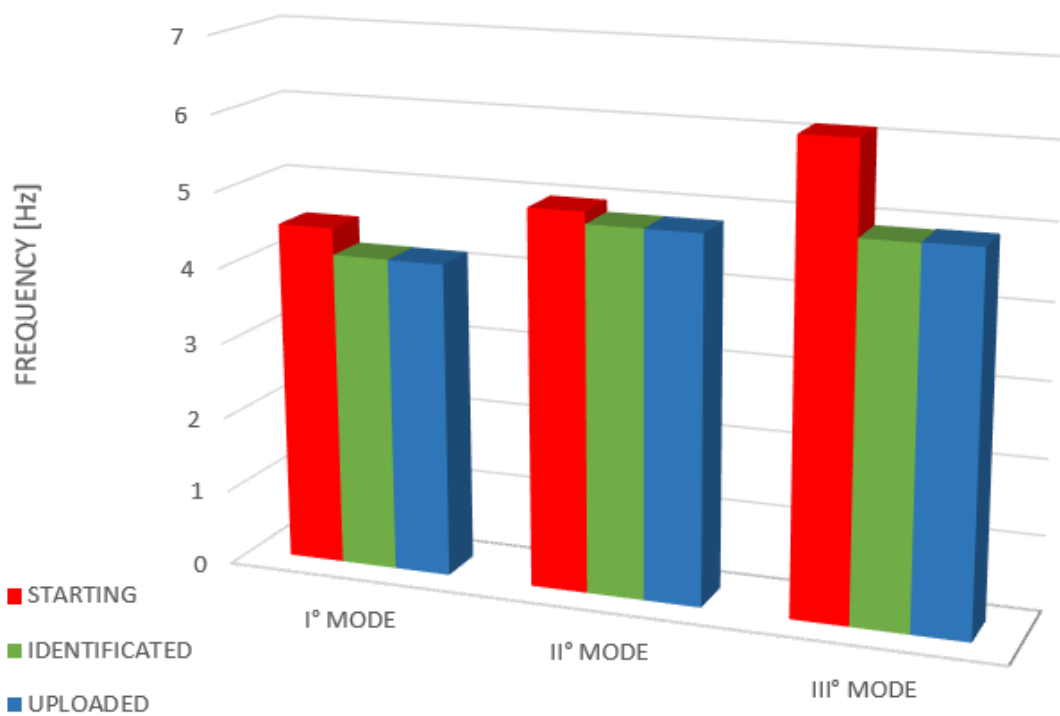


Figure 6.13 Frequency of model

### 6.9.1 Upload parameters found

The 51 parameters analysed belong to various categories, as already mentioned in the previous paragraph. Most of these are part of the stiffness group of floor and another part of the density of the walls and slabs. Only a small part are the external parameters of the structure.

- STIFFNESS

	STIFFNESS [kg/m <sup>2</sup> ]	
	UPLOADED	STARTING
<b>E38</b>	1,43E+09	1,90E+09
<b>E43</b>	1,20E+09	1,90E+09
<b>E40</b>	2,17E+09	1,90E+09
<b>E44</b>	1,90E+09	1,90E+09
<b>E47</b>	2,14E+09	1,90E+09
<b>E51</b>	1,19E+09	1,90E+09
<b>E24</b>	2,31E+09	1,90E+09
<b>E55</b>	3,09E+09	1,90E+09
<b>E31</b>	3,07E+09	1,90E+09
<b>E48</b>	5,02E+09	1,90E+09
<b>E37</b>	7,34E+09	1,90E+09
<b>E26</b>	1,03E+10	1,90E+09
<b>E34</b>	1,73E+10	1,90E+09

Table 6.6 Stiffness MUR\_1 MUR\_3

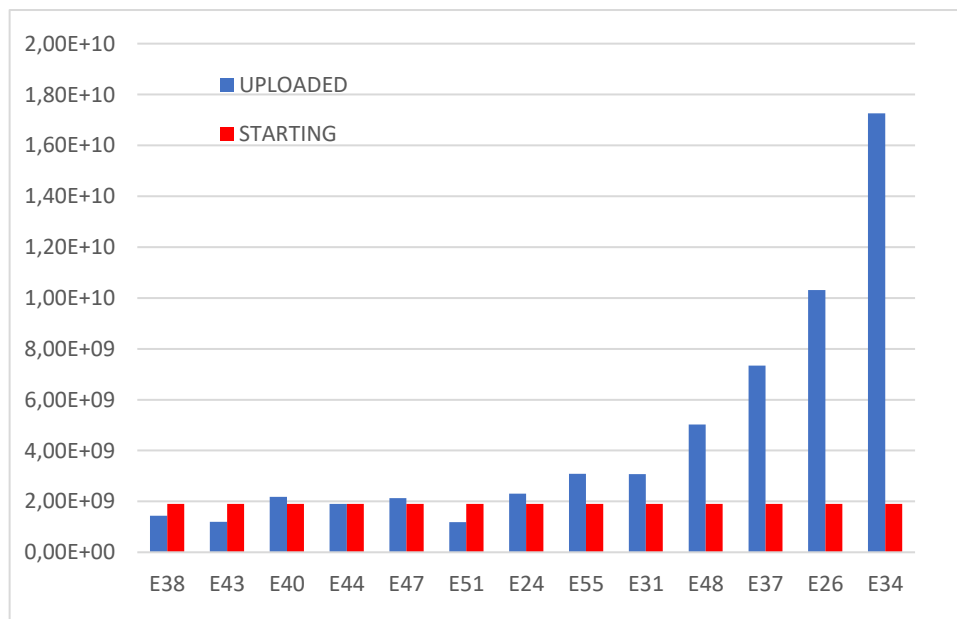


Figure 6.14 Stiffness MUR\_1 MUR\_3

	STIFFNESS [kg/m <sup>2</sup> ]	
	UPLOADED	STARTING
<b>E11</b>	4,52E+08	1,50E+09
<b>E16</b>	1,24E+09	1,50E+09
<b>E23</b>	9,97E+08	1,50E+09
<b>E18</b>	1,48E+09	1,50E+09
<b>E21</b>	5,84E+08	1,50E+09
<b>E1</b>	1,47E+09	1,50E+09
<b>E55</b>	3,09E+09	1,50E+09
<b>E39</b>	3,49E+09	1,50E+09
<b>E2</b>	4,52E+09	1,50E+09

Table 6.7 Stiffness MUR\_2

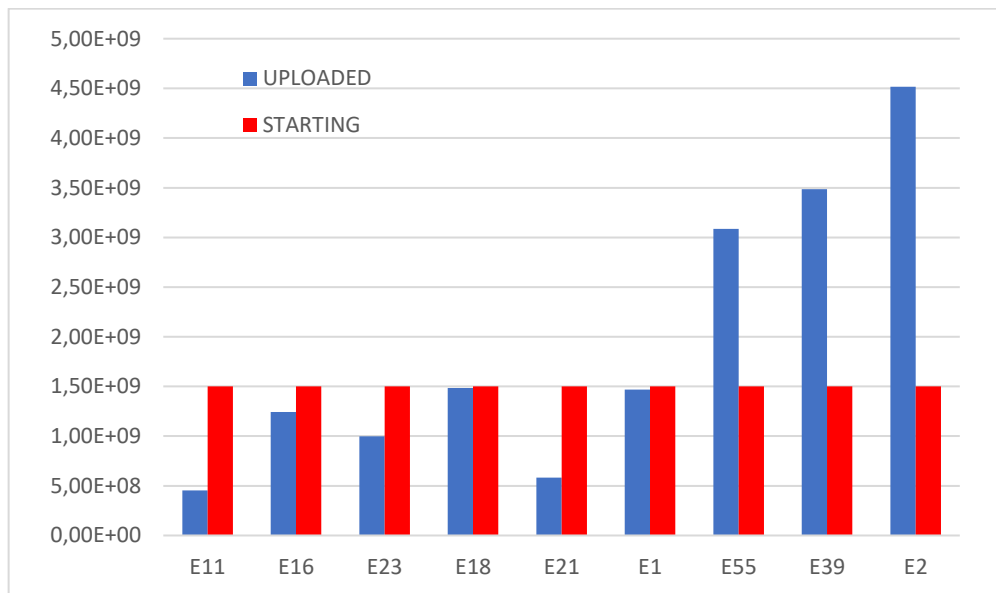


Figure 6.15 Stiffness MUR\_2

- DENSITY

	DENSITY [kg/m <sup>3</sup> ]	
	UPLOADED	STARTING
<b>D49</b>	1100	1800
<b>D24</b>	1900	1938,8
<b>D16</b>	2100	2142
<b>D11</b>	2100	2142
<b>D30</b>	1775	1800
<b>D1</b>	3420	2142
<b>D38</b>	2863	1938,8

Table 6.8 Density of wall

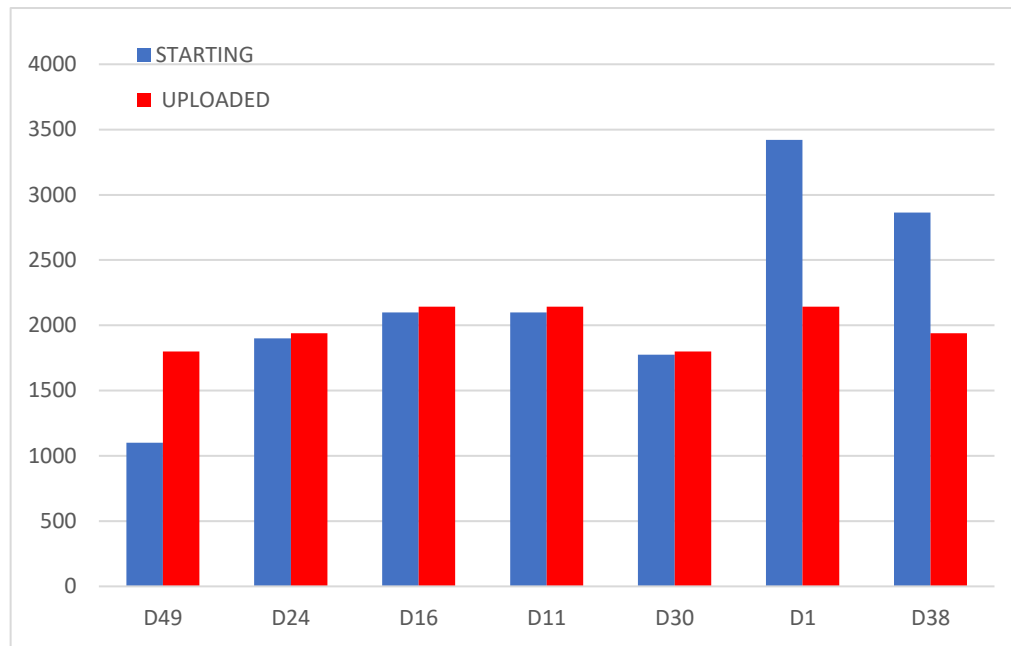


Figure 6.16 Density of wall

	DENSITY [kg/m <sup>3</sup> ]	
	UPLOADED	STARTING
D6	300	544
D7	256,25	291
D8	300	219
D4	695,75	700
D5	628,13	600

Table 6.9 Density of slab

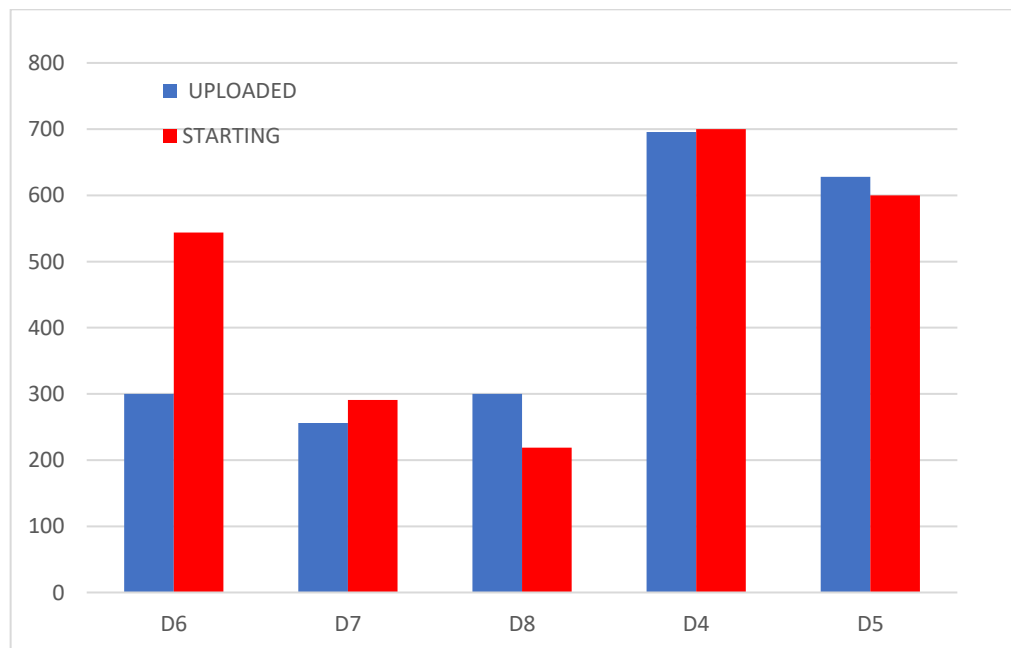


Figure 6.17 Density of slab

- EXTERNAL PARAMETERS

<b>K_SOIL [Mpa]</b>	35575
<b>K_SPRING [Mpa]</b>	11604
<b>MASS_ROOF [ Kg]</b>	198962
<b>vpoiss [-]</b>	0,31

Table 6.10 External parameters uploaded

### 6.10 MAC

The fundamental parameter that has been taken to validate the correspondence between FEM and real model is the MAC. The values that are shown in the table confirm the good adherence of the calibrated model.

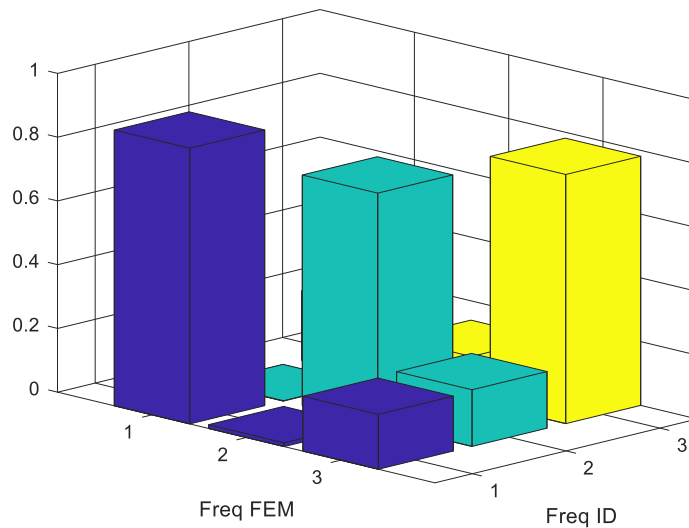


Figure 6.18 MAC uploaded model

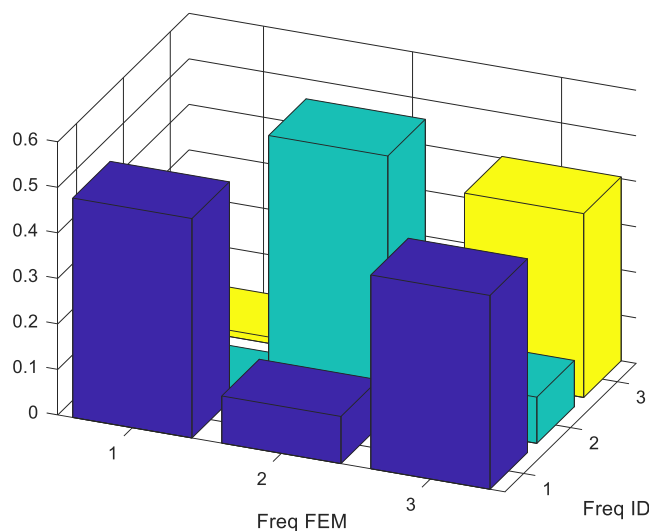


Figure 6.19 MAC starting model

# CHAPTER VII

## 7 MODEL BEHAVIOUR UNDER EARTHQUAKE

The model created, has been calibrated, and now s possible study its behaviour with numerous analyses. In fact, besides modal analyses, also structural analyses to evaluate the deformation and stress level. In this chapter, however, will be cope the behaviour of the structure under earthquake, in particular, those belonging to the seismic sequence that struck Norcia in 2016. The objective is to assess the degree of damage caused by these earthquakes, thus verifying the safety of the building. This assessment is of paramount importance because, after the renovation, the structure has undergone a change of destination in the first two floors, becoming a public kindergarten.

### 7.1 Simulated earthquakes

EARTHQUAKE	DATE, HOUR	M <sub>W</sub>	DIST. EP [Km]	PGA N-S [g]	PGA W-E [g]
1	24/08/2016, 01:36	6,0	75,59	0,0425	0,0521
2	26/10/2016,17:10	5,4	53,96	0,025	0,029
3	26/10/2016,19:10	5,9	48,8	0,081	0,087
4	30/10/2016,06:40	6,5	58,79	0,038	0,053
5	18/01/2017,10:14	5,0	101,13	0,007	0,007

Table 7.1 Earthquake considered

The data acquired by the sensors of the structure were used, in particular were taken into account, the recordings of the sensor in the basement, whose channels 29,30,31, recorded a sequence of accelerations with a sampling time of 0.004 s.

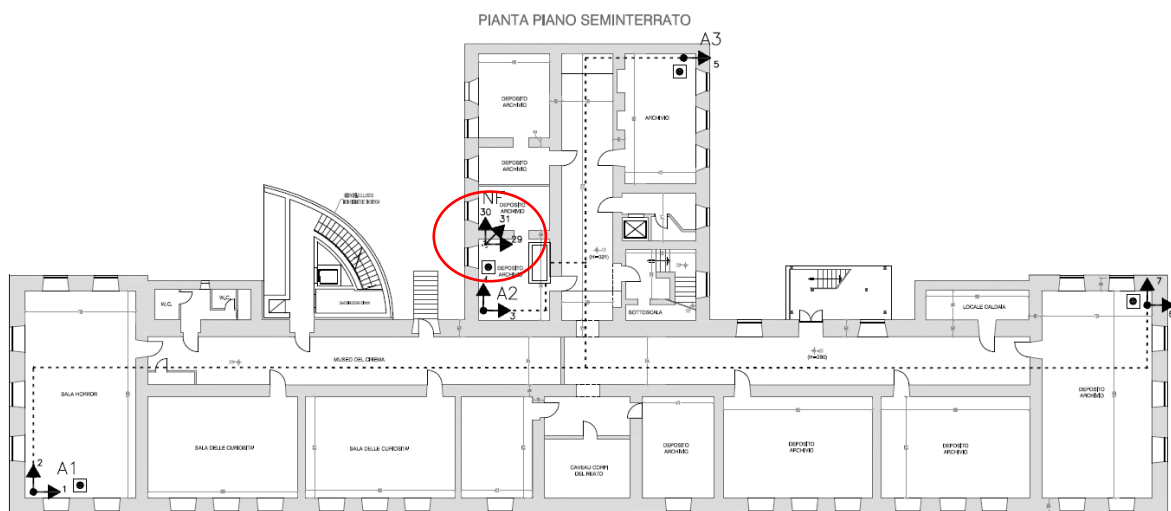


Figure 7.1 Earthquake output sensor



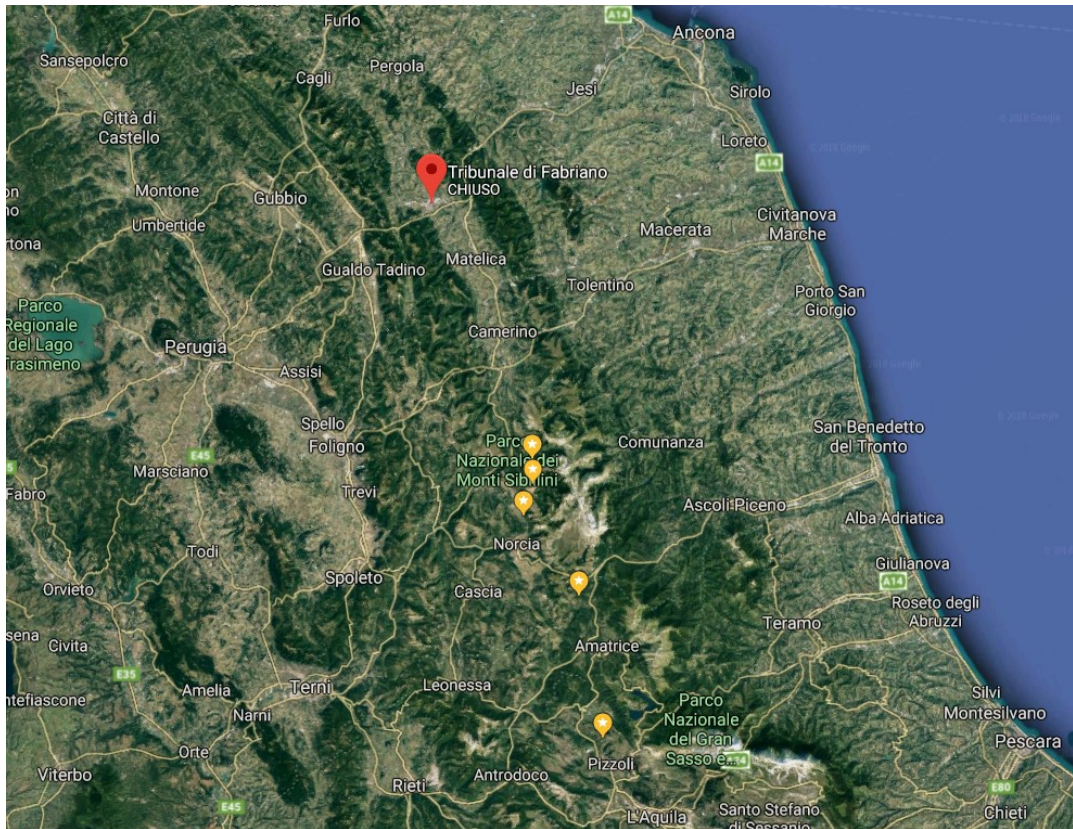


Figure 7.2 Earthquakes distance from Fabriano

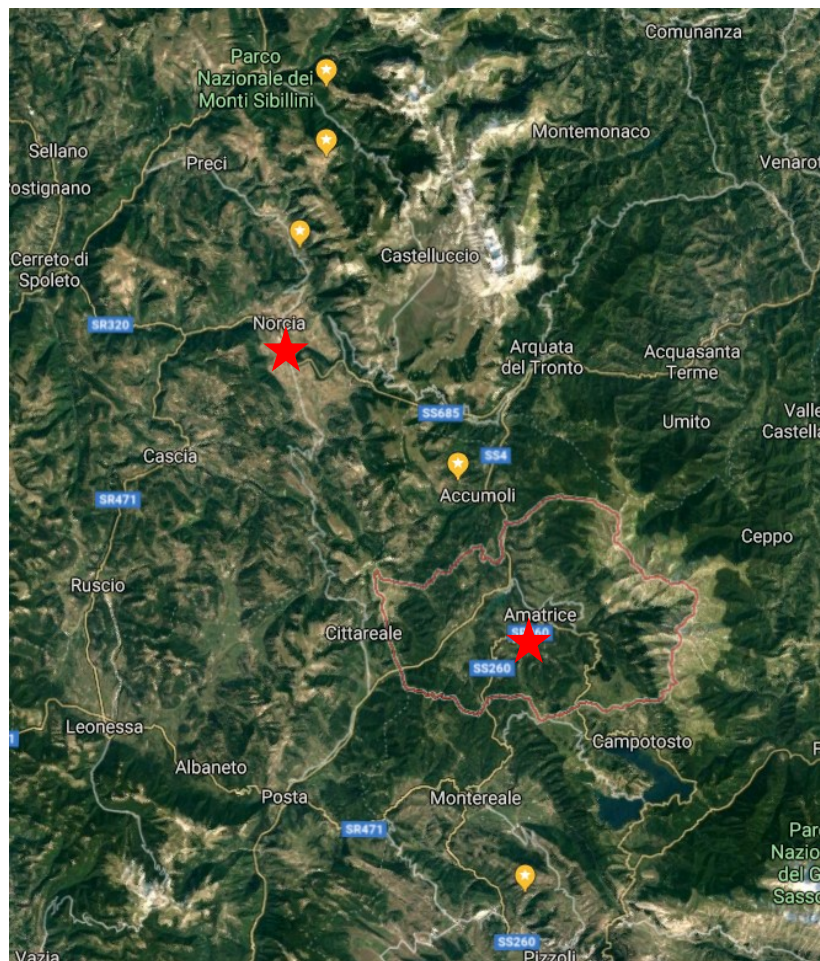


Figure 7.3 Earthquakes distance from Amatrice and Norcia



The previous images show the distances of the epicenters of the five earthquakes, the figure 7.2 with the site of Fabriano and the figure 7.3 with Amatrice and Norcia, cities that have suffered the greatest damage considering human losses and structural collapses. As is possible see from the table 7.1 and from following images, The PGA to which the structure has undergone are not to be elevated, in fact the earthquakes have modest epicentral distances. For example, the earthquake of 24-08-2017 magnitude 5.9 was resented by the structure with PGA of 0.089g, but the same earthquake have a far greater value in epicentral site, this in fact is due to the laws of attenuation and distance. The shaking maps give an orientation of a value of the PGA felt according to the distance. The double yellow triangle shows the position of Fabriano, for when it concerns the first earthquake, even if the magnitude is lower, the PGA in the area of Fabriano is around 9% of g fig 7.5, while for the second earthquake, the one with the magnitude of 6.5 , in the same area the PGA is lower, reaching a value around 5% of g fig 7.4. These shaking maps confirm the validity of the recored accelerations and of the PGA values shown in table 7.1

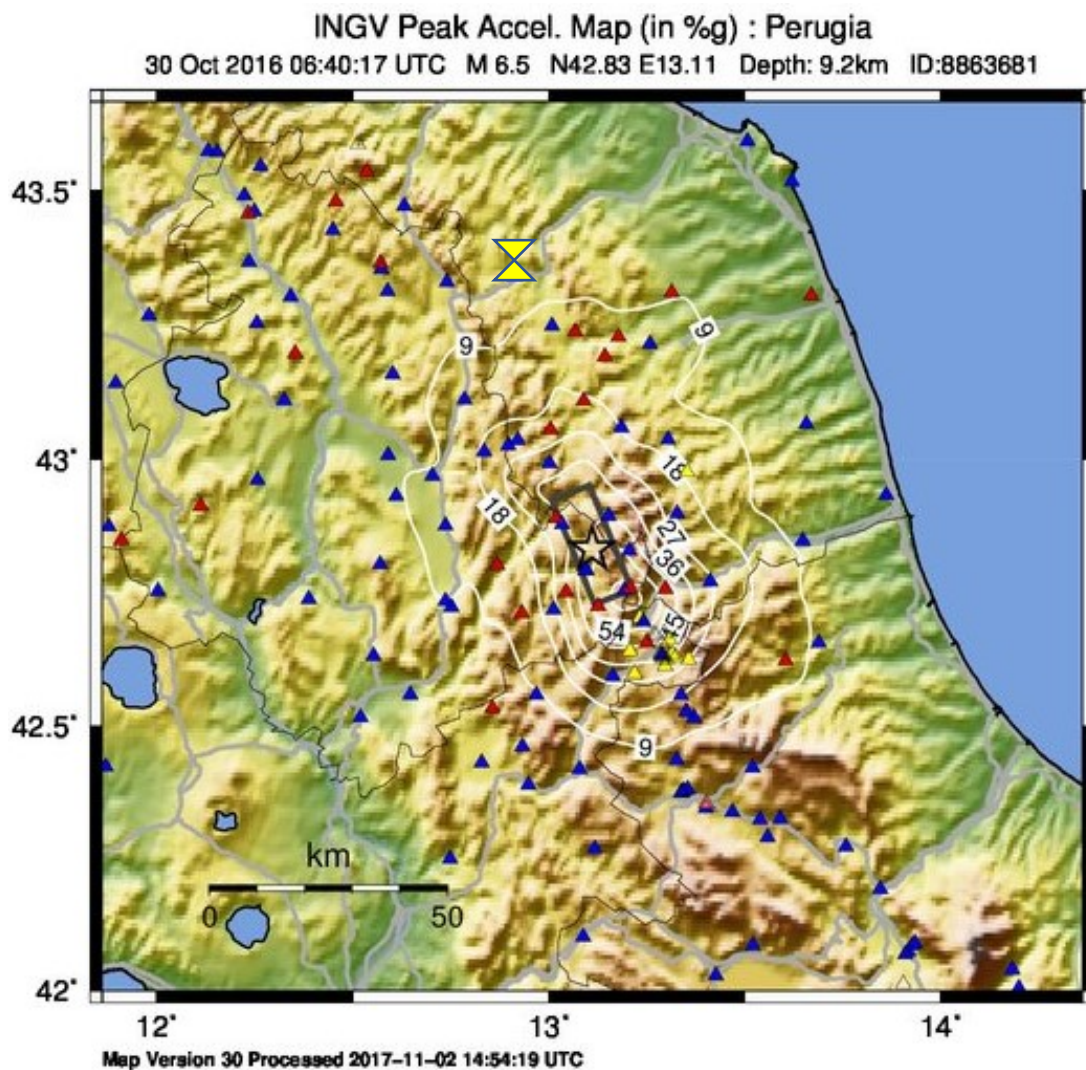
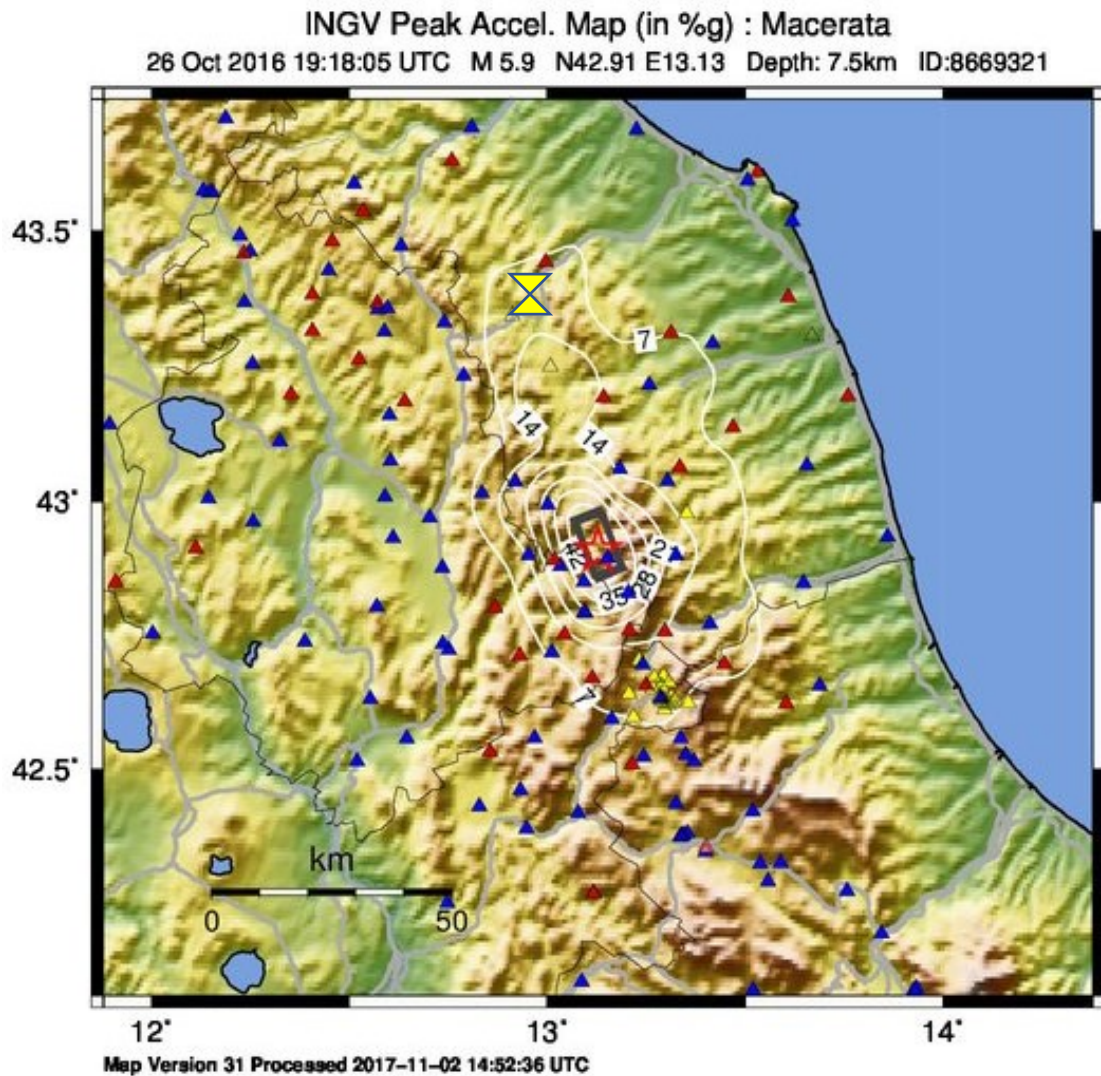


Figure 7.4 Shaking map earthquake n.4



*Figure 7.5 Shaking map earthquake n.3*

the values of accelerations that were used as seismic input to the structure are listed below, by noting in addition to component in two four cardinal directions: North, South, East, and West, the Pga has also been reported in reference to component, in Z direction, which usually has lower values than the other.

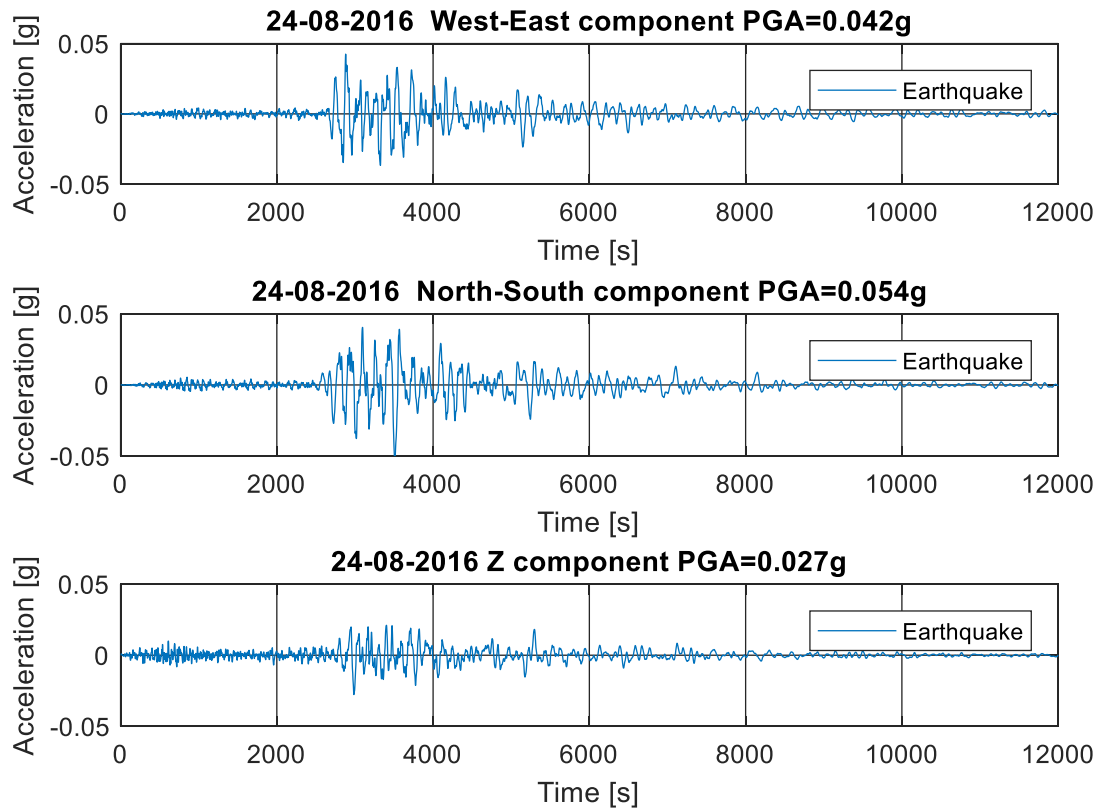


Figure 7.6 Seismic acceleration Earthquake n.1

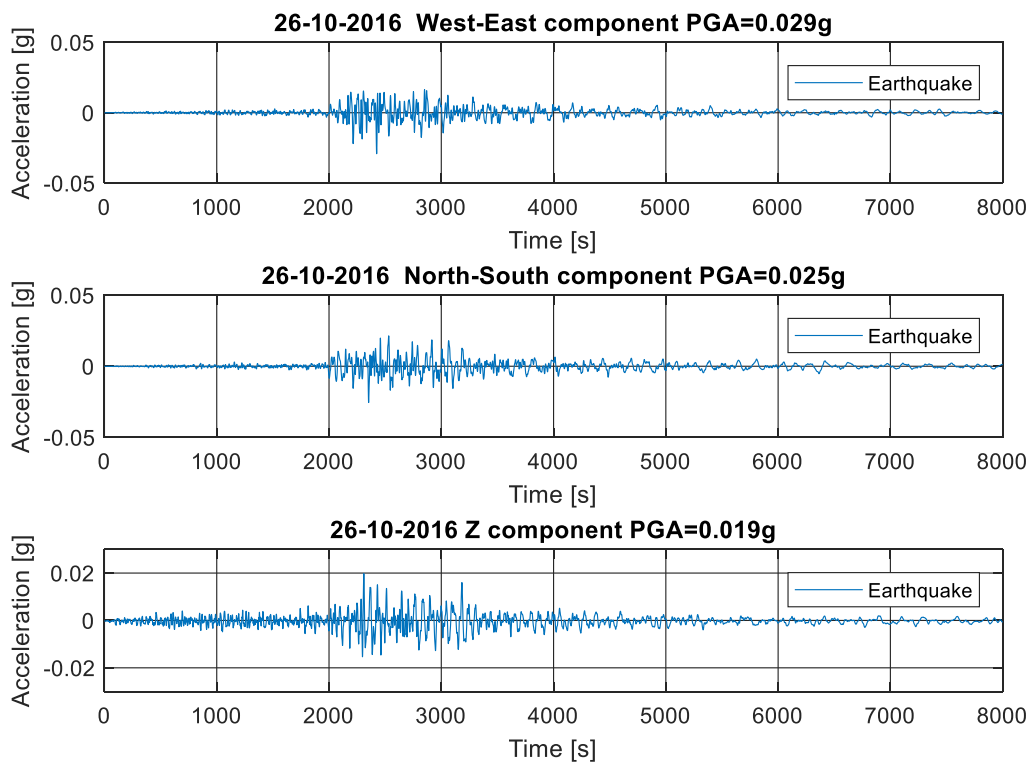


Figure 7.7 Seismic acceleration Earthquake n.2

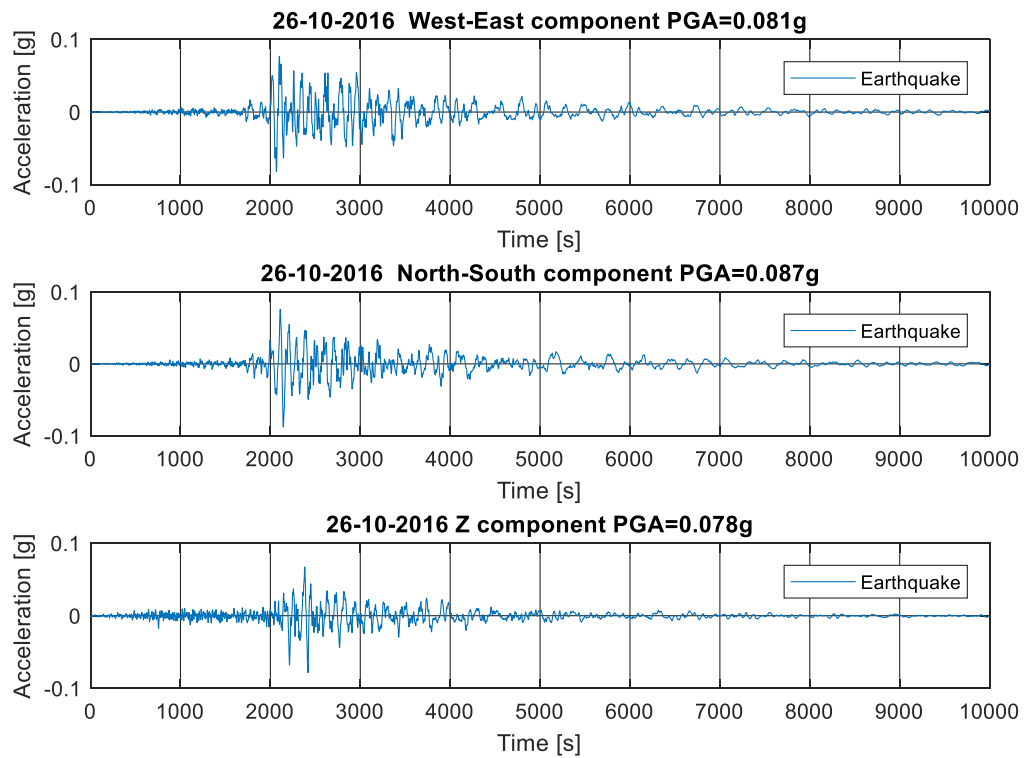


Figure 7.8 Seismic acceleration Earthquake n.3

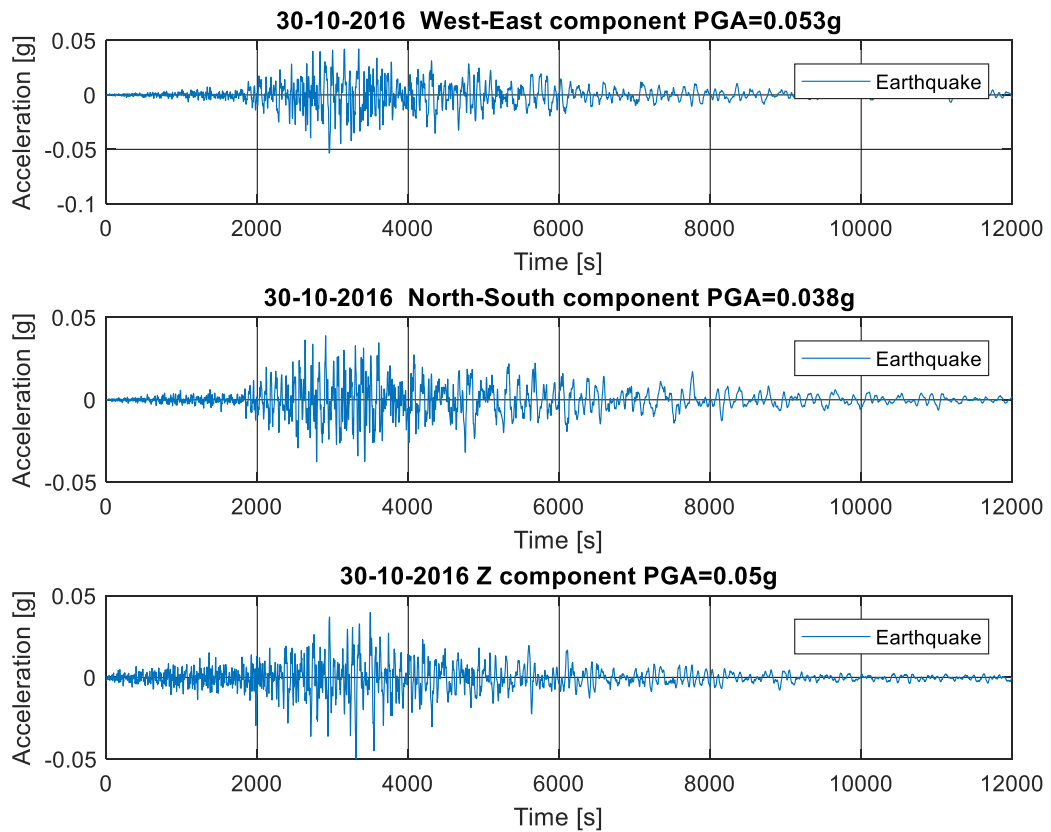


Figure 7.9 Seismic acceleration Earthquake n.4



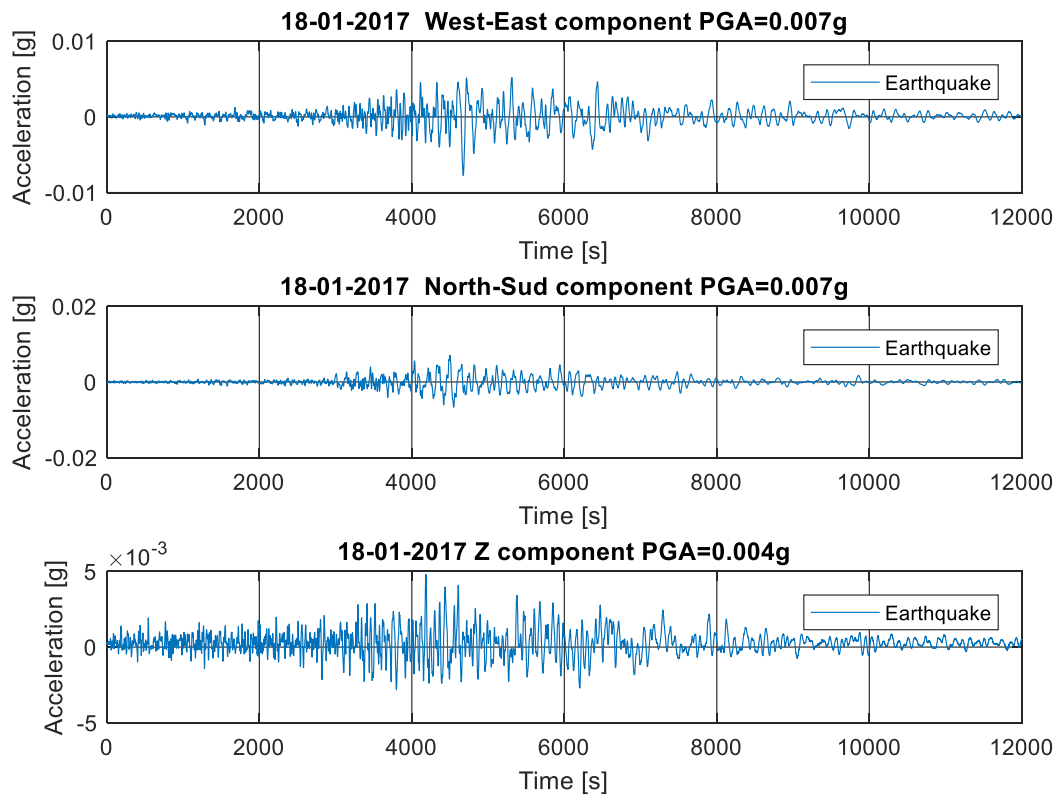


Figure 7.10 Seismic acceleration Earthquake n.5

The earthquakes reported, belong to the same seismic swarm begun in August of 2016, and still not permanently interrupted. These five one were those which had a greater relief of liberated energy and damage caused.



Figure 7.11 Damage caused by seismic shock 24-08-2016



## 7.2 Acceleration comparison

Another comparison that can be made is to compare the accelerations of the FEM model and the experimental ones (ID) at the points where the sensors are installed. This comparison can be made for each earthquake and for each channel, but below the graphs report the accelerations for the first earthquake. Two significant points of the second floor were chosen.

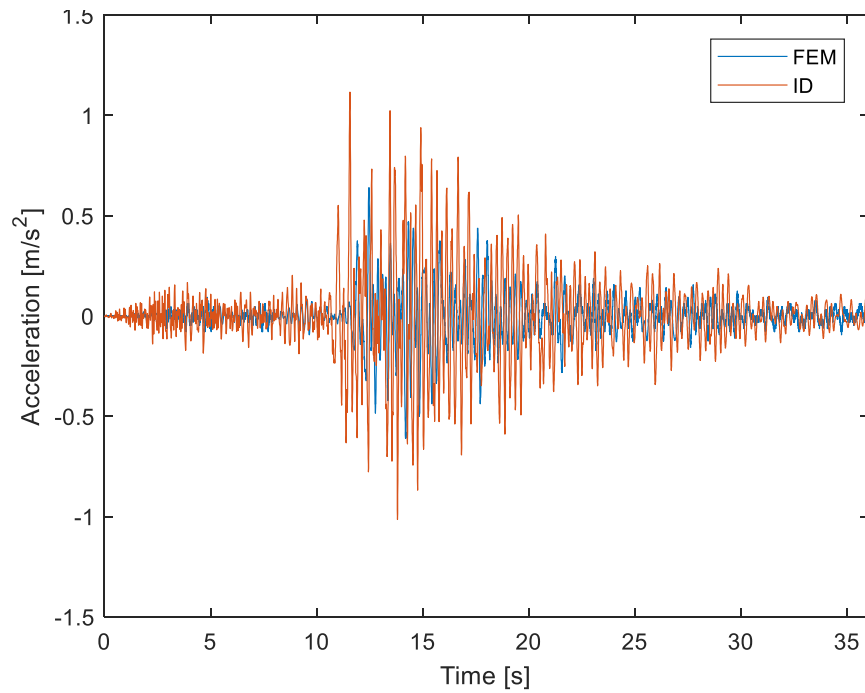


Figure 7.12 Acceleration FEM, ID channel 22

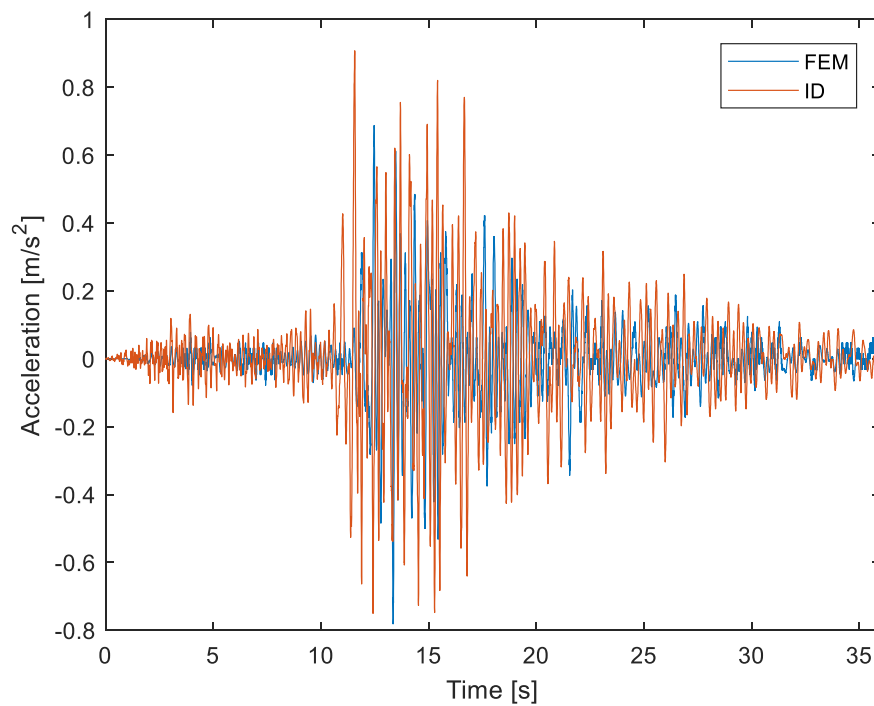


Figure 7.13 Acceleration FEM, ID channel 24

### 7.3 Displacements

The movements of the structure play a key role, in fact, they are a very useful parameter that allows to understand how the structure is "suffering" under the earthquake. A first step is to compare the movements of our model with those measured by the sensors.

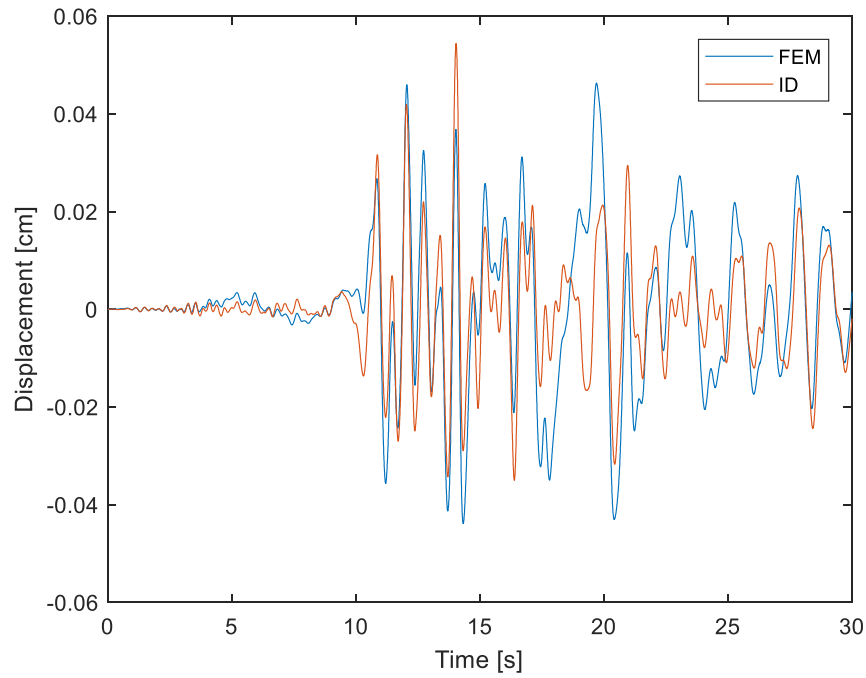


Figure 7.14 Displacement channel 22

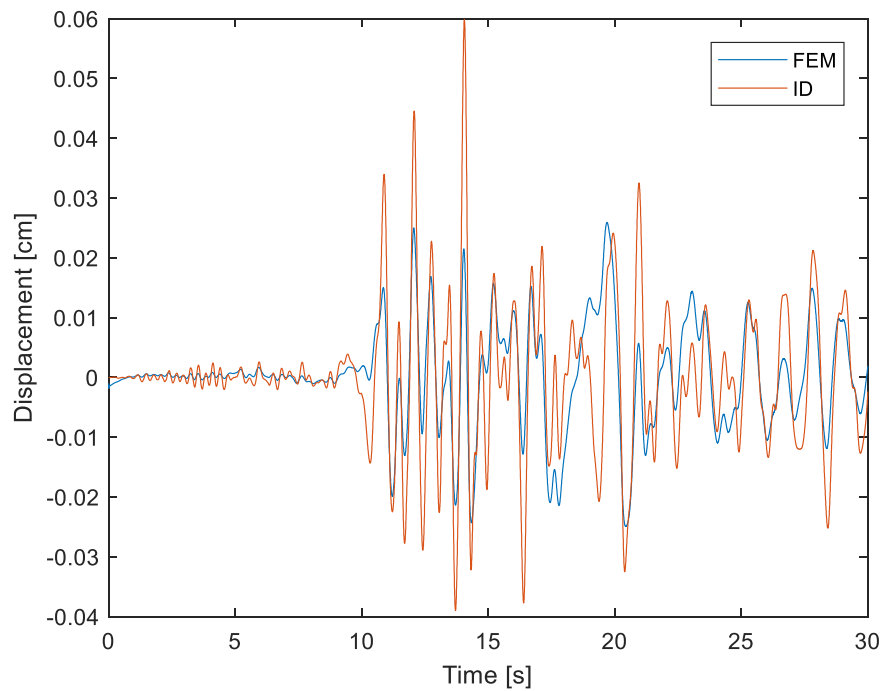


Figure 7.15 Displacement channel 24

## 7.4 Drift of floor

The drift is a useful parameter to value the level of stress or structure. This parameter is nothing more than the difference in displacement between two adjacent planes. For the study the drift is calculated to carry out evaluations with the state limit of damage, in fact, through its evaluation it is possible to determine whether the structure in question is injured, if it needs immediate interventions of consolidation, and in the best of the cases, if such a structure has not been damaged. In the case of civil and industrial constructions, according to the provisions of paragraph 7.3.7.2 NTC08, the verification of the State of damage is deemed to be fulfilled if the drift is:

$$dr < 0,005 h$$

Where h is the height between two floors.

In addition to considering the drift calculated by the calibrated model (FEM), it will compared to the experimental (ID), seeing if there is a correspondence.

The experimental Drift (ID), are calculated considering the position of the sensors and their channel orientation. Each channel measures the movement in one direction, to make the calculation require do the difference of two measurements, with two sensors belonging to the same channel, in the same is point but at different altitude

EARTHQUAKE 1					
	DIR.DRIFT	CHANNEL	ID [cm]	FEM [cm]	0,005 H [cm]
FLOOR 1/2	X	20	0,02	0,01	2,04
		27			
	X	19	0,04	0,02	2,04
		24			
	Y	21	0,09	0,07	2,04
		28			
	Y	16	0,06	0,05	2,04
		23			
FLOOR 0/1	X	20	0,07	0,15	2,68
		13			
	X	19	0,04	0,03	2,68
		8			
	Y	21	0,18	0,43	2,68
		14			
	Y	16	0,12	0,23	2,68
		10			

Table 7.2 Drift under earthquake n.1

EARTHQUAKE 2			ID [cm]	FEM [cm]	0,005 H [cm]
DIR.DRIFT	CHANNEL				
FLOOR 1/2	X	20	0,06	0,01	2,04
		27			
	X	19	0,02	0,01	2,04
		24			
	Y	21	0,07	0,07	2,04
		28			
	Y	16	0,04	0,03	2,04
		23			
FLOOR 0/1	X	20	0,05	0,03	2,68
		13			
	X	19	0,04	0,03	2,68
		8			
	Y	21	0,09	0,06	2,68
		14			
	Y	16	0,07	0,23	2,68
		10			

Table 7.3 Drift under earthquake n.2

EARTHQUAKE 3			ID [cm]	FEM [cm]	0,005 H [cm]
DIR.DRIFT	CHANNEL				
FLOOR 1/2	X	20	0,09	0,02	2,04
		27			
	X	19	0,05	0,04	2,04
		24			
	Y	21	0,017	0,015	2,04
		28			
	Y	16	0,08	0,10	2,04
		23			
FLOOR 0/1	X	20	0,078	0,017	2,68
		13			
	X	19	0,045	0,070	2,68
		8			
	Y	21	0,016	0,040	2,68
		14			
	Y	16	0,014	0,020	2,68
		10			

Table 7.4 Drift under earthquake n.3

EARTHQUAKE 4			ID [cm]	FEM [cm]	0,005 H [cm]
DIR.DRIFT	CHANNEL				
FLOOR 1/2	X	20	0,045	0,025	2,04
		27			
	X	19	0,017	0,017	2,04
		24			
	Y	21	0,013	0,015	2,04
		28			
	Y	16	0,013	0,023	2,04
		23			
FLOOR 0/1	X	20	0,045	0,015	2,68
		13			
	X	19	0,017	0,005	2,68
		8			
	Y	21	0,012	0,003	2,68
		14			
	Y	16	0,013	0,019	2,68
		10			

Table 7.5 Drift under earthquake n.4

EARTHQUAKE 5			ID [cm]	FEM [cm]	0,005 H [cm]
DIR.DRIFT	CHANNEL				
FLOOR 1/2	X	20	0,050	0,001	2,04
		27			
	X	19	0,007	0,005	2,04
		24			
	Y	21	0,008	0,007	2,04
		28			
	Y	16	0,005	0,008	2,04
		23			
FLOOR 0/1	X	20	0,045	0,037	2,68
		13			
	X	19	0,017	0,003	2,68
		8			
	Y	21	0,012	0,002	2,68
		14			
	Y	16	0,013	0,023	2,68
		10			

Table 7.6 Table Drift under earthquake n.4

### 7.4.1 Drift variation with the PGA

Another interesting thing to note is that the drift varies according to the PGA, or the earthquakes to which the structure was subjected. To make this comparison, only the second-floor drift of three significant points were taken into account:

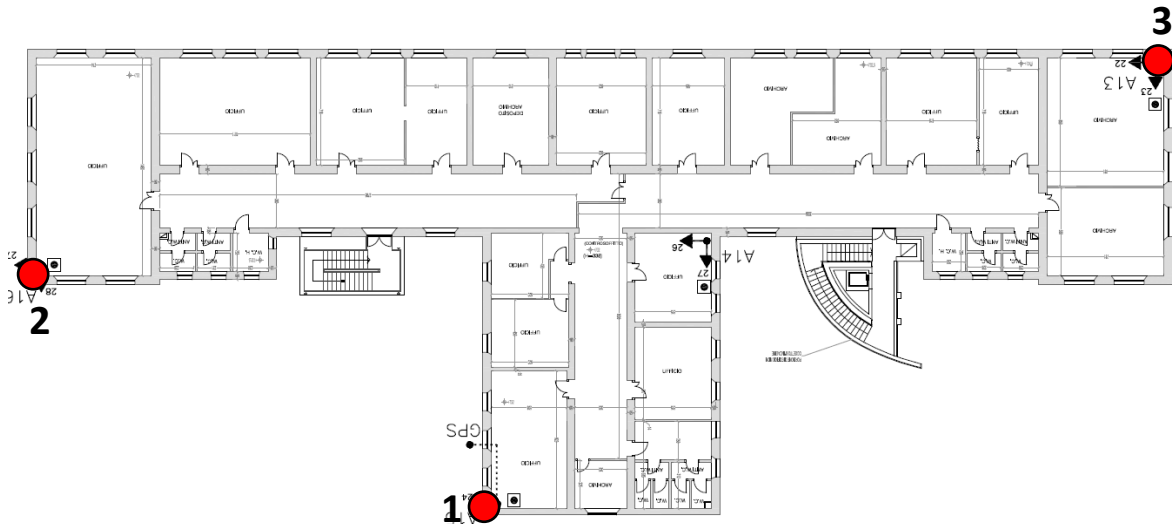


Figure 7.16 Location of DRIFT calculated second floor

The values of the interplane movements, calculated from the calibrated model, are shown below

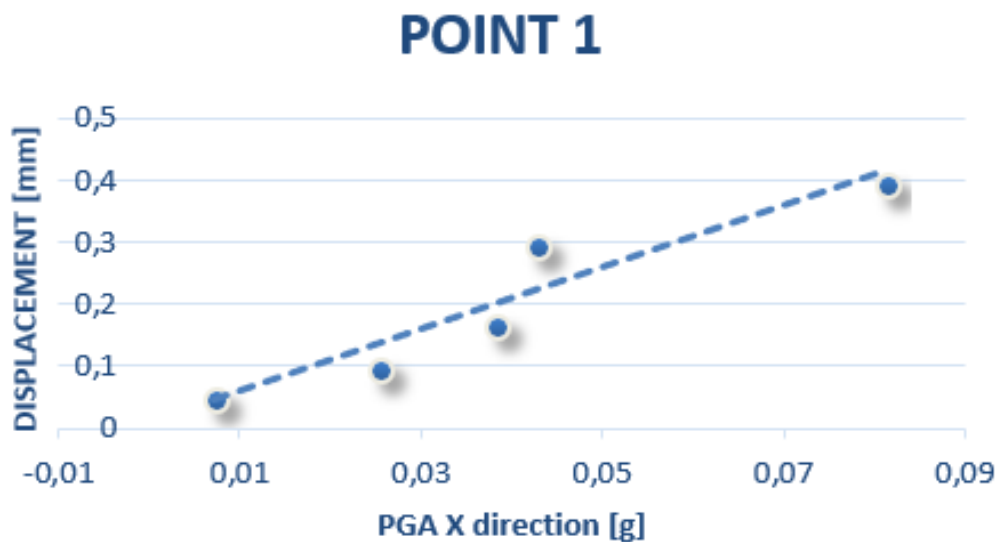


Figure 7.17 Displacement of point 1 with PGA



## POINT 2

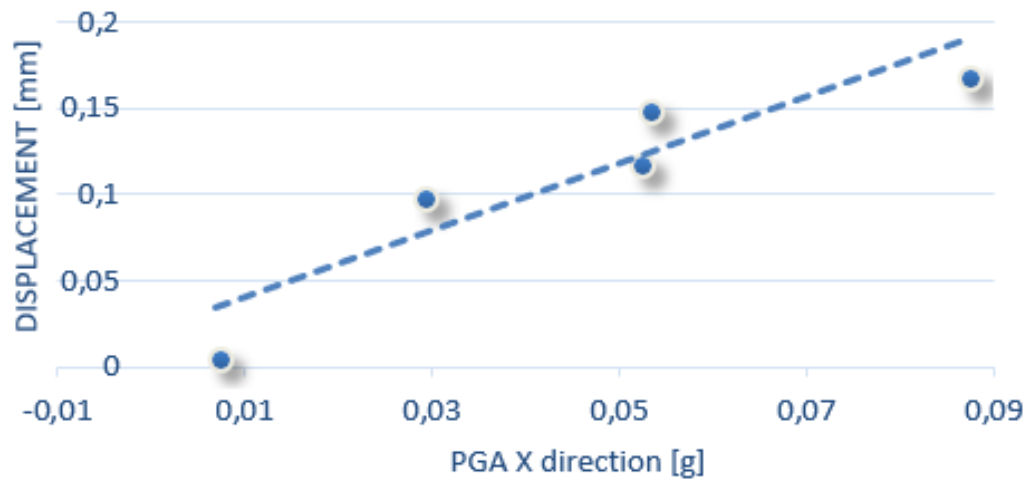


Figure 7.18 Displacement of point 2 with PGA

## POINT 3

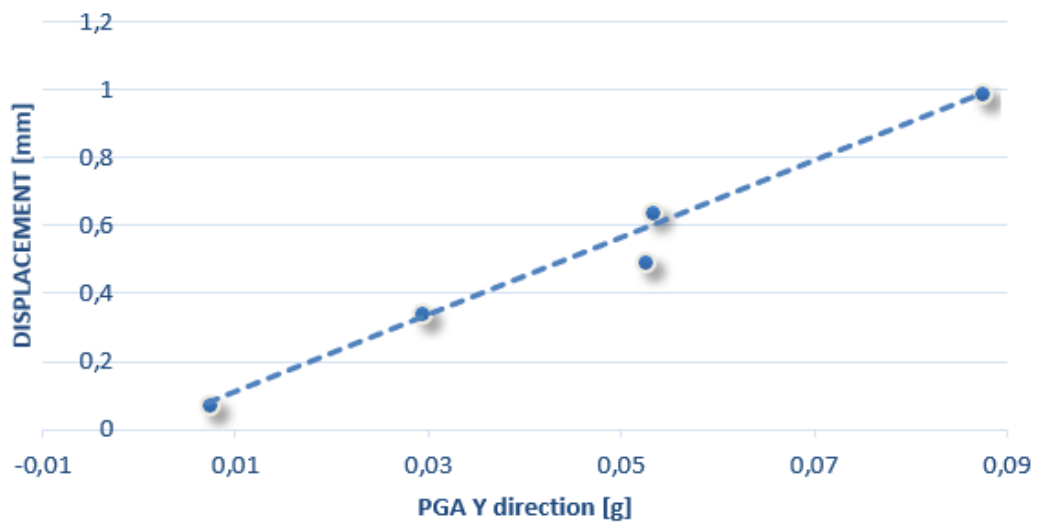


Figure 7.19 Displacement of point 3 with PGA

as shown above, there is a pattern similar to the linear one as the intensity of the earthquake increases.

### 7.4.2 Comparison Drift ID and FEM

At this point it is possible to make a comparison between the identified drift and those of FEM, in order to verify a correspondence and eventually to detect any errors, if the differences should be too pronounced.

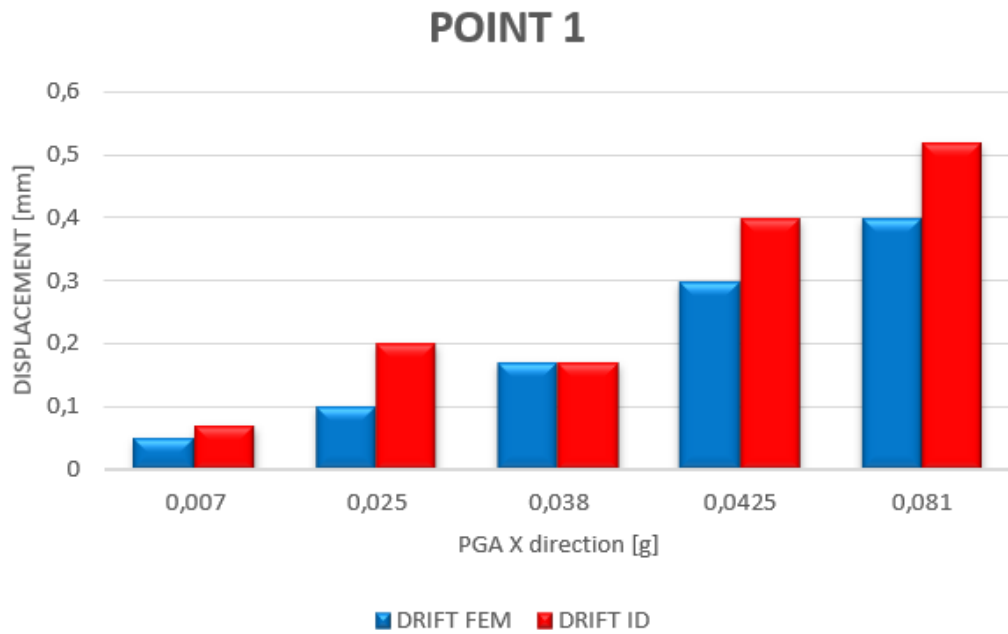


Figure 7.20 Comparison DRIFT point 1

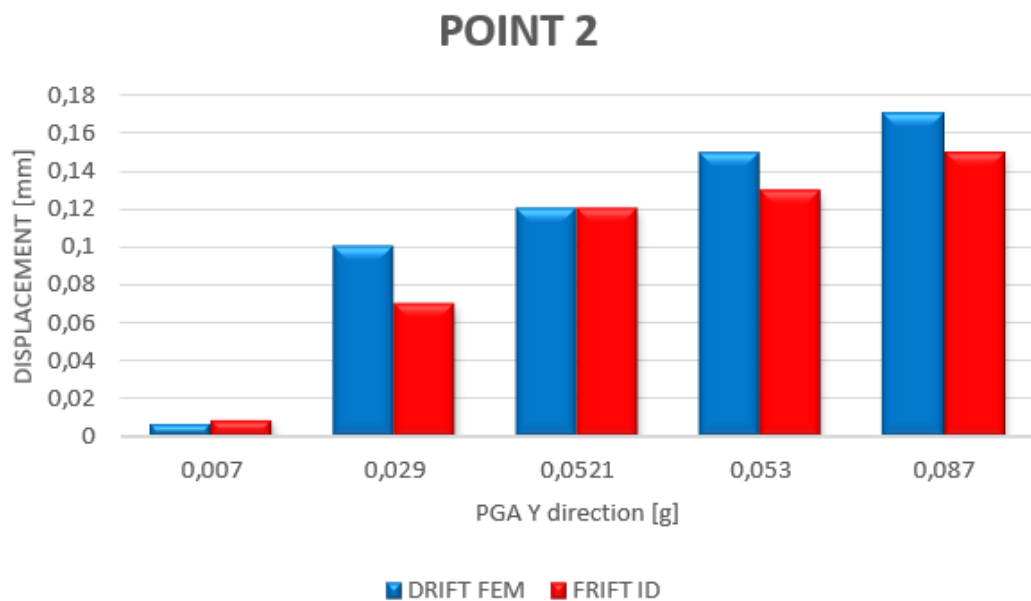
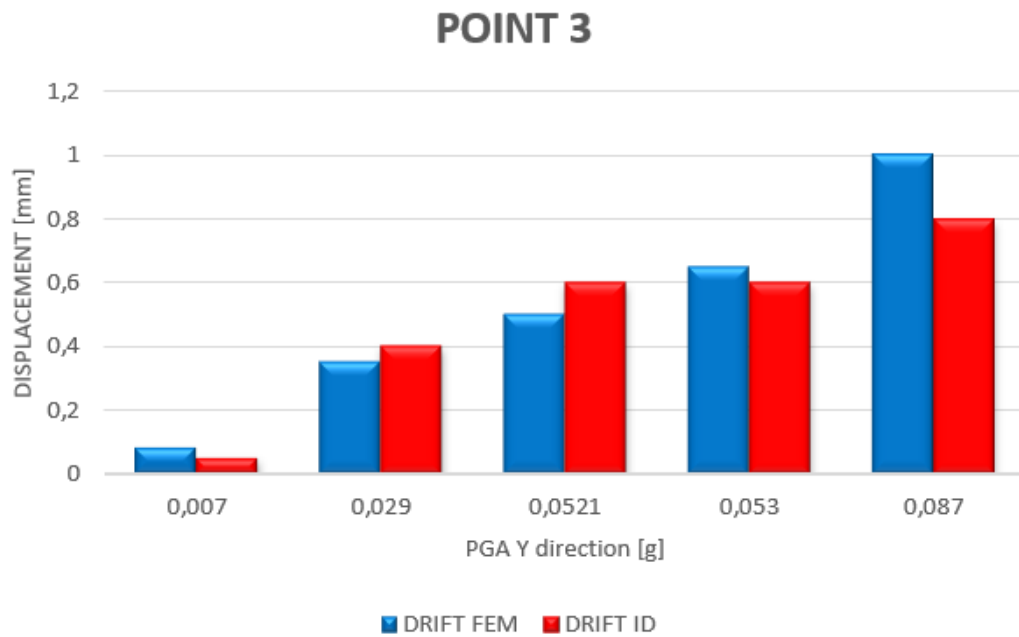


Figure 7.21 Comparison DRIFT point 2



*Figure 7.22 Comparison DRIFT point 3*

From the graphs do not denote any appreciable difference, however this check should also be made to the other two floors to have a greater assurance of the goodness of the results.

### 7.4.3 Drift for height of floor

At this point it is useful to see how the drift varies depending on the height of the plane. The three points in figure 7.15 were always taken in reference and only the Earthquake n.3 is considered, which has the highest PGA.

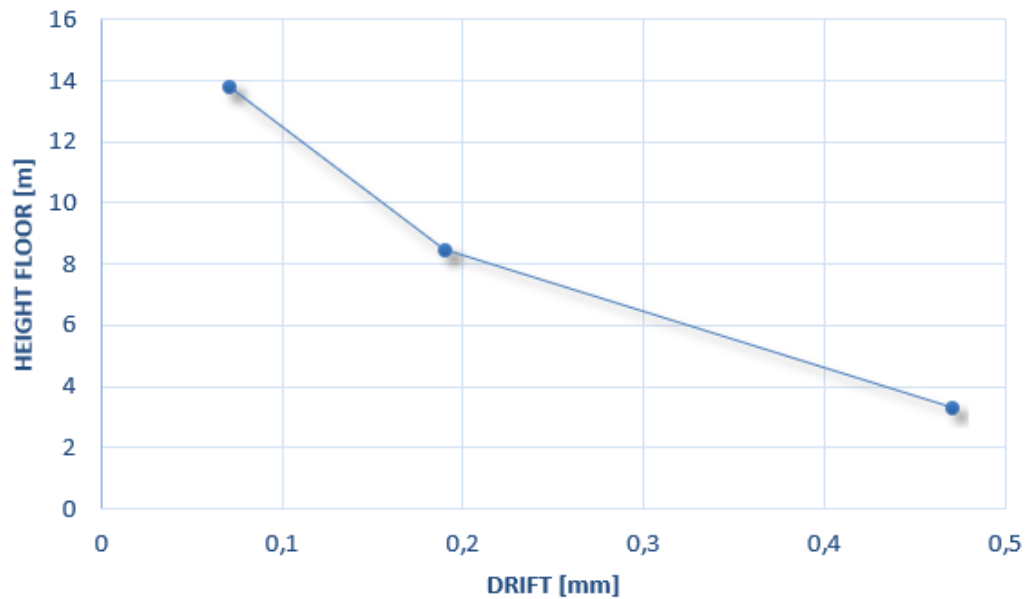


Figure 7.23 DRIFT FEM point 1

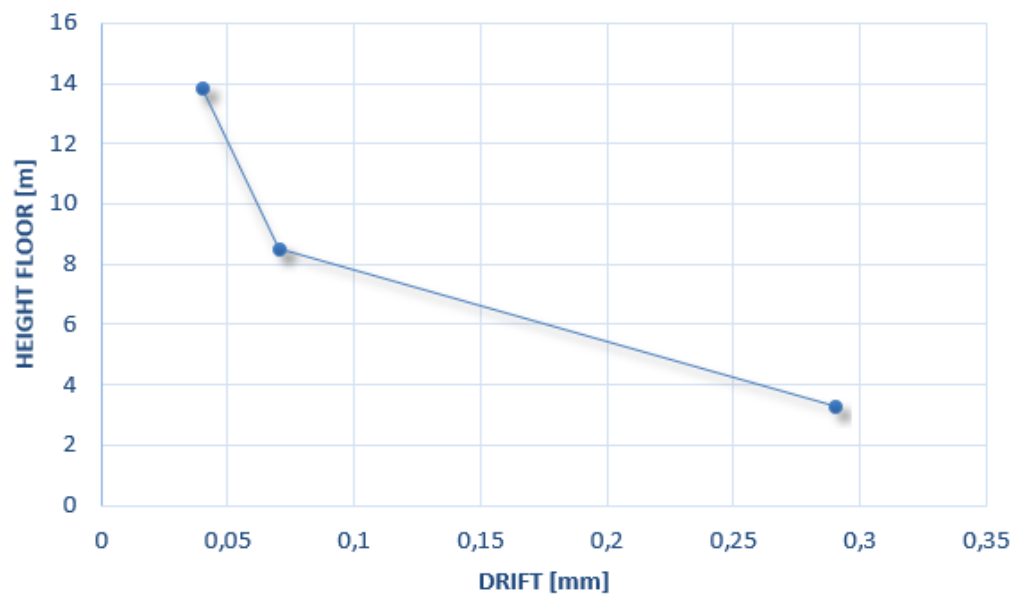


Figure 7.24 DRIFT FEM point 2

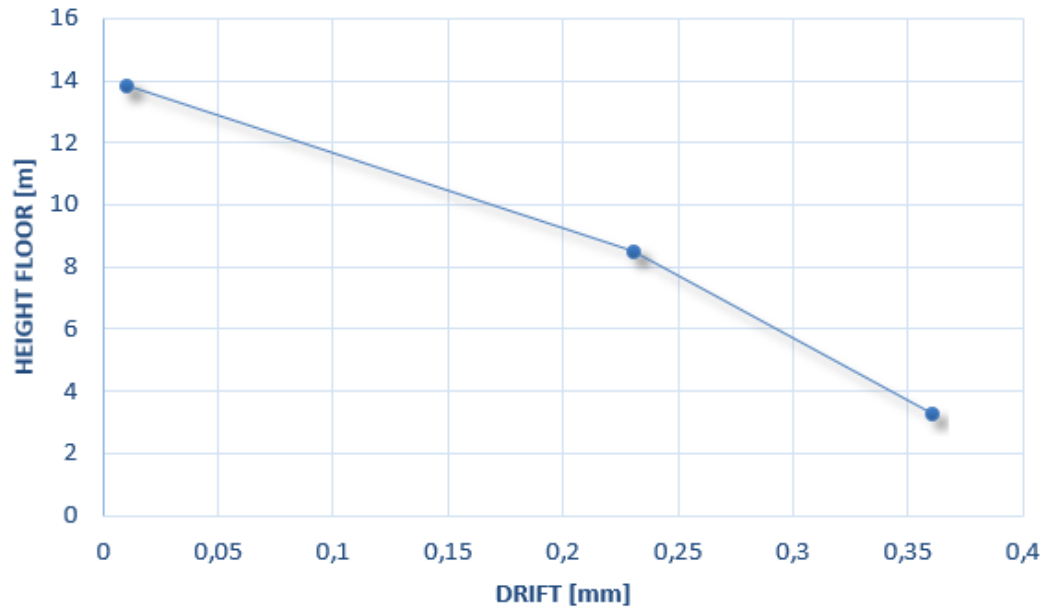


Figure 7.25 DRIFT FEM point 3

It is possible to notice a linear trend as the height of the plane increases, with very low values.

## 8 CONCLUSION

The modelling of the structure in question has led to satisfactory results even if the information about the structural characteristics provided by the civil protection has been summary and often not very specific. A very good calibration needs a few independent parameters and a simple implementation model. The calibration has been assessed with a good result but a further improvement is possible, extending the study to at least two modes of vibration. The model made, in fact, constitutes a good start, for further studies. A fundamental point that can and must be resumed is the study of the sensitive data acquired by the sensors. The acceleration and displacement signals available, were ordered in an order that did not respect the legend provided by the civil protection, and such data were affected by distortions that only a careful analysis of the signals could correct. The structure under examination, after the seismic sequence of Norcia, has not been damaged, as can be verified by paragraph 7.4. Public and civil activities can be resumed without any danger.

With a calibrated model it is possible to perform time history analysis considering real recorded earthquakes or with recreated by software to evaluate the response of the building and eventually to identify the area in which it can intervene thus guaranteeing its accessibility also immediately after the shock. The calibration, thanks to which the actual behaviour of the structure is simulated, is an important diagnostic tool that is available, especially for the most vulnerable buildings, those belonging to the historical-architectural heritage. In a larger perspective, thesis work is part of a seismic prevention project that is gradually taking shape in an increasingly large number of historic buildings to be protected.

Without prevention there is no protection, every study on structural behaviour is essential and must collect as many fields of study as possible. This is what it is doing, with good results the project Reluis. Seismic operating on prevention that plays a fundamental role especially in the preservation of historical buildings, where in Italy they are most of the built.



## ATTACHMENT

	PARAMETER ID	VALUE	TYPE/FLOOR
1	'E15'	5,55E+07	2
2	'E28'	1,44E+12	1
3	'E48'	5,02E+09	G
4	'E55'	3,09E+09	WALLS PARTITIONS G,1,2
5	'E53'	3,57E+12	2_ROOF
6	'E10'	1,29E+10	2_ROOF
7	'E52'	1,36E+14	2_ROOF
8	'E39'	3,49E+09	G
9	'E40'	2,17E+09	G
10	'E44'	1,90E+09	G
11	'E47'	2,14E+09	G
12	'E51'	1,19E+09	G
13	'E25'	1,24E+10	1
14	'E26'	1,03E+10	1
15	'E31'	3,07E+09	1
16	'E34'	1,73E+10	1
17	'E37'	7,34E+09	1
18	'E12'	4,33E+10	2
19	'E13'	2,45E+10	2
20	'E23'	9,97E+08	2
21	'E18'	1,48E+09	2
22	'E21'	5,84E+08	2
23	'E2'	4,52E+09	WALL PARTITIONS U
24	'E4'	6,90E+09	SLAB
25	'K_SOIL'	3,63E+09	SOIL SPRNGS
26	'E1'	1,47E+09	UNDERGROUND
27	'E38'	1,43E+09	G
28	'E43'	1,20E+09	G
29	'E24'	2,31E+09	1
30	'E29'	4,97E+11	1
31	'E11'	4,52E+08	2
32	'E16'	1,24E+09	2
33	'K_SPRING'	1,18E+09	SOIL SPRNGS
34	'MASS_ROOF'	5,47E+02	WEIGHT OF ROOF
35	'vpoiss'	3,10E-01	MODULE OF POISSON
36	'D4'	6,96E+02	SOL_1

# ATTACHMENT

37	'D38'	2,86E+03	G
38	'D49'	1,10E+03	G
39	'D24'	1,90E+03	1
40	'D30'	1,78E+03	1
41	'D16'	2,10E+03	2
42	'D11'	2,10E+03	2
43	'D1'	3,42E+03	UNDERGROUND
44	'D5'	6,28E+02	SOL_3
45	'D6'	3,00E+02	SOL_3
46	'D7'	2,56E+02	SOL_4
47	'D8'	3,00E+02	SOL_4
48	D54'	1,20E+03	ROOF
49	D10'	5,00E-02	ROOF
50	D52	5,00E-02	ROOF
51	D53	5,00E-02	ROOF

*Table Attachment n..1 Calibrated Values Parameters*

## REFERENCES

- Aarts, E., e J. Korst. *Simulated Annealing and Boltzan Machines*. Jhon Wiley & Sons, 1990.
- Allemang, R.J. *The modal assurance criterion (MAC): twenty years of use and abuse, Proceedings 20th International Modal Analysis Conference*. Los Angeles, 2002.
- Bathe, K.J. *Finite Element Procedures*. 2007.
- Chopra, A.K. *Dynamics of Structures: Theory and Applications to Earthquake engeneering*. Prentice-hall Internacional Series, 2016.
- Clough, R.W., and J. Penzien. *Dynamics of Structures*. Mc Graw-Hill Education, 1993.
- Daquarti. *Identificazione Dinamicae Model Updating i torri campanarie in muratura tesi di Laurea*. Torino: Politecnico di Torino, 2012.
- Ewins, D.J. *Modal Testing: Theory and Practice, Research Studied press LTD*. 1984.
- Gilbert, E.G. *Controllability and Observability in Multivariable Control Sytem*. SIAM, 1963.
- Ibrahim, R.A. *Parametric Rando Vibration*. Research Studies Press LTD, s.d.
- Kalman, R.E. *Mathematicl Description of Linear Dynamical Systems*. SIAM Journal on Control, 1998.
- Kirkpatrick, S., C.D. Gellat, and M.P. Vechi. *Optimization by Simulated Anneling*. 1983.
- Leuridan, J. *Some direct Parameter Model Identification Methods Applicable for Multiple Modal Analysis*. Department of Mechanical and Industrial Engineeering, University of Cincinnati, 1984.
- Ljung, L. *System Identification-Theory for user*. New Jersey: Prentice-Hall, 1999.
- Lundy , M., and A. Mess. *Convergence of an Annealing Algorithm, Mathematical Programming*. 1986.
- Palm , W. *Introduction to Matlab 7 for Engineers*. McGraw-Hill Science, 2003.
- Paulay, T., e M. J. N. Priestley. *Seismic Design of Reinforced Concrete and Masonry Buildings*. Wiley, 1992.
- Piras, F. *Monitoraggio sismico di edifici strategici: analisi di dati registrati durante l'evento sismico dell'Appennino Tosco Emiliano in data 27 Gennaio 2012*. Torino: Politecnico Torino, 2012.